PLACE IN RETURN BOX to remove this checkout from your record. TO AVOID FINES return on or before date due.

DATE DUE	DATE DUE	DATE DUE
<u>Jan£39</u> 00 23 8		
-		

MSU is An Affirmative Action/Equal Opportunity Institution

FUNDAMENTAL STUDIES OF ANALYTE/FILM INTERACTIONS AND THEIR APPLICATIONS FOR CHEMICAL SENSOR DEVICES

Ву

Edwin B. Townsend IV

A DISSERTATION

Submitted to
Michigan State University
in partial fulfillment of the requirements
for the degree of

DOCTOR OF PHILOSOPHY

Department of Chemistry

ABSTRACT

FUNDAMENTAL STUDIES OF ANALYTE/FILM INTERACTIONS AND THEIR APPLICATIONS FOR CHEMICAL SENSOR DEVICES

By

EDWIN B. TOWNSEND IV

Coated Surface Acoustic Wave (SAW) devices typically measure vapor concentrations during vapor/film equilibrium. However, many practical sensor applications require the analysis of pulsed sample streams. Thus, the research described was motivated by the desire to develop SAW chemical sensor systems to detect environmentally important compounds utilizing pulsed sample introduction.

A semi-automated pulsed injection and data analysis system utilizing 200 MHz SAW resonators has been constructed. A cell consisting of separate sample splitting chamber, sample transfer lines, and sensor device areas allows temperature control over the individual regions. Injections involving hexane, trichlorobenzene, and 1% (w/v) of biphenyl in hexane show that all three temperatures play an important role in the magnitude and time dependency of the SAW response.

The interactions of various classes of compounds with poly(isobutylene) [PIB] coated SAW devices and quartz crystal microbalances (QCM) have been examined. For the pulsed system, a new parameter ("pulse coefficient") has been developed that is analogous to the partition coefficient in a continuous flow system. Using the pulse coefficients, Linear Solvation Energy Relationships (LSER) were calculated that provided insight into analyte/film interactions. Pulse coefficients and LSER calculations compare favorably with values reported for continuous flow SAW and GLC experiments.

PIB films coated on SAW devices and FTIR/ATR internal reflection elements were exposed to nitromethane, isooctane, and perchloroethylene vapors. A correlation

was found between a spectroscopic indication of vapor induced polymer swelling and the responses of the polymer coated SAW devices. Sorption of perchloroethylene and isooctane caused PIB films to swell significantly while sorption of nitromethane swelled PIB films to a lesser degree. The observed polymer swelling occurs nearly simultaneously with analyte sorption, and both IR and SAW results indicate that the polymer swelling changes were reversible.

The responses of uncoated, PIB, poly(vinyl alcohol), and OV-275 coated SAW devices to 4% (w/v) biphenyl or 500 ppm pentachlorobiphenyl (PCB) in acetone, methanol, or hexane have been determined. SAW results obtained from the PIB coated devices indicate that dispersion forces are most important for both biphenyl and PCB. The nature of the solvent does not affect the sensor response to biphenyl. However, the response to PCB in hexane is larger than for PCB in methanol and acetone, regardless of polymer coating.

For Mom and Dad

who showed me the path

For Maria,

who has chosen to share her path with mine

For Sara

a wonderful addition to our path

ACKNOWLEDGMENTS

There are many who played important roles during the course of my graduate school experience. First and foremost was Prof. Jeff Ledford, who dispensed advice, guidance, and encouragment along with whatever else he felt was needed. Believe it or not, these words were appreciated. I learned more from you about the philosophy of science and life than I ever thought existed. I would like to thank Prof. Chris Chang, who allowed me the freedom to orchastrate the TAC program however I saw fit. Finally, Prof. Stan Crouch also deserves special mention. I admire and appreciate your professionalism. Finally, Profs. Blanchard, Harrison, and Galloway along with Drs. Funkhauser and Atkinson have always been available when I needed them.

There were others in the department who made significant contributions to my experience. To Beth Thomas and Cathy Allison; I don't think I could have survived without you. Everybody should be lucky enough to have you on their side. I can't thank you enough for all the help you've given me throughout the years. Dick Menke, my master cell constructor. Very little of this work could have been acomplished without your mechanical skills.

I have several friends who deserve special comment:

Kurt & Tracy K.- Thanks for everything. I'm sure that via Maria and Tracy, the phone companies will always be profitable.

Laura "Admiral" P. - Thank you for your support and encouragement. You deserve a lot from life, and I know you'll get it. Thanks for showing me what a very positive, upbeat outlook can do for a person.

Jim "Odie" R. - I'm not sure that anything I could write would be printable. Lets just say that you're the most unique, but no less valued, entry on my list.

Stephen M. - Thanks for all of your computer advice. I hope everything works out for you.

Kris K.- My favorite pool and bar partner. When are you going to get those acknowledgements done?

Greg N. - I hope that you're able to find someone who can help you during your final months as much as you helped me. Despite our "ideological" differences, I very much value your friendship. If only you couldn't just go run 6 miles at 7 minute pace whenever you wanted...

Jim N. - From you I have learned truth, honesty, and integrity. Mr. Moral fiber and all that stuff. I also want to remind you about the job you've promised me.

I have made many other friends during my time in my graduate school. The "original" group of cronies, Karen W-L, Jon W., Dave G., Gary S., Jeff G., Berly G., Jason R., Sue R., Mark S., Mary S., Eric H., and the others who started me off (in)correctly. The second generation of friends included Per "Calbert" A., Mike T., Paul "Gamemaster" P., Kathy S. (& family), Jeff R., Tim "Rabbit" M., Dana S., and all the others. I'm sure that I've inadvertantly forgot a few and I apologize. I wish you all well and thank you for your contributions to my sanity and well-being.

A dissertation could never be completed without the support of family. Even though I'm not sure they always understood why some events were occurring, they were supportive nonetheless. From my side, thanks go to Mom & Dad, Beef, Mary, and Drew, and all of my grandparents. On Maria's side, thanks go to Joanne, Michele, John, and Michael, along with Joe, Amy, & the kids. John, if it weren't for your inspiration, I don't know if I'd still be running. Thanks for the hobby (oh, excuse me, way of life).

I owe everyting to the two most important women in my life, Maria and Sara. The contributions that you make to my life are indescribable. Maria, the only way I can thank you is to make sure you get yours. And you will.

Now, Get to Work!!!

This work has been performed by a contractor of the U.S. Government under Contract DE-ACO5-84OR21400. The work performed at Michigan State University was performed under subcontract 19KMP607C to Martin Marietta Energy Systems Inc. A U.S. Patent has been applied for to cover various aspects of this development effort. Accordingly the U.S. Government retains a nonexclusive, royalty-free license to publish or reproduce the published form of this contribution, or allow others to do so, for U.S. Government purposes.

TABLE OF CONTENTS

		Page
List of Tabl	es	vi
List of Figu	res	vii
Chapter 1.	Introduction to Surface Acoustic Wave Sensors	1
1.1	Focus of Research	1
1.2	Acoustic Devices	3
	1.2.1 Introduction to Acoustic Devices	3
	1.2.2 Quartz Crystal Microbalance	4
	1.2.3 Surface Acoustic Wave Devices	6
1.3	Factors Contributing to SAW Response	12
	1.3.1 Mass Loading	12
	1.3.2 Mechanical Properties	14
1.4	Coatings for SAW Devices	
	1.4.1 Introduction	18
	1.4.2 Coordination Chemistry, Charge Transfer, Host/Guest	
	Mechanisms	19
	1.4.3 Solubility	20
1.5	Solubility Models and the Interpretation of SAW Response	21
	1.5.1 Partitioning	21
	1.5.2 Boiling Point Model and Hildebrand Solubility Parameters	23
	1.5.3 Linear Solvation Energy Relationships	24
	1.5.4 Application of LSERs to SAW Response	
1.6	References	29
Chapter 2.	Effect of Silanization and Operating Temperature on the Response of	
ош тр 101 д.	uncoated and Poly(isobutylene) Coated Surface Acoustic Wave	
	(SAW) Sensors	34
2.1	Abstract	34
2.2	Introduction	
2.3	Experimental	
2.4	Results and Discussion	
2.7	References	

Chapter 3.	Development and Performance of a Semi-automated 200 MHz	
	Surface Acoustic Wave Resonator Array-Based Sensor Test	
	Apparatus	51
3.1	Abstract	51
3.2	Introduction	
3.3	Experimental	
3.4	Results and Discussion	
3.5	References	
Chapter 4.	Study of Poly(isobutylene) Coated Piezoelectric Mass Sensors in a	
C.Lupior	Pulsed Injection System	72
4.1	Abstract	72
4.2	Introduction	
4.3	Experimental	
4.4	Results and Discussion	
4.5	Conclusion	
4.6	References	
Chapter 5.	An FTIR/ATR Study of Sorbent Induced Polymer Swelling:	
	Application to the Study of Surface Acoustic Wave Sensors	105
5.1	Abstract	105
5.2	Introduction	
5.3	Experimental	
5.4	Results	
5.5	Discussion	
5.6	Conclusion	
5.7	References	
Chapter 6.	Detection of Biphenyl and Pentachlorobiphenyl in Organic Solvents	
onupor o	Using Polymer Coated Surface Acoustic Wave Devices	137
6.1	Abstract	
6.2	Introduction	
6.3	Experimental	
6.4	Results	
6.5	Discussion	
6.6	References	162

List of Tables

Table		Page
Table 2.1.	Analytes and their responses at 30°C	42
Table 2.2.	Analytes and their responses at 60°C	47
Table 4.1.	List of analytes, boiling points, and the solvation energy parameters used in this work	78
Table 4.2.	Response ratios, pulse coefficients, and partition coefficients for the blank and PIB coated QCM and SAW devices.	91
Table 4.3.	Comparison of $LogP_{SAW}$, $LogP_{QCM}$, and $LogK_{SAW}$ with $LogK_{SAW}$ and $LogK_{GLC}$ values from the literature	96
Table 4.4.	Results of LSER fits using the QCM and SAW data and different solvation parameters.	98
Table 4.5.	Comparison of the contributions from each of the common statistically significant interaction parameters to logK _{SAW} and logP _{SAW} for poly(isobutylene).	100
Table 5.1.	Assignments of the major IR bands for poly(isobutylene), isooctane, perchloroethylene, and nitromethane	118
Table 5.2.	Comparison of vapor induced polymer swelling estimates to the change in integrated intensity of the C-H bending band of PIB (1235 cm ⁻¹)	121
Table 5.3.	List of analytes, boiling points, refractive indicies, and solvation energy parameters.	130

Table 6.1.	The average measured and calculated responses (Hz) to the solvent, biphenyl/solvent mixtures, and biphenyl measured using uncoated and coated SAW devices held at 30°C and 60°C	148
Table 6.2.	The average measured and calculated responses (Hz) to the solvent, 2,3,3',4,4'-pentachlorobiphenyl(PCB)/solvent mixtures, and PCB measured using uncoated and coated SAW devices held at 75°C	152
Table 6.3.	List of boiling points and solvation parameters for compounds used in this work and selected related species. The LSER coefficients available for the polymer films examined are also included	155

List of Figures

Figure	Page .
Figure 1.1.	General overview of a SAW device and measurement scheme. An alternating rf voltage, applied at one transducer, strains the piezoelectric substrate and generates the SAW. The wave travels along the surface of the crystal and any surface perturbations will affect the velocity and amplitude of the wave. The wave is subsequently detected at the other side of the device by the second set of IDTs. Any change in wave velocity is indirectly measured as a frequency change using an oscillator circuit
Figure 1.2.	The dual delay line SAW device10
Figure 1.3.	The SAW resonator11
Figure 1.4.	An illustration of the contribution of mass and viscoelastic effects to SAW response
Figure 1.5.	The partitioning phenomena between molecules in the vapor phase and the film on the SAW sensor substrate
Figure 2.1.	Schematic diagram of sensor test apparatus39
Figure 3.1.	View of the cell bottom showing the platform array device inserted. Individually mounted SAW devices are mounted perpendicular to the devices on the platform
Figure 3.2.	Schematic diagram of the complete sensor test apparatus56
Figure 3.3.	Output created by the LabView software written to process 6 channels of SAW data

Figure 3.4.	The effect of sensor cell temperature on the response of an uncoated device to injections of 3 µL of hexane followed by 3 µL of a 1% (w/v) mixture of biphenyl in hexane. Sensor cell temperatures = (a) 60°C, (b) 45°C, and (c) 30°C. Splitting chamber temperature = 250°C. Transfer line temperature = 50°C. Carrier gas flow rate = 80 cc/min	61
Figure 3.5.	Effect of various combinations of splitting chamber/transfer line temperatures on the response of an uncoated device to injections of 3 μ L of hexane followed by 3 μ L of a 1% (w/v) mixture of biphenyl in hexane. Splitting chamber/transfer line temperatures = (a) 100/38°C, (b) 200/49°C, (c) 300/63°C, and (d) 400/77°C. Sensor cell temperature = 30°C. Carrier gas flow rate = 80 cc/min	63
Figure 3.6.	The effect of transfer line temperature on the uncoated device response to 0.1 µL injections of trichlorobenzene. Transfer line temperatures = (a) 75°C and (b)150°C. Splitting chamber temperature = 400°C. Sensor cell temperature = 30°C. Carrier gas flow rate = 80 cc/min	66
Figure 3.7.	Effect of carrier gas flow rate on the uncoated device response to injections of 3 μ L of hexane followed by 3 μ L of a 1% (w/v) mixture of biphenyl in hexane. Carrier gas flow rate = (a) 20 cc/min, (b) 50 cc/min, and (c) 100 cc/min. Splitting chamber temperature = 250°C. Transfer line temperature = 50°C. Sensor cell temperature = 30°C	67
Figure 3.8.	Calibration curves for hexane injected on a blank () and poly(isobutylene) coated (Δ) device	69
Figure 4.1.	Schematic diagram of the SAW sensor test cell. The sample is introduced as a pulse and then split equally into 6 streams. Each of the streams is delivered directly onto the SAW surface. (a) is one of the six delivery arms, (b) is the mixing chamber, and (c) is one of the 6 resonators mounted on a gold stage	80
Figure 4.2.	Schematic diagram of the QCM sensor test cell. The QCM is positioned in the center of the cell, and the sample is introduced as a pulse and then split equally into 2 streams. The streams are delivered to the left and the right of the device	83

Figure 4.3.	Variation of uncoated QCM device response (Hz/μmole) versus analyte boiling point	86
Figure 4.4.	Variation of uncoated SAW device response (Hz/nanomole) versus analyte boiling point	88
Figure 4.5.	Variation in the response of poly(isobutylene) coated QCM device response (Hz/µmole) as a function of analyte boiling point	90
Figure 4.6.	Variation in the response of poly(isobutylene) coated SAW device (Hz/nanomole) as a function of analyte boiling point for the pulse injection (O) and continuous flow (+) methods. The response for nonane (78 Hz/nanomole) has not been included in this plot (see text)	92
Figure 5.1.	Normalized PIB coated SAW device responses to (a) nitromethane, (b) isooctane, and (c) perchloroethylene using continuous flow and pulsed injection sample introduction. Equilibrium and pulse responses have been normalized to analyte concentrations of 0.02 g/L and 0.01 g/L, respectively	113
Figure 5.2.	Variation in the normalized equilibrium frequency shifts versus time following $t^{1/2}$ for a PIB coated SAW device exposed to nitromethane (Δ), perchloroethylene (), and isooctane (O). (a) Rising and (b) Falling edges	114
Figure 5.3.	IR spectra of (a) nitromethane, (b) perchloroethylene, (c) isooctane, and (d) poly(isobutylene)	117
Figure 5.4.	(a) IR spectra of a PIB film before exposure to nitromethane (solid line) and at maximum analyte intensity (dashed line) using pulsed sample introduction. (b) IR spectra before exposure to nitromethane (solid line) and during vapor/film equilibrium (dashed line) using continuous flow sample introduction	119
Figure 5.5.	(a) IR spectra of a PIB film before exposure to isooctane (solid line) and at maximum analyte intensity (dashed line) using pulsed sample introduction. (b) IR spectra before exposure to isooctane (solid line) and during vapor/film equilibrium (dashed line) using continuous flow sample introduction	122

Figure 5.6.	(a) IR spectra of a PIB film before exposure to perchloroethylene (solid line) and at maximum analyte intensity (dashed line) using pulsed sample introduction. (b) IR spectra before exposure to perchloroethylene (solid line) and during vapor/film equilibrium (dashed line) using continuous flow sample introduction	123
Figure 5.7.	IR spectra obtained as a function of time for a PIB film exposed to a continuous vapor stream of perchloroethylene	124
Figure 6.1.	Overview of the sensor test apparatus	142
Figure 6.2.	Typical response profiles obtained for the solvent and the biphenyl/solvent mixtures using poly(isobutylene), poly(vinyl alcohol), and OV-275 coated devices held at 30°C	147
Figure 6.3.	Typical response profiles obtained for the solvent and the biphenyl/solvent mixtures using poly(isobutylene), poly(vinyl alcohol), and OV-275 coated devices held at 60°C	149
Figure 6.4.	Typical response profiles obtained for the solvent and the PCB/solvent mixtures using poly(isobutylene), poly(vinyl alcohol), and OV-275 coated devices held at 75°C	151

Chapter 1

Introduction to Surface Acoustic Wave Chemical Sensors

1.1 Focus of Research

Surface acoustic wave (SAW) devices belong to a general class of acoustic microsensors that are sensitive to surface mass changes. The potential of these devices is best illustrated by noting that a SAW device operating at 200 MHz exhibits a 904 Hz frequency shift when perturbed by 1 ng of surface mass. The small size and extreme sensitivity of these devices has motivated researchers to investigate their potential use as chemical sensors. The chemical selectivity of SAW devices is enhanced through the application of a coating to the device surface. Using a good coating, Ballantine and Wohltjen [1] have suggested that it is possible to detect vapors at the 10-100 ppb concentration level, with selectivity of 1000:1 or more over commonly encountered interferences, with a linear dynamic range of 3-4 orders of magnitude.

Typically, the coated device is exposed to a continuous stream of vapor. We are exploring an alternate method of sample introduction, the pulsed method, where the analyte of interest reaches the SAW device as a plug, interacts with the coated surface, desorbs, and is rapidly swept out of a test cell. This importance of this style of sample introduction technique in relation to mass sensors has been discussed previously [2-10]. For example, Janghorbani and Freund have successfully used a quartz crystal microbalance (QCM) as a GC detector [8].

Edmonds and West have used pulsed sample introduction in combination with QCMs coated with gas chromatographic phases to detect various organic species [9]. Grate and Abraham have pointed out that this type of sample introduction can be used in conjunction with laser or thermal desorption [2]. Grate *et al.* [10] later used thermal desorption of analyte in preconcentrator tubes to deliver pulses of gas to an array of SAW devices.

The research described in this dissertation was motivated by the desire to develop SAW chemical sensors that detect environmentally important compounds utilizing pulsed sample introduction. Chapters 2-6 detail knowledge gained regarding the different aspects of sensor operation in the pulsed sampling environment. Chapter 2 explores the effects of temperature and surface silanization on uncoated and poly(isobutylene) coated mass sensor responses. Chapter 3 details a new pulsed sensor system and a SAW cell used to illustrate the effects of various operating parameters and to provide new insight into phenomena occurring in pulsed sampling sensor systems. Chapter 4 demonstrates that data obtained from poly(isobutylene) coated acoustic devices in pulsed injection systems can be used in combination with Linear Solvation Energy Relationships to obtain molecular level insight into analyte/film interactions. Chapter 5 demonstrates that FTIR/ATR spectroscopy can be used to probe phenomena that occur during the sorption of an analyte into a film and how these processes can influence SAW response. Chapter 6 demonstrates the influence of solvent matrix on SAW device response.

1.2 Acoustic Devices

1.2.1. Introduction to Acoustic Devices

Piezoelectricity was first observed in 1880 by Pierre and Jacque Curie [11], who found that, for particular compounds, the application of a mechanical force resulted in the generation of an electrostatic voltage. They also found that the application of an electric field to these compounds induced crystal deformations. Since these initial findings, a large number of materials have been found that exhibit the piezoelectric effect. Quartz is the piezoelectric material used most often for chemical sensing applications because of its chemical inertness and the insensitivity of its wave properties to changes in temperature.

Piezoelectric materials may support a wide range of acoustic waves. Waves can travel either through the bulk or along the surface of the material, or by reflections along multiple surfaces. Transverse or shear waves have particle displacements that are normal to the direction of wave propagation, and can be subsequently polarized so that the displacements are parallel or normal to the surface of the sensor. Surface acoustic (or Rayleigh) waves are confined to an area at the surface of the crystal that is roughly one acoustic wavelength thick. Surface particles affected by these Rayleigh waves move in an elliptical path, with both surface-parallel and surface normal components.

Acoustic microsensors normally consist of a piezoelectric material in combination with some type of metal transducer. The transducers launch acoustic waves into the crystal at high frequencies. The types of waves generated depend on the crystal

orientation, thickness, and the geometry of the metal transducers. There are four basic kinds of acoustic devices, so named because of the types of waves generated and detected. They are the quartz crystal microbalance, the surface acoustic wave, flexural plate wave, and acoustic plate mode devices. Because this dissertation includes only quartz crystal microbalances and surface acoustic wave devices, the discussion is limited to those two devices.

1.2.2. Quartz Crystal Microbalance

The first type of microbalance to be developed using the piezoelectric properties of materials was the quartz crystal microbalance (QCM). The dominant acoustic wave generated and monitored in a QCM is the bulk transverse wave, which travels perpendicular to the sensing surface. The thickness of the QCM determines the wavelengths of the fundamental and the harmonic resonances. Typical resonant frequencies for the fundamental mode are between 5 and 10 MHz.

The use of QCMs as detectors was first demonstrated by Sauerbrey [12], who derived an expression that related a change in thickness of the crystal (caused by an increase in mass at the surface of the crystal) to shifts in frequency according to equation (1), where ρ_q and ν_q are the density and shear wave velocity of quartz , and f_q is the fundamental frequency of the quartz oscillator.

$$\Delta f = -2f_q^2 \, \Delta m / \left(\rho_q v_q \right) \tag{1}$$

This expression assumes that the material deposited on the QCM surface only increases the thickness of the crystal. The consequences of changes in density, viscosity or shear modulus of the added layer are ignored. However, the utility of this expression was illustrated by adding mass to the crystal using vacuum metal evaporation [12] and later verified by others [13-15].

Kanazawa has derived the most recent expression that describes the frequency dependence of the QCM on both the mass and physical properties of an overlayer [16]. The relationship is shown in equation (2), and was developed to describe the response of a QCM in contact with liquids, but is applicable to any viscous overlayer,

$$\Delta f = -f_0^{3/2} \left(\rho_L \eta_L / \pi \rho \mu \right)^{1/2} \tag{2}$$

where f_O is the frequency of the uncoated crystal, η_L is the absolute viscosity of the liquid, μ is the shear modulus, ρ is the density of quartz, and ρ_L is the overlayer density. This equation has been supported using results obtained from 5 and 9 MHz QCMs [17].

QCMs have been used as GC detectors [18], for monitoring trace amounts of atmospheric gases [19], or for polymer film characterization [20]. Many reviews have been published that discuss coating materials and the use of QCMs to detect analytes at low concentrations [19-27]. Sensors designed using guest/host chemistry have also been reported [28-30]. Chemometric techniques have been used to analyze the responses obtained from QCM arrays [31,32].

1.2.3. Surface Acoustic Wave Devices

Surface waves were first described by Lord Rayleigh [33] and are often referred to as Rayleigh waves. Devices utilizing these types of waves were created [34] after White and Voltmer developed the interdigital transducer (IDT) [35]. Wohltjen and Dessey first introduced the concept of SAW chemical sensors in 1979, and subsequently described operational concerns and demonstrated possible applications [34,36-39]. The concepts of coated SAWs as detectors for gas chromatography, to probe film properties, and for gas phase analyte detection were also introduced.

Typically, a SAW device is constructed using ST-cut quartz and two sets of interdigital transducers (IDTs) formed by photolithographic patterning of a thin metal film (see Figure 1.1). When an alternating potential is applied to one transducer, an alternating strain is generated in the substrate due to its piezoelectric nature. If this alternating potential is at the appropriate frequency, the strain launches a Rayleigh (SAW) wave which travels along the surface of the substrate. The SAW has most of its energy confined within one wavelength of the surface and thus, is strongly affected by any material in contact with the surface. Consequently, the properties of the material have an effect on the velocity and amplitude of the SAW wave.

SAW devices normally operate in the 3-300 MHz range. The actual resonant frequency depends upon the spacing between the IDTs, as illustrated by equation (3) where f_O is the resonant frequency, ν is the velocity of the SAW wave, and d is the distance between the transducers.

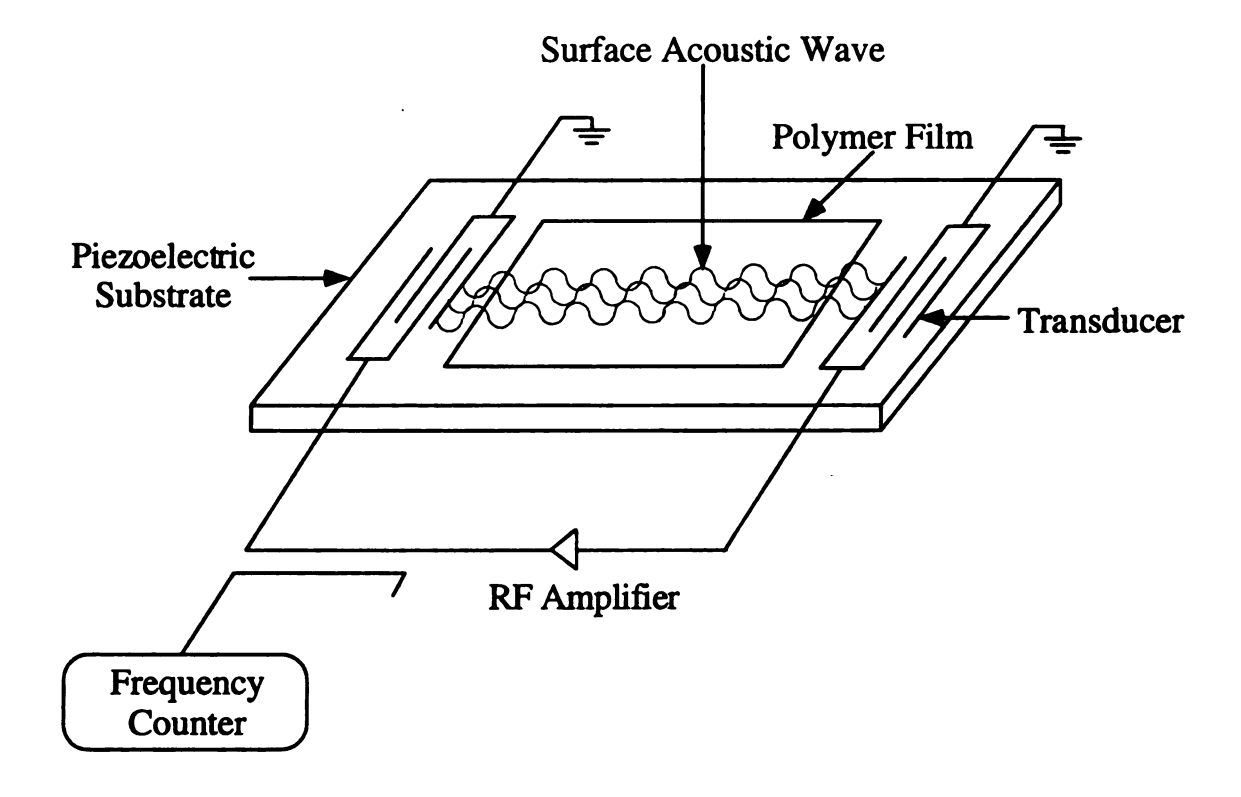


Figure 1.1. General overview of a SAW device and measurement scheme. An alternating rf voltage, applied at one transducer, strains the piezoelectric substrate and generates the SAW. The wave travels along the surface of the crystal and any surface perturbations will affect the velocity and amplitude of the wave. The wave is subsequently detected at the other side of the device by the second set of IDTs. Any change in wave velocity is indirectly measured as a frequency change using an oscillator circuit.

$$f_o = \frac{v}{d} \tag{3}$$

This expression illustrates that the closer the spacing between the IDTs, the higher the resonant device frequency. As will be discussed in Section 1.3.1, the theoretical sensitivity of the device increases with the square of the operating frequency. Thus, it appears that increased sensitivity can be achieved with smaller devices.

Velocity and amplitude measurements can be made using a signal generator and a vector voltmeter [40]. An rf voltage at a fixed frequency matched to the resonant frequency of the device is supplied to the input transducer by a signal generator. A vector voltmeter monitors the change in insertion loss and any phase shift between input and output ports. Attenuation is evaluated from the insertion loss while the change in wave velocity is obtained from the phase change. The frequency shift can be calculated from the change in wave velocity.

However, a simpler and more common measurement method involves the indirect determination of acoustic velocities by using the SAW device as the frequency control element of an oscillator circuit. In this case the SAW device is used as an amplifier feedback path. Fractional changes in wave velocity lead to equivalent changes in oscillation frequency. Thus, monitoring the oscillation frequency provides a precise, indirect measurement of acoustic wave velocities. Devices based on these circuits are relatively simple and inexpensive to construct.

There are two major surface acoustic wave device configurations. One is the dual delay line device (illustrated in Figure 1.2) and the other is termed a SAW resonator (illustrated in Figure 1.3). The dual delay line device is made so that the IDTs are placed at opposite ends of the surface. It is called a delay line device because the electrical signal at the input transducer reaches the output transducer 5 orders of magnitude slower as an acoustic wave than it would as an electromagnetic signal [23]. One disadvantage of the dual delay line device is that the surface wave is launched in both directions from the transducer, thus half the wave is lost.

SAW resonators place transducers inside reflector arrays. These reflector arrays reflect the SAW back towards the center of the device from the edges of the crystal to create a standing wave. The standing wave effectively traps the acoustic energy through constructive interference of the reflected waves. Because the acoustic energy is not lost at the ends of the crystal, the resonator (as opposed to the delay line) is considered a high Q device [41,42]. The configuration of the reflector arrays permits only 1 standing wave to exist at a frequency corresponding to the spacing of the transducers. Thus, efficient signal transmission (and oscillation) is restricted to the frequency of the standing wave. This decreases the amount of noise compared to the delay line system. Consequently, the most significant advantage of a resonator device is the improved mass detection limits achieved by increasing the signal/noise ratio. Other factors affecting the sensitivity of these devices will be discussed in Section 1.3.1.

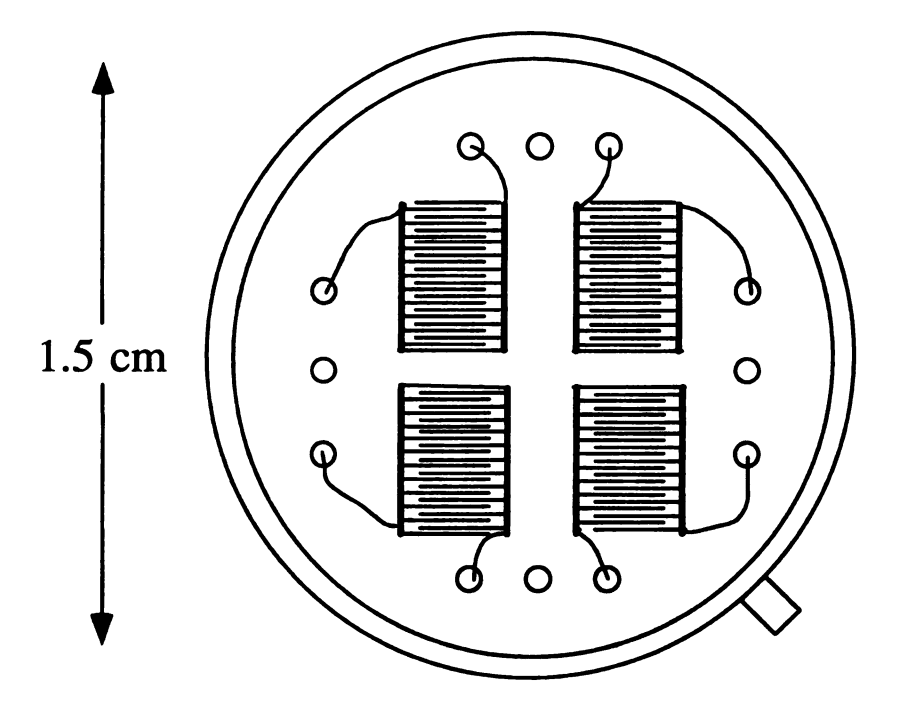


Figure 1.2. The dual delay line SAW device.

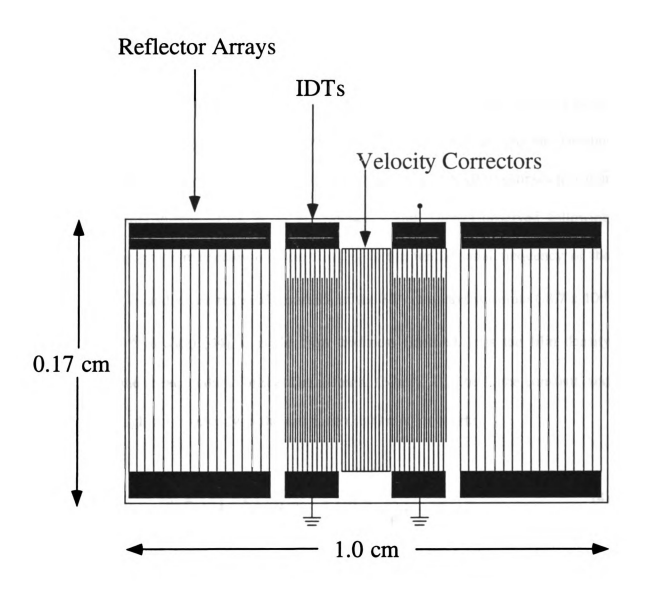


Figure 1.3. The SAW resonator.

1.3 Factors Contributing to SAW Response

1.3.1 Mass Loading

In 1978, Tiersten and Sinha [43] derived an equation relating SAW velocity to the properties of acoustically thin, elastic films. Wohltjen [39] later applied the Tiersten expression as shown in equation (4) to interpret polymer coated SAW responses to vapor sorption. In this interpretation, Δf is the frequency shift (hertz) observed following sorption of gas phase molecules into the film, f_0 is the fundamental frequency of the device (hertz), k_1 and k_2 are material constants of the ST cut quartz substrate (-8.7 x 10⁻⁸ and -3.9 x 10⁻⁸ m²s/kg) [44], h is the film thickness (meters), ρ is the film density (kg/m³), μ is the shear modulus of the film material (N/m²), λ is the Lamé constant, and V_r is the Rayleigh wave velocity in the substrate (3300 m/s for quartz).

$$\Delta f = (k_1 + k_2) f_0^2 h \rho - k_2 f_0^2 h \left(\frac{4\mu}{V_R^2} \left(\frac{1+\mu}{1+2\mu} \right) \right)$$
 (4)

The first term describes the frequency shift due to mass loading and the second term represents the influence of film mechanical properties. If the shear modulus of the coating is small compared to the square of the wave velocity $(4\mu/V_R^2 < 100)$, then the second term is negligible and equation (5) simplifies to an expression resembling the Sauerbrey equation (1):

$$\Delta f = (k_1 + k_2) f_0^2 h \rho \tag{5}$$

This equation assumes that the film is an isotropic, nonconducting, nonpiezoelectric polymer film held above its glass transition temperature with a thickness less than one percent of the acoustic wavelength. Ideally, since $h\rho$ is the mass per unit area, Δf is proportional to the change in surface mass.

Expression (5) clearly shows that the response of the SAW device increases with the square of the operating frequency. This offers exciting opportunities for microsensors, because the operating frequency increases as the spacing between the IDTs decrease. Consequently, smaller devices should be more sensitive. However, this is not strictly true, because as device frequency increases, sensing area decreases. Grate and Klusty [42] have shown that as the sensing area decreases, the thickness of the applied polymer coating must also decrease. Consequently the amount of vapor/unit area that can be collected also decreases. Thus, increasing device frequency is offset by decreased sensing area when considering SAW sensitivities.

The fact that device sensitivity increases with the square of the operating frequency also applies to the QCM. However, the operating frequency of the QCM increases with decreasing crystal thickness. Thus, there is a practical, physical limitation for the QCM because as the device is made thinner, it becomes much more difficult to manipulate. Because the frequency of the SAW device depends on the spacing of the IDTs rather than the crystal thickness, much higher frequencies can be obtained without

sacrificing ruggedness. For this reason, high frequency SAW devices are normally chosen over QCMs for gas phase sensor applications.

1.3.2 Mechanical Properties

Consideration of the mechanical contributions to SAW response is best separated into two cases. The first is the frequency decrease observed when a polymer film is applied to the surface of a bare SAW, and the second is the frequency decrease obtained when a vapor is sorbed by the polymer. These two instances are shown in Figure 1.4.

The inherent sensitivities of acoustic wave devices to the physical properties of viscoelastic thin films were noted in early models for SAW sensors based on perturbation analysis [39,45]. These models predicted that the resonant frequency of a SAW device would be altered by both the mass and the shear modulus when a thin, nonconducting, isotropic film was applied to its surface.

Using Langmuir-Blodgett layers of known mass/area, Grate and Klusty [42] have demonstrated that when a film is applied to a bare crystal, the mass of the coating is the primary source of the frequency decrease. In theory, the modulus effect is only 10-15% of the mass effect if the modulus of the film is 10⁹ N/m² (typical of glass polymers) at a given SAW device operating frequency. Grate and Klusty suggest that if the modulus is 10⁶ N/m², then the modulus contribution to SAW response should be negligible [42,46]. Rubbery polymers typically have a film modulus of 10⁶ N/m², but that value can increase to approximately 10⁹ N/m² at the high frequencies employed by typical SAW devices [47].

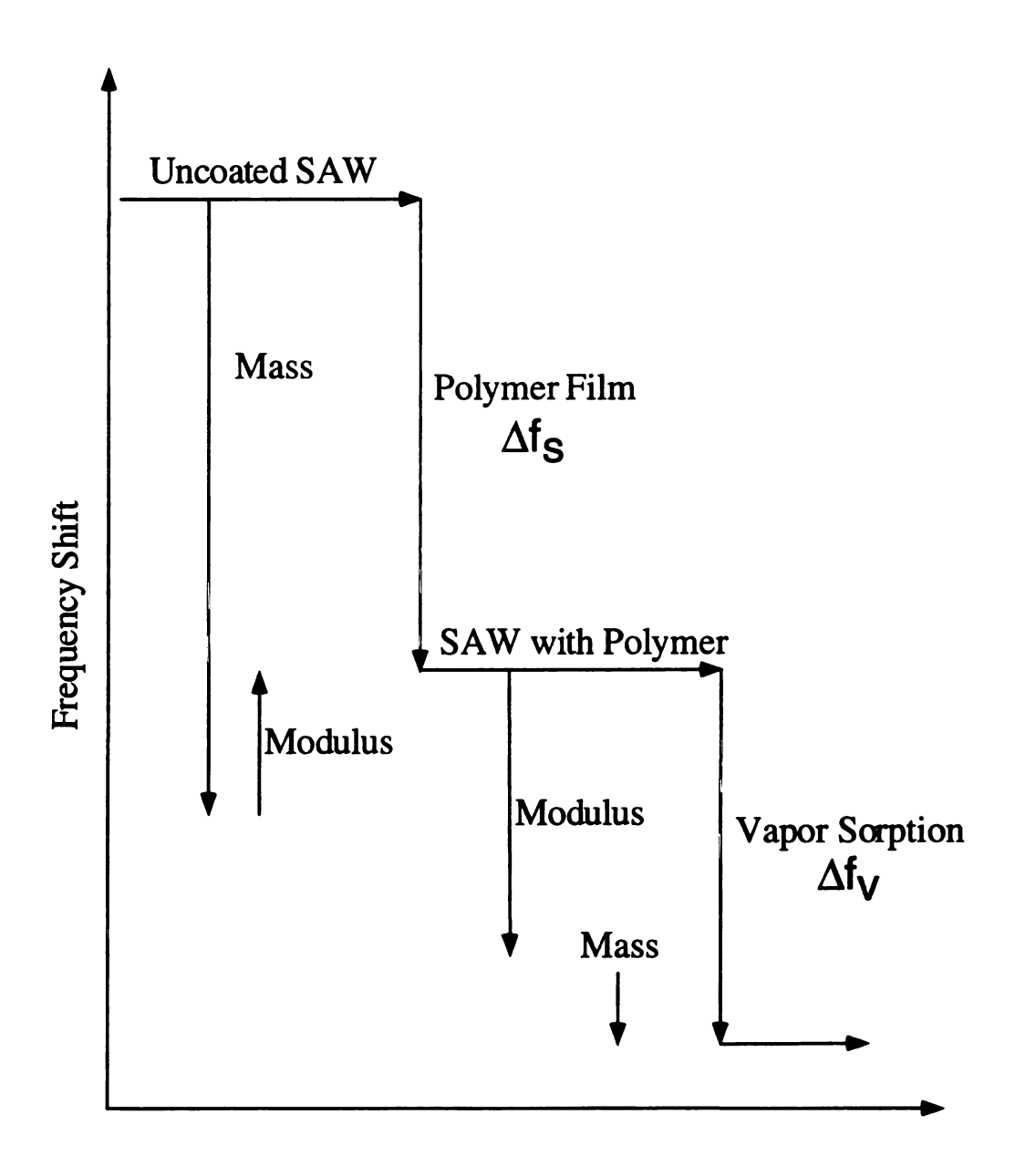


Figure 1.4. An illustration of the contribution of mass and viscoelastic effects to SAW response.

The sorption of vapor into a polymer is known to expand the polymer volume by the free volume of the sorbed molecules [48]. Effectively, vapor sorption acts to dilute the polymer chain segments with increasing volume. Increasing the polymer volume decreases the chain-chain interactions because the polymer chain segments are farther apart and the intermolecular interactions are decreased. Thus, it is reasonable to conclude that vapor sorption changes polymer modulus by increasing the free volume of the polymer.

In the case of vapor sorption on a coated SAW device, it was initially presumed that for a polymer well above its glass transition temperature (T_g), the second term in equation 3 was negligible and that the frequency response was dominated by the mass loading term. However, recent investigations have provided substantial evidence that mechanical effects are not negligible and may, in fact, represent a significant contribution to the frequency response to vapors [46,49].

Martin et al. [50] found that changes in film viscoelastic properties affect SAW response, and proposed that the response could be described by the Maxwell model. In this model, the resistance of the polymer chains moving against each other is represented by the shear viscosity, and the polymer chains reorienting and reorganizing is the shear stiffness. In the case of vapor sorption, the vapor diffuses into the free volume of the polymer, causing the shear viscosity to decrease and a change in the shear stiffness. This changes the elasticity of the polymer, which alters the SAW response.

Grate et al. [46] began to assemble a more complete explanation of the effects of viscoelastic thin films on acoustic wave devices while investigating differences between

partition coefficients determined from GLC measurements (K_{GLC}) and partition coefficients from SAW measurements (K_{SAW}) [51]. These authors reported that K_{SAW} was approximately 4 times larger than K_{GLC} for six analytes sorbed into fluoropolyol, poly(epichlorohydrin), and poly(isobutylene) polymers. In an effort to explain this finding, they proposed that changes in thin film mechanical properties resulting from vapor induced polymer swelling makes a significant contribution to the responses of polymer-coated SAW devices [46]. These researchers assumed that the change in free volume of the polymer caused by vapor sorption would be similar to the change in free volume induced by thermal expansion. This is reasonable because new volume created by polymer thermal expansion above the glass transition temperature is characterized as free volume [52].

Thus, using known thermal expansion rates for polymer films and the experimentally determined effects of thin film expansion on SAW device resonant frequencies, the volume effect was estimated to be 10-20 kHz per percent of volume increase [46]. Volume increases caused by vapor sorption were estimated from test vapor concentrations, K_{GLC} values, and liquid densities of vapors. These estimates suggested polymer swelling of 0.3-3% by certain vapors. Thus, estimated swelling can be multiplied by a volume effect calibration to calculate the frequency decreases that occur in response to vapor induced swelling. It was reported that polymer coated sensor responses can be modeled (equation 6) by summing the response expected from mass loading and the response expected from swelling-induced modulus changes.

$$\Delta f_{v} = \left(\frac{\Delta f_{s} C_{V} K_{GLC}}{\rho_{s}}\right) + \left(\frac{\Delta f_{s} C_{V} K_{GLC}}{\rho_{L}}\right) \left(\frac{A_{SAW}}{\alpha}\right)$$
(6)

All of the terms are as defined before, and C_V is the vapor concentration, ρ_S is the density of the polymer coating when in equilibrium with the sorbed vapor, ρ_L is the density of the vapor in the liquid state, α is the polymer thermal expansion coefficient, and A_{SAW} is the frequency change of a polymer coated SAW due to thermally induced swelling.

Martin et al. [49] have recently interpreted the dynamics and response of polymercoated SAW devices in terms of film viscoelastic properties and film resonance effects.

They have proposed that there are two distinct regimes of SAW response. The first, when
the film is considered to be acoustically thin, and the second, when the film is considered
to be acoustically thick. Using the information presented by Martin et al. [49], values for
polymer modulus caused by either vapor sorption or a temperature change may now be
determined, and the resultant velocity and attenuation changes can be modeled using the
appropriate equations. In this dissertation, all films are calculated to be acoustically thin.

This suggests that changes in wave velocity (frequency) are proportional to changes in the
analyte concentration in the film.

1.4 Coatings for SAW Devices

1.4.1 Introduction

There are several review articles that discuss coatings and the selectivity of piezoelectric chemical sensors [53-56]. Interaction mechanisms for chemically selective

layers have also been reviewed extensively [2,21,24,27,57-63]. Films typically interact with vapor through coordination chemistry, charge transfer, host/guest mechanisms, or solubility interactions.

1.4.2 Coordination Chemistry, ChargeTransfer, Host/Guest Mechanisms

A compromise between selectivity and reversibility can be found in coordination chemistry or charge-transfer complex formation. The potential use of coordination interactions has been discussed by Nieuwenhuizen *et al.* [58,64]. Selectivity in coordination and charge transfer chemistry can also be influenced by the choice of the central metal ion or the ligands from both an electronic and a steric point of view. For example, these interactions have been used to detect NO₂ using metal phthalocyanines [23,65]. Zellers *et al.* [66-68] have reported SAW sensors which respond to select olefins by coordination to Pt complexes. Lewis acid/Lewis base interactions have been utilized in the detection of SO₂ (Lewis acid) using basic amines [21].

In an alternate approach, a chemical reaction between the vapor of interest and the coating leads to selectivity. For example, Snow and Wohltjen have developed an irreversible cyclopentadiene sensor [69]. Zellers *et al.* [70] have demonstrated styrene and vinyl acetate sensors. These sensors are not intrinsically reversible but can be made so by regenerating the device using a reagent [71].

A special case of complexation for potential use in sensors involves cage or inclusion compounds. Dickert has been a pioneer in the application of cage molecules and guest/host interactions for the construction of piezoelectric based chemical sensors

[72-79]. Cyclodextrins [80] and calixarenes [81] will complex hydrophobic compounds of appropriate size within their hydrophobic cavities. The cavity provides a site where solubility interactions occur in a particular steric arrangement. For example, modified cyclodextrins have been applied to QCM devices for the detection of benzene [82].

1.4.3 Solubility

Typically, polymeric materials have been used in organic vapor sensing applications because vapor sorption in rubbery polymers is rapid and reversible; they tend to form adherent thin films, and some selectivity can be achieved by varying the chemical structure of the film [24]. Vapor selectivity is determined only by slight differences in the partition coefficients between the polymer coating and the various vapors. To a great extent, the partition coefficient is influenced by the solubility properties of the coating and the vapor of interest. Grate and Abraham [2] have extensively discussed the importance of solubility for vapor/polymer interactions.

In practice, it is not possible to make a material that will interact via a single solubility property. For example, all organic materials will undergo significant dispersion interactions. Because solubility interactions are not completely selective, the use of sensor arrays with pattern recognition has been investigated as a means of improving selectivity [31,32,83,84].

There has been interest in using chromatographic stationary phases as coatings for SAW devices. McCallum has summarized work involving the interaction of seven analytes with nine chromatographic stationary phases [60]. Several researchers have used

Carbowax phases as coatings for SAW devices [19,21,63,85-88]. Methyl- and phenyl siloxanes have also been examined [89-91].

1.5 Solubility Models and the Interpretation of SAW Response

1.5.1 Partitioning

Traditionally, the partition coefficient (K) is used as a measure of the amount of analyte that sorbs into a film. The similarity between the partitioning of analytes into stationary phases in gas-liquid chromatography and the partitioning between analytes and sensor phases (see Figure 1.5) was recognized early for quartz crystal microbalances [18,92,93] and was more recently applied to the study of SAWs [46,51]. The partition coefficient, K, is defined in equation (7).

$$K = \frac{C_s}{C_v} \tag{7}$$

 C_S represents the amount of analyte in the stationary phase and C_V is the concentration of the analyte in the vapor phase.

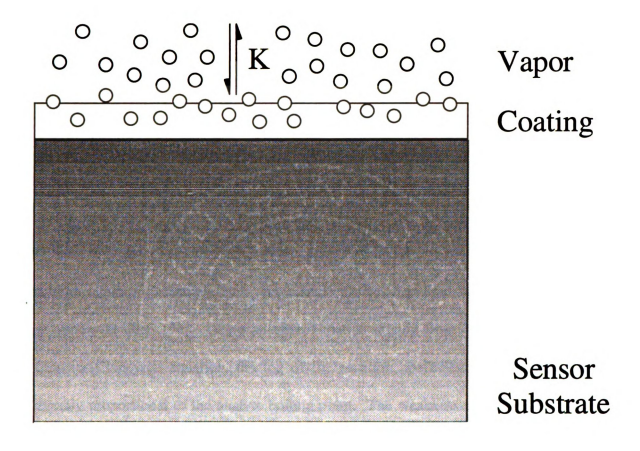


Figure 1.5. The partitioning phenomena between molecules in the vapor phase and the film on the SAW sensor substrate.

1.5.2 Boiling Point Model and Hildebrand Solubility Parameters

The simplest model that attempts to account for the interactions between the vapor and the film is the boiling point model [94]. This model relates the partition coefficient to the analyte saturation vapor pressure as given in equation (8).

$$K = \frac{\rho_1 RT}{\gamma_2 M_1 p_2} \tag{8}$$

K is the partition coefficient, ρ_1 is the density of the stationary phase, M_1 is the molecular weight of the stationary phase, γ_2 is the vapor activity coefficient, and p_2 is the analyte saturation vapor pressure. Expression (8) was first used to describe the retention of vapors in GLC [94]. Using an approximation arising from Trouton's rule and the Clausius-Clapeyron equation, the log of the partition coefficient can be shown to be directly proportional to the analyte boiling point. The weakness of this model is that it fails to account for deviations from ideality.

Deviations from the ideal vapor-polymer solution behavior described above are observed in most real systems. A model using Hildebrand solubility parameters was developed that intended to take into account non-ideal behavior. The regular solution theory developed by Hildebrand assumes that deviations from ideality arise from the nonzero heat of mixing, which can be related to the infinite-dilution activity coefficient and to the solubility parameters of the polymer, δ_1 and solute vapor δ_2 by equation (9), where V_2 is the vapor molar volume.

$$\log \gamma_2^{\infty} = \frac{\Delta H_m}{2.303RT} = \frac{V_2 (\delta_1 - \delta_2)^2}{2.303RT} \tag{9}$$

The solubility parameter of a substance is defined as the square root of the molar vaporization energy per unit volume and, as such, is a measure of cohesive energy (or enthalpy). Since solubility parameter values generally increase with increasing polar constituents in a molecule, solubility parameters are commonly used as indices of overall polarity. In general, the more similar the solubility parameter values of two materials, the lower their heat of mixing and the greater their mutual solubility. The solubility parameter model predicts the following relationship:

$$\log K = \log \left(\frac{\rho_1 RT}{M_1 \rho_2} \right) - \frac{V_2 (\delta_1 - \delta_2)^2}{2.303 RT}$$
 (10)

which indicates that for situations where δ_1 and δ_2 differ appreciably ($\gamma > 1$), the partition coefficient will be reduced relative to the ideal case.

This model fails when specific oriented chemical interactions are the dominant mode of intermolecular interaction. In addition, regular solution theory is most applicable for nonpolar or slightly polar materials. Thus, this model still provides only a limited picture of vapor/film interactions.

1.5.3 Linear Solvation Energy Relationships

Linear solvation energy relationships are a combination of Linear Free Energy Relationships (LFER) [95,96], which attempt to determine the correlation between

structure and reactivity, and Quantitative Structure-Activity Relationships (QSAR), whose premise is that microscopic structural features of a chemical compound can be related to its macroscopic properties [97]. The first application of LFER examined the effect of aromatic substitution on the acidity of a number of benzoic acids [98]. Current applications of LFERs have been reviewed recently [99,100]. In general, QSAR analysis involves a regression equation that correlates selected microscopic features of a set of chemical compounds with a specific property. QSAR is now used predominantly to predict and understand biological, pharmacological, and physical properties [101-105].

Early examples of LSER explained solvent effects on various free energy based properties [106-108]. Two solvation equations (Equations 11 and 12) have been developed [109,110] that have been applied to various processes that involve transfer of a series of solutes from the gas phase to a condensed phase or transfer of a series of solutes from one condensed phase to another.

$$\log SP = c + a \sum \alpha_2^H + b \sum \beta_2^H + l \log L^{16} + rR_2 + s\pi_2^H$$
 (11)

$$\log SP = c + a \sum_{\alpha} \alpha_{2}^{H} + b \sum_{\alpha} \beta_{2}^{H} + v V_{x} + r R_{2} + s \pi_{2}^{H}$$
 (12)

SP is a standard property for a series of solutes in a given phase. For example, SP might be the partition coefficient for a number of solutes on a given stationary phase, or a biological property for a series of solutes. $\Sigma \alpha_2^H$, $\Sigma \beta_2^H$, $\log L^{16}$, R_2 , π_2^H , and V_x are called molecular descriptors, and are combined with the standard property in a multiple

linear regression to determine the constants. These constants can be used to characterize the solvent phase.

 $\sum \alpha_2^H$ and $\sum \beta_2^H$ are measures of the solute hydrogen-bond acidity and basicity, and thus the constant a would be a measure of the solvent hydrogen bond basicity and the constant b would be a measure of the solvent hydrogen bond acidity. The values for these descriptors are obtained from hydrogen-bond complexation constants of acids by reference bases (such a pyridine) in a reference solvent (such as carbon tetrachloride) or complexation of bases by reference acids (such as 4-fluorophenol) in carbon tetrachloride [111,112], and more recently from chromatographic or partition measurements [113].

logL¹⁶ is a descriptor derived from the solute gas-liquid partition coefficient on hexadecane at 298K [114]. They have been obtained by gas chromatography and several hundred values are now available [111-114]. V_x is McGowan characteristic volume and can be calculated for any solute based on its chemical structure [115]. Both of these descriptors are considered to be a measure of dispersion interactions, and represent the energy of the endoergic creation of a cavity within the solvent, the incorporation of the solute in the solvent, and the reorganization of the solvent around the solute and the associated interactions.

 R_2 is an excess molar refraction term that is determined using the refractive index of a compound, i.e., the molar refraction in excess of the molar refraction (MR) of an alkane of the same characteristic volume (V_x) [116].

 $R_s = MR_x - MR_x$ for an alkane of the same V_x

By subtracting the molar refraction for an alkane of the same characteristic volume, the dispersive component of molar refraction (already accounted for by $\log L^{16}$) is removed. This descriptor represents the tendency of a solute to interact through π or n electrons, and thus r is a measure of a solvents' ability to stabilize π or n electron interactions.

 π_2^H is a measure of the compounds dipolarity/polarizability. It is obtained experimentally from gas-liquid chromatographic measurements [109,110]. This parameter is important with regard to the dipole/dipole and dipole/induced-dipole interactions. For non-protonic, aliphatic solutes with a single dominant dipole, π_2^H values are approximately proportional to molecular dipole moments.

1.5.4 Application of LSERs to SAW Response

Grate and Abraham proposed [2,46] using K_{SAW} in combination with Linear Solvation Energy Relationships to help elucidate the chemical interactions occurring between a vapor and a film. This expression is given in equation (14).

$$\log K_{SAW} = c + a \sum_{h} \alpha_{2}^{H} + b \sum_{h} \beta_{2}^{H} + llogL^{16} + rR_{2} + s\pi_{2}^{H}$$
 (14)

They also discussed the prediction of SAW responses through LSER expressions that were obtained based on GLC data. It was hypothesized that a films' performance as a GLC phase should be an accurate predictor of the film as a SAW coating. They detailed this approach for SAW devices and also suggested possible coatings that might interact through specific terms.

It is important to realize that models based on solubility and partitioning are simply logical places to start when attempting to understand vapor/film interactions. All of these models calculate partition coefficients assuming SAW device response to be strictly mass loading. Grate *et al.* [46] have shown that vapor induced changes in film properties are important. However, this was accomplished using only 6 analytes and 3 films. Thus, the effect of vapor induced changes in film mechanical properties for individual analytes is not well defined.

However, Patrash and Zellers [117] have recently examined OV-275 (poly[bis(cyanoallyl)-siloxane]), OV-25 ([25% methyl] poly(methylphenylsiloxane)), poly(isobutylene), and poly(phenyl ether) as SAW coatings and exposed each to 37 analytes and then determined the LSER coefficients for the films. They found that interaction predictions from GLC data were reasonable approximations for the SAW device.

1.6 References

- 1. Ballantine, D. S., Jr.; Wohltjen, H. Anal. Chem. 1989, 61, 704A.
- 2. Grate, J. W.; Abraham, M. H. Sens. & Act. B. 1991, 3, 85.
- 3. Suleiman, A; Guilbault, G. G. Anal. Chim. Acta 1984, 162, 97.
- 4. Thompson, M.; Stone, D. C. Anal. Chem. 1990, 62, 1895.
- 5. Hecki, W. M.; Marassi, F. M.; Kallury, K. M. R.; Stone, D. C.; Thompson, M. *Anal. Chem.* **1990**, *62*, 32.
- 6. Thompson, M.; Stone, D. C.; Nisman, R. Anal. Chim. Acta 1991, 248, 143.
- 7. Yan, Y.; Bein, T. J. Phys. Chem. 1992, 96, 9387.
- 8. Janghorbani, M.; Freund, H. Anal. Chem. 1973, 45, 325.
- 9. Edmonds, T. E.; West, T. S. Anal. Chim. Acta 1980, 117, 147.
- 10. Grate, J. W.; Rose-Pehrsson, S. L.; Venezky, D. L.; Klusty, M.; Wohltjen, H. *Anal. Chem.* 1993, 65, 1868.
- 11. Curie, J.; Curie, P. Bull. Soc. Min. Paris 1880, 3, 90.
- 12. Sauerbrey, G. Z. Phys. 1959, 155, 206.
- 13. Mueller, R. M.; White, W. Rev. Sci. Instum. 1968, 39, 291.
- 14. Mueller, R. M.; White, W. Rev. Sci. Instum. 1969, 40, 1646.
- 15. Stockbridge, C. D. in *Vacuum Microbalance Techniques, Vol. 5*; Behrndt, K. H. Ed.; Plenum Press: New York, NY, **1966**, 135.
- 16. Kanazawa, K. K.; Gordon, J. G. Anal. Chim. Acta 1985, 175, 99.
- 17. Kanazawa, K. K.; Gordon, J. G. Anal. Chem. 1985, 57, 1770.
- 18. Janghorbani, M.; Freund, H. Anal. Chem. 1973, 45, 325.
- 19. Edmonds, T. E.; West, T. S. Anal. Chim. Acta 1980, 117, 147.
- 20. Martin, S. J.; Frye, G. C. *Proc. 1991 IEEE Ultrason. Symp.* **1991**, 393.
- 21. Hiavay, J.; Guilbault, G. G. Anal. Chem. 1977, 49, 1890.
- 22. Guilbault, G. G.; Jordan, J. M. CRC Crit. Rev. Anal. Chem. 1988, 19, 1.
- 23. Grate, J. W.; Martin, S. J.; White, R. M. Anal. Chem. 1993, 65, 940A.
- 24. Grate, J. W.; Martin, S. J.; White, R. M. Anal. Chem. 1993, 65, 987A.
- 25. Alder, J. F.; McCallum, J. J. Analyst 1983, 108, 1169.

- 26. Munoz Leyva, J. A.; Hidalgo De Cisneros, J. L.; Garcia Gomez DE Barreda, D.; Beerra, Fraidias, A. J. *Talanta* 1994, 41, 159.
- 27. Ward, M. D.; Buttry, D. A. Science 1990, 249, 1000.
- 28. Dickert, F. L.; Bauer, P.A. Adv. Mater. 1991, 3, 436.
- 29. Dickert, F.L.; Schuster, O. Adv. Mater. 1993, 5, 826.
- 30. Dickert, F. L.; Haunschild, A. Adv. Mater. 1993, 5, 887.
- 31. Carey, W. P.; Kowalski, B. R. Anal. Chem. 1986, 58, 3077.
- 32. Carey, W. P.; Beebe, K. R.; Kowalski, B. R. Anal. Chem. 1987, 59, 1529.
- 33. Lord Rayleigh London Math. Soc. Proc. 1887, 17, 14.
- 34. Wohltjen, H. U.S. Patent 4,312,228, Jan. 26, 1982.
- 35. White, R. M.; Voltmer, F. W. Appl. Phys. Lett. 1965, 7, 314.
- 36. Wohltien, H.; Dessy, R. Anal. Chem. 1979, 51, 1458.
- 37. Wohltjen, H.; Dessy, R. Anal. Chem. 1979, 51, 1465.
- 38. Wohltjen, H.; Dessy, R. Anal. Chem. 1979, 51, 1470.
- 39. Wohltjen, H. Sens. Actuators 1984, 5, 307.
- 40. Frye, G. C.; Martin, S. J. Appl. Spectrosc. Rev. 1991, 26, 73.
- 41. Bowers, W. D.; Chuan, R. L.; Duong, T. M. Rev. Sci. Instrum. 1991, 62, 1624.
- 42. Grate, J. W; Klusty, M. Anal. Chem. 1991, 63, 1719.
- 43. Tiersten, H. F.; Sinha, B. K. J. Appl. Phys. 1978, 49, 87.
- 44. Ballantine, D. S., Jr. Anal. Chem. 1992, 64(24), 3069.
- 45. Tiersten, H. F.; Sinha, B. K. J. Appl. Phys. 1978, 49, 87.
- 46. Grate, J. W.; Klusty, M.; McGill, R. A.; Abraham, M. H.; Whiting, G.; Andonian-Haftvan, J. Anal. Chem. 1992, 64, 610.
- 47. Ferry, J. D. Viscoelastic Properties of Polymers, 3rd ed.; John Wiley and Sons: New York, 1980.
- 48. Rogers, C. E. in Polymer Permeability; Comyn, J., Ed.; Elsevier: New York, 1985; p 11-73.
- 49. Martin, S. J.; Frye, G. C.; Senturia, S. D. Anal. Chem. 1994, 66, 2201.
- 50. Martin, S. J.; Ricco, A. J.; Frye, G. C. 1990 Solid State Sensor & Actuator Workshop, ACS Spring Meeting, San Francisco.

- 51. Grate, J. W.; Snow; A.; Ballantine; D. S., Jr.; Wohltjen, H.; Abraham, M. H.; McGill, R. A.; Sasson, P. *Anal. Chem.* **1988**, *60*, 869.
- 52. Roe, R.-J. Encyclopedia of Polymer Science and Engineering, 2nd ed.; John Wiley and Sons, Inc.: New York, 1987; Vol. 7, 531-544.
- 53. Janata, J. Anal. Chem. 1992, 64, 196R.
- 54. Janata, J.; Josowicz, M.; De Vaney, D. M. Anal. Chem. 1994, 66, 207R.
- 55. Bastians, G. J. in T. E. Edmonds (Ed.), *Chemical Sensors*, Blackie: London, 1988, Chp. 14, p. 295.
- 56. Janata, J., Principles of Chemical Sensors, Plenum: New York, 1989.
- 57. Mierzwinski, A.; Witkiewicz, Z. Environ. Pollut. 1989, 57, 181.
- 58. Nieuwenhuizen, M. S.; Venema, A. Sens. Mater. 1989, 5, 261.
- 59. D'Aminco, A.; Verona, E. Sens. Actuators 1989, 17, 55.
- 60. McCallum, J. J. Analyst(London) 1989, 114, 1173.
- 61. Fox, C. G.; Alder, J. F. Analyst (London) 1989, 114, 997.
- 62. Katritzky, A. R.; Offerman, R. J. CRC Anal. Chem. 1989, 21(2), 83.
- 63. Alder, J. F.; McCallum, J. J. Analyst (London) 1983, 108, 1169.
- 64. Nieuwenhuizen, M. S.; Barendsz, A. W. Sens. Actuators 1987, 11, 45.
- 65. Snow, A. W.; Barger, W. R. in A. B. P. Lever and C. C. Leznoff (Eds.), *Phthalocyanines Properties and Applications*, VCH Publishers: New York, 1989, Chp. 5, pp. 341.
- 66. Zellers, E. T. In Chemical Sensors and Microinstrumentation; Murray, R. W., Ed.; ACS Symposium Series 403; American Chemical Society: Washington, DC, 1989; pp.176-190.
- 67. Zellers, E. T.; Hassold, N. C.; White, R. M.; Rappaport, S. M. *Anal. Chem.* 1990, 62, 1227.
- 68. Zellers, E. T.; Zhang, G.-Z. Anal. Chem. 1992, 64, 1277.
- 69. Snow, A. W.; Wohltjen, H. Anal. Chem. 1984, 56, 1411.
- 70. Zellers, T. E.; White, R. M.; Rappoport, S. M.; Wenzel, S. W. Transducers'87, 459.
- 71. Zhang, G.-Z.; Zellers, E. T. Anal. Chem. 1993, 65, 1340.
- 72. Dickert, F. L.; Bauer, P.A. Adv. Mater. 1991, 3, 436.

- 73. Dickert, F. L.; Haunschild, A.; Hofmann, P.; Mages, G. Sens. Actuators B 1992, 6, 25.
- 74. Dickert, F. L.; Baumler, U. P. A.; Zwissler, G. K. Synth. Met. 1993, 61, 47.
- 75. Dickert, F. L.; Bruckdorfer, Th.; Feigl, H.; Haunschild, A.; Kuschow, V.; Oberveier, E.; Bulst, W.-E.; Knauer, U.; Mages, G. Sens. Actuators B. 1993, 13-14, 297.
- 76. Dickert, F. L.; Haunschild, A. Adv. Mater. 1993, 5, 887.
- 77. Dickert, F. L.; Haunschild, A.; Maune, V. Sens. Actuators B 1993, 12, 169.
- 78. Shurig, V.; Novotny, H. P.; Schmalzing, D. Angew. Chem. Int. Ed. Engl. 1989, 28, 736.
- 79. Dickert, F.L.; Schuster, O. Adv. Mater. 1993, 5, 826.
- 80. Stoddart, R.; Zarycki, R. Cyclodextrins, Royal Society of Chemistry: London, 1989.
- 81. Gutsche, C. D. Calixarenes, Royal Society of Chemistry: London, 1989.
- 82. Lai, C. S.-I., Moody, G. J.; Thomas, J. D. R.; Mulligan, D. C.; Stoddart, J. F.; Zarzycki, R. J. Chem. Soc., Perkin Trans. 2 1988, 319.
- 83. Ballantine, D. S.; Rose, S. L.; Grate, J. W.; Wohltjen, H. Anal. Chem. 1986, 58, 3058.
- 84. Ema, K.; Yokoyama, M.; Nakamoto, T.; Moriizumi, T. Sens. Actuators 1989, 18, 291.
- 85. Ho, M. H.; Guilbault, G. G. Reitz, B. Anal. Chem. 1983, 55, 1830.
- 86. Ho, M. H.; Guilbault, G. G.; Reitz, B. Anal. Chem. 1980, 52, 1489.
- 87. Lopez-Roman, A.; Guilbault, G. G. Anal. Lett. 1972, 15, 225.
- 88. Tomita, Y.; Ho, M. H.; Guilbault, G. G. Anal. Chem. 1979, 51, 1475.
- 89. Brady, J. E.; Bjorkman, D.; Herter, C. D.; Carr, P. W. Anal. Chem. 1984, 56, 278.
- 90. Lucklum, R.; Henning, B.; Hauptmann, P.; Schierbaum, K. D.; Vaihinger, S.; Göpel, W Sens. Actuators A 1991, 25-27, 705.
- 91. Schierbaum, K. D.; Gerlach, A.; Haug, M.; Göpel, W. Sens. Actuators A 1992, 31, 130.
- 92. King Jr., W. H. Anal. Chem. 1964, 36, 1735.
- 93. Karasek, F. W.; Guy, P.; Hill Jr., H. H.; Tiernay, J. M. *J. Chromatogr.* **1976**, 124, 179-186.

- 94. Littlewood, A. B. Gas Chromatography, Academic Press: New York, 1970; 44.
- 95. Burkhardt, G. N. Nature (London) 1935, 17, 125.
- 96. Hammett, L. P. Chem. Rev. 1935, 17, 125.
- 97. Chemial Applications of Atomic and Molecular Electrostatic Potentials; Politzer, P., Truhlar, D. G., Eds.; Plenum: New York, 1981.
- 98. Hammett, L. P. J. Am. Chem. Soc. 1937, 59, 96.
- 99. Exner, O. Correlation Analysis of Chemical Data; Shorter, J., Ed.; Plenum: New York, 1988.
- 100. Exner, O. Prog. Phys. Org. Chem. 1990, 18, 129.
- 101. Weinstein, H.; Osman, R. Green, J. P.; Topiol, S. in *Chemial Applications of Atomic and Molecular Electrostatic Potentials*; Politzer, P., Truhlar, D. G., Eds.; Plenum: New York, 1981, 309.
- 102. Hansch, C.; Fujita, T. H. J. Am. Chem. Soc. 1964, 86, 1616.
- 103. Hall, L. H.; Kier, L. B. Rev. Comput. Chem. 1991, 2, 367.
- 104. Bersuker, I. B.; Dimoglo, A. S. Rev. Comput. Chem. 1991, 2, 423.
- 105. Hansch, C. Acc. Chem. Res. 1993, 26, 147.
- 106. Abboud, J.-L. M.; Kamlet, M. J.; Taft, R. W. J. Am. Chem. Soc. 1977, 99, 8325.
- 107. Kamlet, M. J.; Taft, R. W. Prog. Org. Chem. 1983, 48, 2877.
- 108. Kamlet, M. J.; Abraham, M. H.; Doherty, R. M.; Taft, R. W. J. Am. Chem. Soc. 1984, 106, 464.
- 109. Abraham, M. H.; Whiting, G. S.; Doherty, R. M.; Shuely, W. J. J. Chromatogr. 1991, 587, 213.
- 110. Abraham, M. H.; Whiting, G. S. J. Chromatogr. 1992, 594, 229.
- Abraham, M. H.; Grellier, P. L.; Prior, D. V.; Duce, P. P.; Morris, J. J.; Taylor, P. J. J. Chem. Soc. Perkin. Trans. 2 1989, 699.
- 112. Abraham, M. H.; Grellier, P. L.; Prior, D. V.; Morris, J. J.; Taylor, P. J. *J. Chem. Soc. Perkin. Trans.* 2 1990, 521.
- 113. Abraham, M. H. Chem. Soc. Rev. 1993, 22, 73.
- 114. Abraham, M. H.; Grellier, P. L.; McGill, R. A. J. Chem. Soc. Perkin Trans. 2 1987, 797.
- 115. Abraham, M. H.; McGowan, J. C. Chromatographia 1987, 23, 243.

- 116. Abraham, M. H.; Whiting, G. S.; Doherty, R. M.; Shuely, W. J. J. Chem. Soc. Perkin. 2 1990, 1451.
- 117. Patrash, S. J.; Zellers, E. T. Anal. Chem. 1993, 65, 2055.

Chapter 2

Effect of Silanization and Operating Temperature on the Response of
Uncoated and Poly(isobutylene) Coated Surface Acoustic Wave (SAW)
Sensors

2.1 Abstract

The effects of silanization and operating temperature (30 and 60°C) on the response of uncoated and poly(isobutylene) coated surface acoustic wave (SAW) devices to alkanes, alcohols, and water have been investigated using pulsed sample introduction. Silanization of the SAW surface with dichlorodimethylsilane "deactivates" the surface primarily through a decrease in the active surface area of the device. Silanization also appears to increase the surface area of the poly(isobutylene) coating and decrease the contribution of vapor induced changes in thin film mechanical properties to sensor response. Increasing the operating temperature of an uncoated or poly(isobutylene) coated, unmodified SAW device decreases the response to alkanes and alcohols, but increases the response to water. The increase in water response has been ascribed to an increase in the number of silanol and silylether groups that are available for adsorption on the quartz surface held at 60°C. At 30°C, these sites are partially occupied by trace water adsorbed from the carrier gas. For the uncoated, silanized SAW device, the response to all analytes except 1-butanol decreases with increasing temperature. The increase in 1-

butanol response has been attributed to adsorption at additional silylether and tracesilanol sites available on the higher temperature surface. Increasing the operating temperature decreases the magnitude of the response of the poly(isobutylene) coated, silanized SAW devices to all analytes examined.

2.2 Introduction

Considerable effort has been devoted to the development of vapor sensors based on surface acoustic wave (SAW) devices [1-17]. Most sensors utilize the sorption properties of a thin film coating of polymeric material to improve the analytical capabilities of the device. The importance of sorption phenomena has led to the application of linear solvation energy relationships (LSERs) to describe analyte/film interaction mechanisms at a molecular level [18-20] and to predict suitable coatings for detection of specific analytes [18,21]. In addition to these chemical aspects, construction of a practical sensor device requires consideration of thin film physical properties such as adhesion and thermal stability. These properties are influenced in part by polymer/device surface interactions. Consequently, a number of investigators have examined the effect of surface modification and operating temperature on sensor response.

Several studies have shown that pretreatment of the SAW device surface (usually SiO₂) improves the uniformity, stability, and performance of sensor coatings. Grate *et al.* [22] reported that higher quality films could be prepared on devices cleaned using a nitrogen plasma versus solvent rinsing. Ballantine [23] used silanized devices to study the influence of poly(isobutylene) film morphology on the sensor response to isooctane.

McGill et al. [24] modified SAW surfaces with diphenyltetramethyldisilazane in order to maintain poly(isobutylene) adhesion and minimize the impact of interfacial adsorption on sensor responses to water. Dickert et al. [25] have suggested that long-chain hydrocarbon substituents of organosilyl compounds form assembled films that can include n-decyl tethers attached to cyclodextrins. These authors attributed a decrease in response time for the modified device to alignment of the included cyclodextrin cavities.

The operating temperature of the device affects the physical properties of the film as well as the sensitivity and selectivity of the sensor. Grate *et al.* [22] showed that thermal expansion of the polymer film decreases the device frequency. They proposed that similar sorbent induced swelling phenomena led to larger sensor responses than would be expected from only mass loading. Martin *et al.* [16] have recently presented an extensive treatise on the effect of film thickness and operating temperature on the properties of poly(isobutylene) coated devices. It is also well known that increasing temperature decreases the magnitude of the sensor response [9,22,26,27]. For example, Grate *et al.* [9] have shown that the response of a fluoropolyol-coated sensor to dimethyl methylphosphonate (DMMP) decreases exponentially with increasing temperature. These authors also reported that increasing temperature decreases the selectivity of the sensor.

Previous studies have shown that surface modification (silanization) and operating temperature can significantly affect the response of SAW devices. However, earlier work focused primarily on detailed studies of the equilibrium response for a limited number of analytes. The present study is part of a larger effort devoted to the development of

practical sensor systems based on pulsed sample introduction. The importance of pulsed sample introduction in chemical sensing has been discussed extensively [18,20,28-36]. In this study, the influence of silanization and operating temperature on the response of uncoated and poly(isobutylene) coated SAW devices to pulses of alkanes, alcohols, and water is reported.

2.3 Experimental

Chemicals. Poly(isobutylene) (abbreviated PIB) was obtained from Aldrich chemical company (MW = 380,000). The alkanes and alcohols were obtained from Aldrich chemical company and used as received. Water was distilled and deionized prior to use.

SAW System. A schematic diagram of the sensor test apparatus is shown in Figure 2.1. The approximate volume of the test cell is 8 mL. Analytes were delivered to the cell as a pulse using a gas chromatograph injector operated at 240°C. The flow rate was 20 mL/min flow of N_2 (99.95%, AGA Gas Co.) dried over molecular sieves. The temperature of the cell was controlled by resistance heating of nichrome wire wrapped around the transfer line. The estimated water content of the carrier stream is < 5 ppm [37].

SAW data were obtained using 158 MHz dual delay line devices manufactured by Microsensor Systems, Inc. (Bowling Green, KY). The SAW device is permanently mounted on a conventional 12 pin gold TO-8 header which has bonded gold wire connections. The device exhibits a resonant frequency shift of approximately 365 Hz

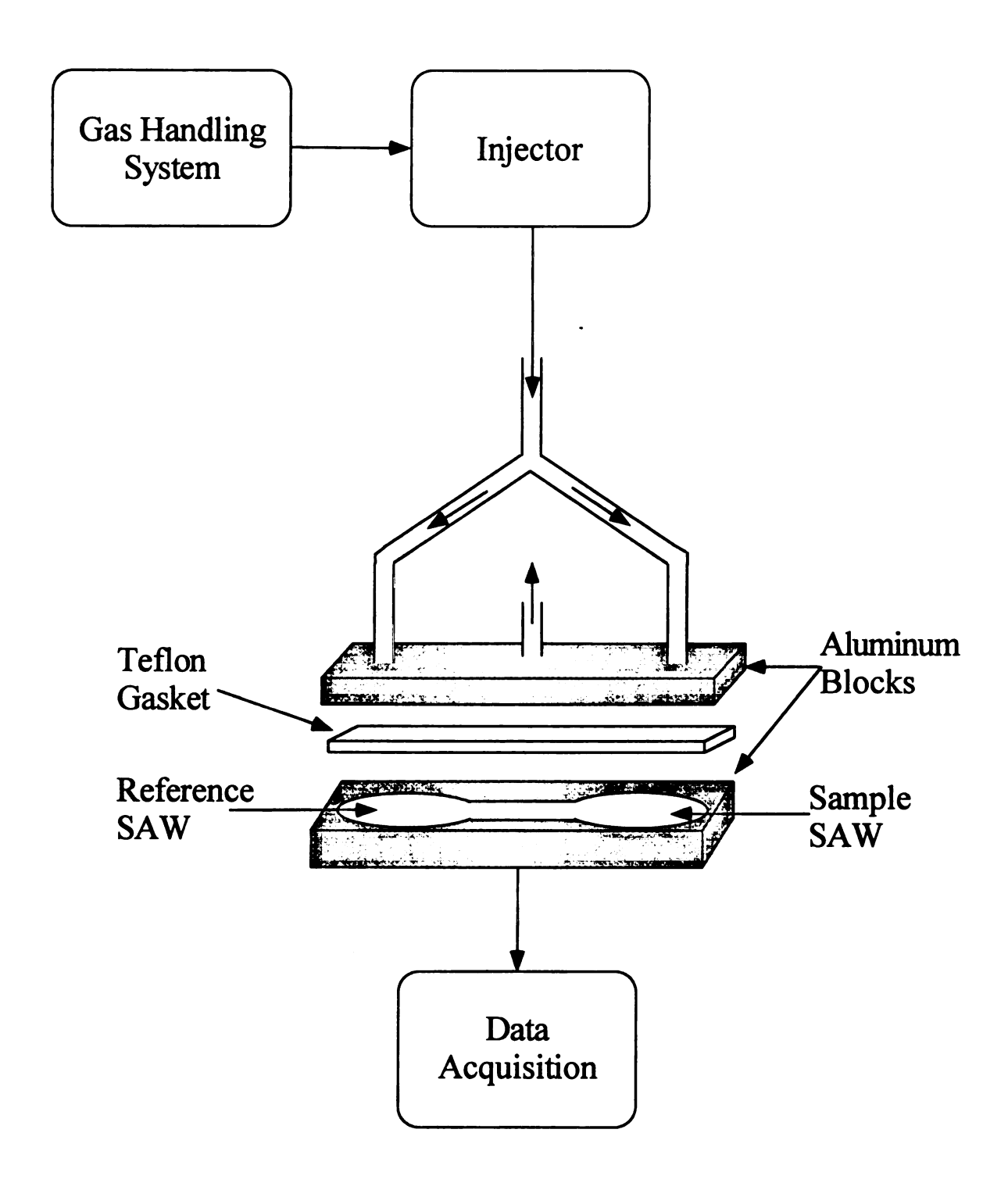


Figure 2.1. Schematic diagram of sensor test apparatus.

when perturbed by a surface mass change of 1 nanogram. An RF electronics module (CEM-158, Microsensor Systems, Inc.) is used to power the sample and reference devices. The output of the electronics module consists of the individual SAW oscillator frequencies as well as the difference frequency between the sample and reference devices.

Software developed in-house is used to convert data from the Microsensor Systems format to one compatible with Microsoft Excel (Microsoft Corporation, Redmond, Washington). The responses reported in this work are the difference frequencies between sample and reference devices contained in the sensor test cell. Both delay lines of the sample device were silanized and/or coated with the polymer. The reference device was a clean, uncoated device that was sealed using a metal lid and epoxy resin (Torr Seal, Varian Vacuum Corporation).

Two methods were used to clean the SAW devices prior to silanization or coating. In the first procedure, the device was rinsed with acetone and methanol, soaked in isopropanol, and then allowed to air dry. The second method involved the same solution and drying steps, followed by a 30 minute treatment in an ozone cleaner (UV Ozone Photoreactor PR-100; UVP, Inc., New Jersey). SAW devices that were either rinsed or rinsed and treated with ozone are designated "unmodified". Both types of unmodified devices showed similar sensor responses. The surface of the quartz was silanized by exposing the device to a 10% solution of dichlorodimethylsilane in toluene for 5 minutes followed by methanol rinsing, isopropanol soaking, and air drying. PIB films are prepared by spray casting from dilute toluene or chloroform solutions (~1000 ppm). Approximately 85 kHz (200 ng, 0.027 µm) films were used in this study.

Operating Procedures. A typical experiment involved 30 seconds of baseline data collection followed by three to six injections of analyte. Injections were separated by a length of time necessary for the frequency to return to baseline. Analytes were injected in random order to minimize any possible effects of exposure history on response data. In addition, some data were collected at 60°C followed by 30°C, while other data sets were collected in the reverse order. Injection volumes were varied from 5 μL for analytes with low boiling points to 0.05 μL for high boiling point samples to produce frequency shifts less than 25 kHz. Sensor responses are reported as the maximum frequency shift in hertz per microgram (or nanomole) of analyte injected to account for differences in the analyte injection volume. For the blanks and each film, data were collected on at least three devices at both temperatures. The device to device SAW response values have typical RSDs of 15%.

2.4 Results and Discussion

Effect of Silanization on Device Response. Uncoated. Table 2.1 shows the responses of the unmodified and silanized devices to alkanes, alcohols, and water at 30° C. Within an analyte class, the responses measured for both types of uncoated SAW devices increase with increasing analyte boiling point. This suggests that the response is strongly affected by analyte physisorption (condensation). Dickert and Haunschild [38] have also shown an increase in sensor response with increasing alkane boiling point

Table 2.1. Analytes and their responses at 30° C ($\pm 15\%$).

			Uncoated	ated			PIB C	PIB Coated	
	Boiling	Unm	Unmodified	Sil	Silanized	Unm	Unmodified	Sil	Silanized
Analyte	Point (°C)	Hz/µgram	Hz/nanomole	Hz/µgram	Hz/nanomole	Hz/µgram	Hz/nanomole	Hz/µgram	Hz/nanomole
hexane	69	20.3	1.75	4.56	0.39	59.4	5.12	65.4	5.64
heptane	86	65.5	6.56	27.7	2.77	223	22.3	221	22.1
octane	126	285	32.6	65.2	7.45	818	93.4	728	83.1
nonane	151	693	88.9	178	22.8	3670	471	2260	290
					-				
methanol	99	5.95	0.19	5.69	0.18	7.34	0.24	15.8	0.51
isopropanol	82	16.8	1.01	6.49	0.39	44.7	2.68	159	9.57
1-butanol	117	108	8.04	28.1	2.08	1290	92.6	2170	161
Water	100	14.5	0.26	7.05	0.13	15.6	0.28	19.5	0.35

(pentane, hexane, and heptane) using a silanized 430 MHz SAW resonator. King [26] reported that higher boiling analytes are able to achieve a larger level of partitioning into a coated sensor device. Patrash and Zellers [19] also reported that an increase in analyte boiling point increases partition coefficients calculated using SAW responses in continuous flow experiments. While it is not possible for partitioning to occur for uncoated devices, it is expected that analyte condensation would produce similar results.

Silanization decreases the magnitude of the responses obtained with the uncoated device. These findings can be explained in terms of the effect of silanization on the physical and chemical properties of the SAW device surface. We believe that silanization lowers the active surface area of the SAW device. Since the response of the uncoated device is strongly influenced by condensation, a decrease in surface area should decrease the response observed with the silanized sensor. Silanization is also known to reduce the surface area of chromatographic supports [39]. It should be noted that dichlorosilanes can polymerize over the quartz surface, thus similar experiments with monochlorosilanization reagents may not yield the same results.

Silanization is also known to deactivate silica surfaces by replacing the active proton on the silanol functionality with a less active, silyl derivative [40,41]. This change in chemical functionality is expected to decrease the sensor response to analytes that can hydrogen bond to the device surface (e.g., alcohols and water). McGill et al. [24] attributed a decrease in interfacial water adsorption on phenyl silane modified SAW devices to a decrease in the number of silanol groups present on the silanized surface. Silanization should improve the chemical affinity of the device for alkanes. However, the

pronounced decrease in alkane response observed following silanization suggests that the decrease in active surface area influences the sensor response more than the change in chemical properties of the SAW surface.

It should also be noted that silanization of the device does not appear to preferentially decrease the responses to alcohols or water compared to the alkanes. Thus, for the short vapor exposure times typical of pulsed sample injection, changes in chemical affinity of the device surface may have less impact on the response magnitude than the decrease in active surface area.

Poly(isobutylene) Coated Silanized. Table 2.1 also shows the responses obtained for the PIB coated unmodified and PIB coated silanized SAW devices operated at 30°C. As anticipated, the responses observed for the PIB coated devices are greater than those obtained with either the unmodified or silanized device.

Alkanes are expected to interact strongly with the PIB film through dispersion forces [18-20,42]. Our results indicate that silanization has little effect on the responses to hexane, heptane, and octane; however, the nonane response is smaller on the PIB coated silanized device. The difference in nonane response observed for the two PIB coated devices can be understood in terms of mechanical phenomena that have been reported for PIB coated SAW devices [16,22,23]. Ballantine [23] reported that the contribution of mechanical effects depends on the coating thickness and the amount of analyte sorbed in the film. We believe that the combination of condensation and sorption during our pulsed sample introduction produces sufficient nonane concentration in the film to cause such effects. However, our results indicate that the magnitude of these

effects are lower on the PIB coated silanized device. It has been suggested that silanization of the SAW device surface before coating enhances the wetting and adhesion of polymer films [23,24]. In addition, Dickert and Haunschild [38] have noted that hydrophobic coatings do not adhere well to quartz surfaces. We propose that the increased adhesion of the PIB film to the silanized surface decreases the mechanical perturbation of the film produced by vapor sorption. This decreases the magnitude of moduli changes for the PIB coated silanized device and results in a lower response to nonane. Similar phenomena may occur for alkanes with lower boiling points; however, the analyte concentration in the film resulting from our pulse injection may be too low to observe any significant effects.

Silanization increases the response of the PIB coated device to alcohols. We ascribe these findings to an increase in PIB surface area resulting from improved wetting and adhesion of the polymer to the surface of the silanized device. Since alcohols are not expected to interact with PIB as strongly as alkanes [18-20], the increased surface area may have a more significant effect on alcohol sorption. Alcohols are also known to self-associate in hydrophobic solvents [43,44]. Thus, increased sorption and self-association both contribute to the enhanced alcohol response observed with the PIB coated silanized device.

The predominant role of dispersion forces in the interaction of analytes with PIB suggests that the PIB coated devices should not show a strong response to water. Indeed, with the exception of methanol, water gives the lowest response of the analytes. McGill et al. [24] have reported that PIB coated SAW devices exposed to concentrated water

vapor streams ([H₂O] > 6194 mg/m³) exhibit fast mass loading responses (decrease in frequency) followed by slowly developing anomalous responses (increase in frequency). For lower concentration water streams, only anomalous responses were observed. These researchers also reported that silanization eliminated the anomalous response and resulted in the low water vapor responses expected for a PIB coated device. We have not observed anomalous responses for any of the analytes. Apparently, the short analyte/surface contact time in a pulsed experiment precludes observation of these slowly developing phenomena.

shows the responses determined using an unmodified device operated at 60°C. Comparison of these responses with those obtained at 30°C (Table I) indicates that increasing the sensor temperature decreases the responses obtained for alkanes and alcohols. Similar results have been obtained for various polymer-coated sensors [9,22,26,27]. In contrast, water shows a larger response at 60°C. This observation can be explained by the effect of temperature on the number of surface silanol and silylether groups that are available for hydrogen bonding interactions. For the device held at 30°C, we believe that trace water present in our carrier gas (< 5 ppm, see Experimental) adsorbs on some of the silanol and silylether groups and essentially decreases the number of active adsorption sites available to the water vapor pulse. Increasing the sensor temperature to 60°C shifts the adsorption equilibrium and, consequently, increases the number of active sites available for interaction with water from the vapor pulse. Thus the

Table 2.2. Analytes and their responses at 60° C ($\pm 15\%$).

			Uncoated	ated			PIB C	PIB Coated	
	Boiling	Unm	Unmodified	Sil	Silanized	Unm	Unmodified	Sil	Silanized
Analyte	Point (°C)	Hz/µgram	Hz/nanomole	Hz/µgram	Hz/nanomole	Hz/µgram	Hz/nanomole	Hz/µgram	Hz/nanomole
hexane	69	8.40	0.72	1.91	0.16	22.3	1.93	20.5	1.76
heptane	86	30.3	3.04	4.87	0.49	62.2	6.23	44.2	4.43
octane	126	81.4	9.29	68.9	0.79	222	25.3	187	21.4
nonane	151	528	8.79	23.2	2.98	1060	136	086	126
methanol	9	2.82	0.09	3.29	0.11	3.36	0.11	3.24	0.10
isopropanol	82	9.42	0.57	4.24	0.25	43.4	2.61	16.8	1.01
1-butanol	117	33.4	2.48	43.8	3.25	143	10.6	135	66.6
Water	100	33.7	0.61	6.47	0.12	35.4	0.64	98.6	0.18

increase in active site density with increasing sensor temperature leads to a larger response to water.

For the silanized SAW device, comparison of the responses measured at 30°C (Table 2.1) and 60°C (Table 2.2) indicate that increasing the sensor temperature decreases the response to all alkanes and alcohols except 1-butanol. As described above, a larger number of silylether (and trace silanol) groups are available on the device surface held at 60°C. These additional sites can participate in hydrogen bonding interactions with 1-butanol. We believe that the adsorption of 1-butanol is enhanced by dispersion interactions between the hydrocarbon portion of the molecule and the methyl groups of the silane. In principle, similar phenomena could occur for isopropanol. However, the interaction of isopropanol with the additional polar sites may be sterically hindered.

Poly(isobutylene) Coated. The responses obtained for PIB coated devices operated at 60°C are also given in Table 2.2. Comparison of these data with the appropriate data from Table I shows that increasing the sensor temperature decreases the response to alkanes and alcohols. Similar response decreases have been reported for several polymer-coated sensors [9,22,26,27]. However, the responses to water measured with the uncoated, unmodified and the PIB coated, unmodified devices are similar. This suggests that the PIB film does not completely cover the unmodified device surface. Thus, the increase in water response with increasing temperature can be attributed to the increase in available hydrogen bonding sites as described previously. McGill et al. [24] have also shown that an unmodified device coated with a 250 kHz PIB film responds to water.

2.5 References

- 1. Wohltjen, H.; Dessy, R. Anal. Chem. 1979, 51, 1458.
- 2. Wohltjen, H.; Dessy, R. Anal. Chem. 1979, 51, 1465.
- 3. Wohltjen, H.; Dessy, R. Anal. Chem. 1979, 51, 1470.
- 4. Grate, J. W.; Martin, S. J.; White, R. M. Anal. Chem. 1993, 65, 940A.
- 5. Grate, J. W.; Martin, S. J.; White, R. M. Anal. Chem. 1993, 65, 987A.
- 6. Ballantine, D. S., Jr.; Wohltjen, H. Anal. Chem. 1989, 61, 704A.
- 7. Fox, C. G.; Alder, J. F. Analyst (London) 1989, 114, 997.
- 8. Nieuwenhuizen, M. S.; Venema, A. Sens. Mater. 1989, 5, 261.
- 9. Grate, J. W.; Snow; A.; Ballantine; D. S., Jr.; Wohltjen, H.; Abraham, M. H.; McGill, R. A.; Sasson, P. Anal. Chem. 1988, 60, 869.
- 10. Ballantine, D. S.; Rose, S. L.; Grate, J. W.; Wohltjen, H. Anal. Chem. 1986, 58, 3058.
- 11. Wohltjen, H. Sens. Actuators 1984, 5, 307.
- 12. Snow, A. W.; Wohltjen, H. Anal. Chem. 1984, 56, 1411.
- 13. Frye, G. C.: Martin, S. J. Appl. Spectrosc. Rev. 1991, 26, 73.
- 14. McCallum, J. J. Analyst(London) 1989, 114, 1173.
- 15. Katritzky, A. R.; Offerman, R. J. CRC Anal. Chem. 1989, 21(2), 83.
- 16. Martin, S. J.; Frye, G. C.; Senturia, S. D. Anal. Chem. 1994, 66, 2201.
- 17. Martin, S. J.; Ricco, A. J.; Ginley, D. S.; Zipperian, T. E. IEEE Trans. Ultrason. 1987, UFFC-34, 142-147.
- 18. Grate, J. W.; Abraham, M. H. Sens. & Act. B. 1991, 3, 85.
- 19. Patrash, S. J.; Zellers, E. T. Anal. Chem. 1993, 65, 2055.
- 20. E.B. Townsend IV, J.S. Ledford and D.P. Hoffmann, submitted to Sensors and Actuators B.
- 21. McGill, R.A.; Abraham, M.H.; Grate, J.W. Chemtech 1994, 24(9), 27.
- 22. Grate, J. W.; Klusty, M.; McGill, R. A.; Abraham, M. H.; Whiting, G.; Andonian-Haftvan, J. Anal. Chem. 1992, 64, 610.
- 23. Ballantine, D. S., Jr. Anal. Chem. 1992, 64(24), 3069.
- 24. McGill, R.A.; Grate, J.W.; Anderson, M.A. Interfacial Design and Chemical Sensing, ACS Symposium Series 561, American Chemical Society, Washington, DC, 1994, 280.

- 25. Dickert, F. L.; Bruckdorfer, Th.; Feigl, H.; Haunschild, A.; Kuschow, V.; Oberveier, E.; Bulst, W.-E.; Knauer, U.; Mages, G. Sens. Actuators B. 1993, 13-14, 297.
- 26. King Jr., W. H. Anal. Chem. 1964, 36, 1735.
- 27. Guilbault, G. G.; Jordan, J. M. CRC Crit. Rev. Anal. Chem. 1988, 19, 1.
- 28. E.B. Townsend IV, J.S. Ledford and D.P. Hoffmann, accepted for publication in *Review of Scientific Instruments*.
- 29. Grate, J. W.; Rose-Pehrsson, S. L.; Venezky, D. L.; Klusty, M.; Wohltjen, H. *Anal. Chem.* **1993**, *65*, 1868.
- 30. Suleiman, A; Guilbault, G. G. Anal. Chim. Acta 1984, 162, 97.
- 31. Thompson, M.; Stone, D. C. Anal. Chem. 1990, 62, 1895.
- 32. Hecki, W. M.; Marassi, F. M.; Kallury, K. M. R.; Stone, D. C.; Thompson, M. *Anal. Chem.* 1990, 62, 32.
- 33. Thompson, M.; Stone, D. C.; Nisman, R. Anal. Chim. Acta 1991, 248, 143.
- 34. Yan, Y.; Bein, T. J. Phys. Chem. 1992, 96, 9387.
- 35. Janghorbani, M.; Freund, H. Anal. Chem. 1973, 45, 325.
- 36. Edmonds, T. E.; West, T. S. Anal. Chim. Acta 1980, 117, 147.
- 37. Private communication, Supelco technical support.
- 38. Dickert, F. L.; Haunschild, A. Adv. Mater. 1993, 5, 887.
- 39. R.L. Grob in Modern Practice of Gas Chromatography, 2nd Edition, R.L. Grob, Ed., John Wiley & Sons, New York, New York, 1985.
- 40. M.L. Lee, F.J. Yang, and K. D. Bartle, Open Tubular Column Gas Chromatography, John Wiley & Sons, New York, New York, 1984.
- 41. R. P. Evershed in Handbook of Derivatives for Chromatography, 2nd Edition, K. Blau and J. Halket, Ed., John Wiley & Sons, New York, New York, 1993.
- 42. Rose-Pehrsson, S. L.; Grate, J. W.; Ballantine, D. S., Jr.; Jurs, P. C. Anal. Chem. 1988, 60, 2801.
- 43. Barton, A.F.M. Pure Appl. Chem. 1985, 57, 905.
- 44. Myers, M. E.; Abu-Isa, I. A. J. Appl. Poly. Sci. 1986, 32, 3515.

Chapter 3

Development and Performance of a Semi-automated 200 MHz Surface

Acoustic Wave Resonator Array-Based Sensor Test Apparatus

3.1 Abstract

A semi-automated pulse injection and data analysis system utilizing 200 MHz surface acoustic wave resonators has been constructed. A cell consisting of separate sample splitting chamber, sample transfer lines, and sensor device areas has been constructed to allow individual temperature control over the regions. Experiments involving injections of n-hexane, trichlorobenzene, and 1% (w/v) of biphenyl in n-hexane show that all three temperatures play an important role in the magnitude and time dependency of the SAW response. Flow rate is also shown to be an important factor. The capabilities of the system have been demonstrated with uncoated and poly(isobutylene) coated devices.

3.2 Introduction

Surface acoustic wave (SAW) devices have been widely studied as mass sensors [1-15]. The use of coatings to enhance the selectivity and sensitivity of the devices is well established [4,5], however, it has become apparent that a single film and device is not adequate for many practical applications. This limitation has led to the use of SAW arrays to obtain more information about the composition of a sample. SAW array data sets are well suited to various data handling, manipulation, and recognition techniques that increase the information content of the results. Pattern recognition techniques have

been applied to mass sensors with some success [16-23] and the application of neural networks has also been suggested [18,23].

There has been considerable interest in the development of SAW technology and associated instrumentation since Wohltjen demonstrated many capabilities of the device in 1979 [1-3]. For example, Grate et al. [24] developed an automated continuous vaporgeneration and data collection system for chemical microsensors. Nederlof and Nieuwenhuizen [25] detailed their automated continuous flow system for testing SAW gas sensors. Munoz Leyva et al. [26] described a test system that can be used to study the effects of pressure, temperature, and relative humidity on the response of a piezoelectric sensor. Grate et al. [19] reported efforts to develop a smart sensor system for the detection of organophosphorus and organosulfur compounds using an array of SAW sensors in conjunction with automated sample preconcentration. Recently, Ricco and Martin [27] have developed multiple frequency SAW devices for sensing and materials characterization.

SAW responses are usually measured with devices that have equilibrated with sample vapor. This method of testing produces a great deal of fundamental information, but many practical sensor applications require the analysis of pulsed sample streams [28-35]. The details of such analyses vary with the specific application. However, in general, a pulse experiment involves a more rapid sequence of analyte sorption and desorption than is commonly associated with equilibrium methods. Grate and Abraham [33] have suggested that this type of sample introduction can be used in conjunction with laser or thermal desorption. Grate *et al.* [19] have also used thermal desorption of analyte from preconcentrator tubes to deliver pulses of gas to an array of SAW devices. In addition to these practical applications, we have recently reported that Linear Solvation Energy Relationships (LSER) derived from data collected using pulsed sample introduction can provide fundamental insight into coating properties [36].

This work is part of a larger study devoted to the development of practical sensor systems for environmental analysis [36,37]. In this paper we describe a sensor test system designed for convenient, unattended collection of response data from SAW resonator arrays. The system employs an autosampler and custom software for data acquisition, manipulation, and storage. We have also developed a sensor test cell that has separate temperature controlled regions for sample splitting, sample transfer, and SAW device containment. The test cell contains a six array 200 MHz SAW resonator device that could ultimately be used for pattern recognition studies. The availability of six channels also allows rapid collection of the large amounts of data needed for fundamental studies of sensor coatings using LSER methods [33,36,38]. Responses measured for uncoated and poly(isobutylene) coated devices have been used to demonstrate the capabilities of the system.

3.3 Experimental

Chemicals. Poly(isobutylene) (MW = 380,000) was obtained from Aldrich chemical company. n-Hexane, trichlorobenzene, and biphenyl were obtained from Aldrich chemical company and used as received.

Surface Acoustic Wave (SAW) Device. Data were obtained using a six element array of 200 MHz SAW resonator microbalances (Femtometrics, Costa Mesa, CA). The 200 MHz resonator has been described previously [39]. The frequency difference between each resonator and a separate reference device (beat frequency) is the measured signal. Power is supplied and frequency counted by an external unit provided by the manufacturer. The SAW resonator exhibits a 904 Hz frequency shift when perturbed by a 1 nanogram mass change.

Prior to use or coating, the SAW devices were rinsed with acetone and methanol, soaked in isopropanol, and dried in air. Poly(isobutylene) coated devices were prepared by spray casting from dilute (~500 ppm) toluene or chloroform solutions of the polymer.

Typi film

reso

this

calc

the a

of c

pins, to ac

the S

volu

The gask

mact

шась 1/16

block

cham Stàinl

splitu

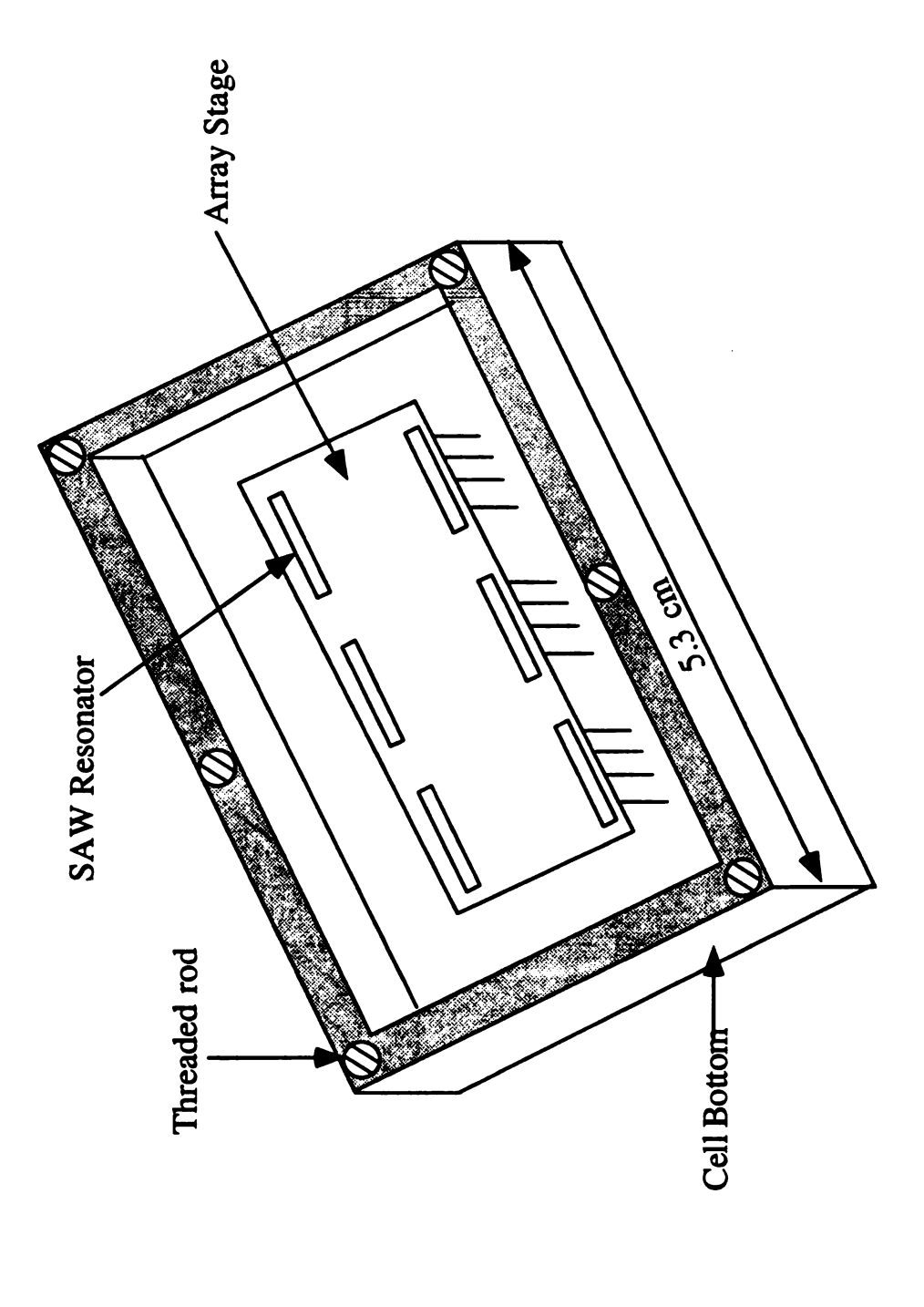
transfe splittin

chamba

Typical film thickness was 100 kHz, which corresponds to a 0.012 µm thick film. This film thickness is calculated using the density of the polymer, the mass deposited as calculated from the frequency shift, and the active area of the SAW device.

Test Cell. Two resonator configurations are available from Femtometrics: single resonators mounted on individual gold platforms and the six element array device used in this work. Figure 3.1 shows a schematic diagram of the bottom part of the test cell with the array platform inserted. The cell bottom is constructed from brass. Electrical contact between the array and the Femtometrics control board is made through a rectangular piece of circuit board using TO-8 pins. High vacuum epoxy (Torr Seal, Varian Vacuum Company) is used to seal all openings in the bottom of the cell (circuit board holes around pins, unused circuit board holes, and circuit board/cell interface). The cell was designed to accommodate either type of SAW device. In the configuration using single devices, the SAWs are installed perpendicular to the devices mounted on the single platform. The volume of the cell bottom is approximately 15 mL.

Figure 3.2 shows a schematic diagram of the complete test cell (top and bottom). The top and bottom are joined using six stainless steel bolts and a thin (~ 1/32") Teflon gasket. The top of the cell is a solid brass block with six holes for the transfer lines machined through directly above the SAW devices. Additionally, a 1/4" i.d. path was machined around the outer edge of the block to allow for water cooling. One end of each 1/16" i.d. (1/8" o.d.) stainless steel transfer line is silver soldered into the top of the brass block. The other end of each transfer line is silver soldered into a stainless steel splitting chamber (internal volume ~ 1 mL). Mounted directly above the splitting chamber is a stainless steel housing designed to accommodate a 1/4" diameter heater cartridge. The splitting chamber is attached to a GC injector via a 1/16" id (1/8" od) stainless steel transfer line and a 1/4" Swagelock connector. The total volume of the system (injector, splitting chamber, transfer lines, and cell) is approximately 20 mL. Equal splitting in the chamber was verified by examining the response of n-hexane on 6 blank devices.



View of the cell bottom showing the platform array device inserted. Individually mounted SAW devices are mounted perpendicular to the devices on the platform. Figure 3.1.

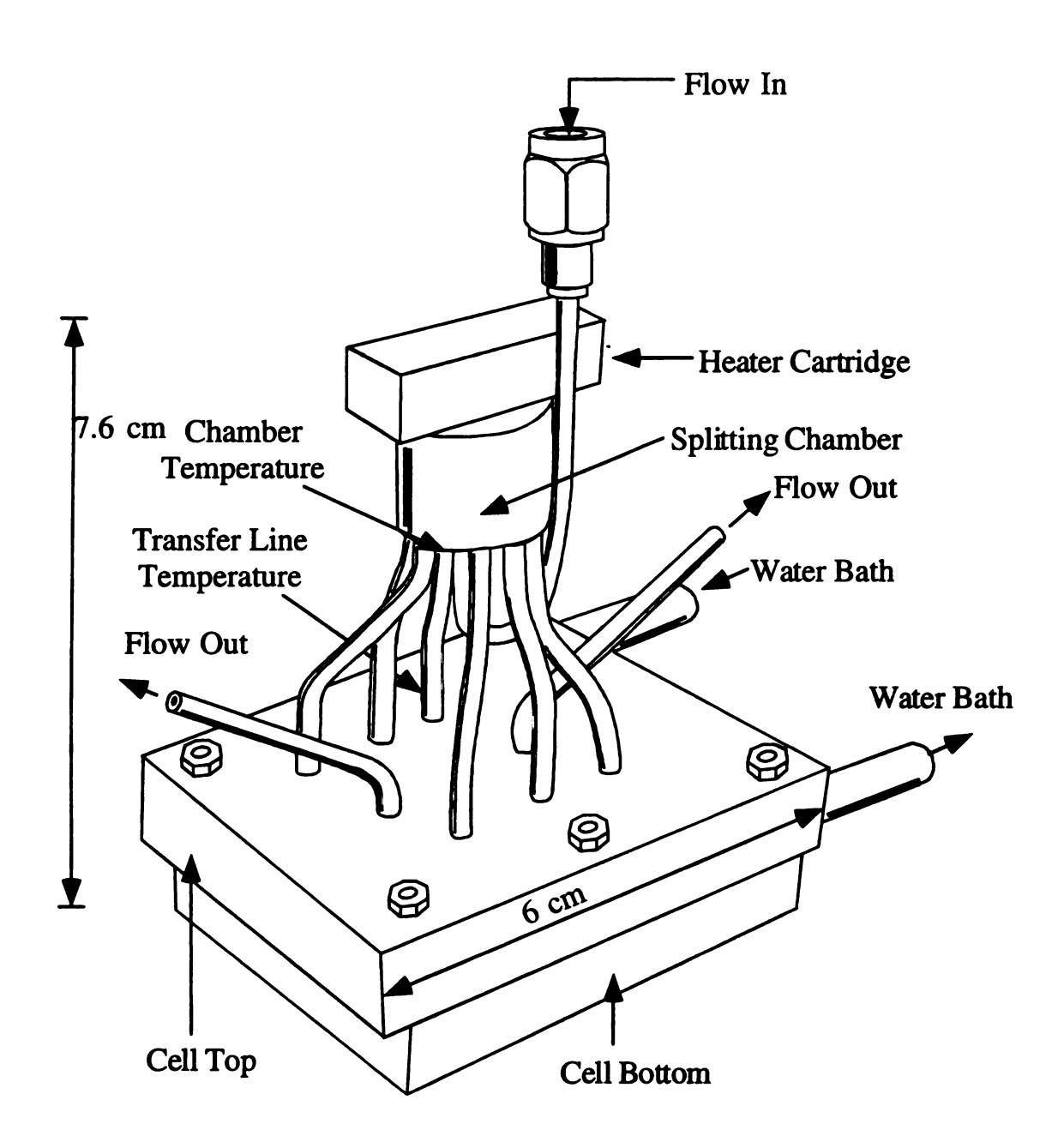


Figure 3.2. Schematic diagram of the complete sensor test cell.

Heat is supplied to the cell top using a 200 W, 1/4" x 1 1/4" heater cartridge (Omega) attached to the splitting chamber and nichrome wire wrapped around the transfer lines. The heated areas of the cell top are insulated using ceramic tape (Wilt, Lake Pleasant, NY) and fiberglass insulation. Temperature is monitored in three places using K-type thermocouples: directly underneath the splitting chamber, at the bottom of one of the transfer lines, and next to the array platform. Transfer line temperatures can range from 70° to 160°C while the splitting chamber temperature can go as high as 500°C. Typical operating temperatures are splitting chamber between 250° and 400°C, transfer line at 100°C, and sensor cell at 30°C. The lid of the cell is either heated or cooled (depending on the temperature of the transfer lines) with a water bath in order to maintain a 30°C sensor cell temperature. With a heated water bath, the temperature of the sensor cell can reach 90°C.

Analytes were delivered to the test cell as a pulse using a Varian autosampler Series 8000 and a Varian gas chromatograph injector operated at 250°C. The autosampler was mounted on a steel plate above the injector to provide mechanical stability to the apparatus. The pneumatic pressure for the autosampler and the carrier gas flow for the injector are provided by a standard laboratory gas cylinder of N_2 (99.95%, AGA Gas Co.). The carrier gas is dried over molecular sieves and the flow rate is controlled by Porter Mass Flow Controllers. Typical carrier gas flow rates vary from 50 to 100 cc/min. We have used either 1.0 or 10.0 μ L syringes for sample introduction. Three injections of each analyte were made on at least three devices to ensure reproducibility. Sensor responses are reported as the maximum frequency shift in hertz. We do not believe that peak area is a valid measure of our sensor response since such a measurement convolutes the amount of analyte sorbed with the residence time of the analyte on the surface of the device. RSDs for SAW responses were approximately 10%.

Data Acquisition and Manipulation. The beat frequencies of the resonators were collected using a digital counting board (MetraByte, Taunton, MA) and stored in a

Gateway 2000 386-25 personal computer. The Femtometrics supplied software is capable of collecting data for all 6 channels at a resolution of either 100 (1pt/0.2sec), 10 (1pt/0.8sec), 5 (1pt/1.5sec), 2 (1pt/3.0sec), or 1 (1pt/6.0sec) Hz. Data presented in this paper were collected with a resolution of 10 Hz in order to provide at least three data points across a typical peak maximum. The standard software has been modified by Femtometrics to allow for timed, multiple runs that allow full utilization of the Varian autoinjector capabilities.

Data analysis was performed using custom software written using LabView for Windows (v2.52, National Instruments, Austin, TX). Figure 3.3 shows an example of the software output. The software separates the Femtometrics file into individual channels, and then simultaneously displays the response of all 6 channels on a single page. In addition, the software determines peaks, peak heights, peak areas, averages, standard deviations, and % RSDs. The user can control the sensitivity of the peak determination and select either none, Savitsky-Goolay smoothing, or median filtering of the data. An output file that contains peak height, peak area, analytical information, and relevant processing information (such as filtering, sensitivity, etc.) can be automatically generated whenever the user is satisfied with the level of data analysis.

3.4. Results and Discussion

We have reported that the response of an uncoated resonator can be understood primarily in terms of analyte physisorption [36]. In contrast, polymer coatings often exhibit selective sorption and mechanical effects [4,5,40,41] that may complicate characterization of a sensor test system. For example, poly(isobutylene) is well known for its ability to selectively interact with alkanes through dispersion interactions [33,36,38] and its susceptibility to viscoelastic effects [40,41,42]. As a result of such possible complications, most of the data presented in the paper were obtained using uncoated SAW devices.

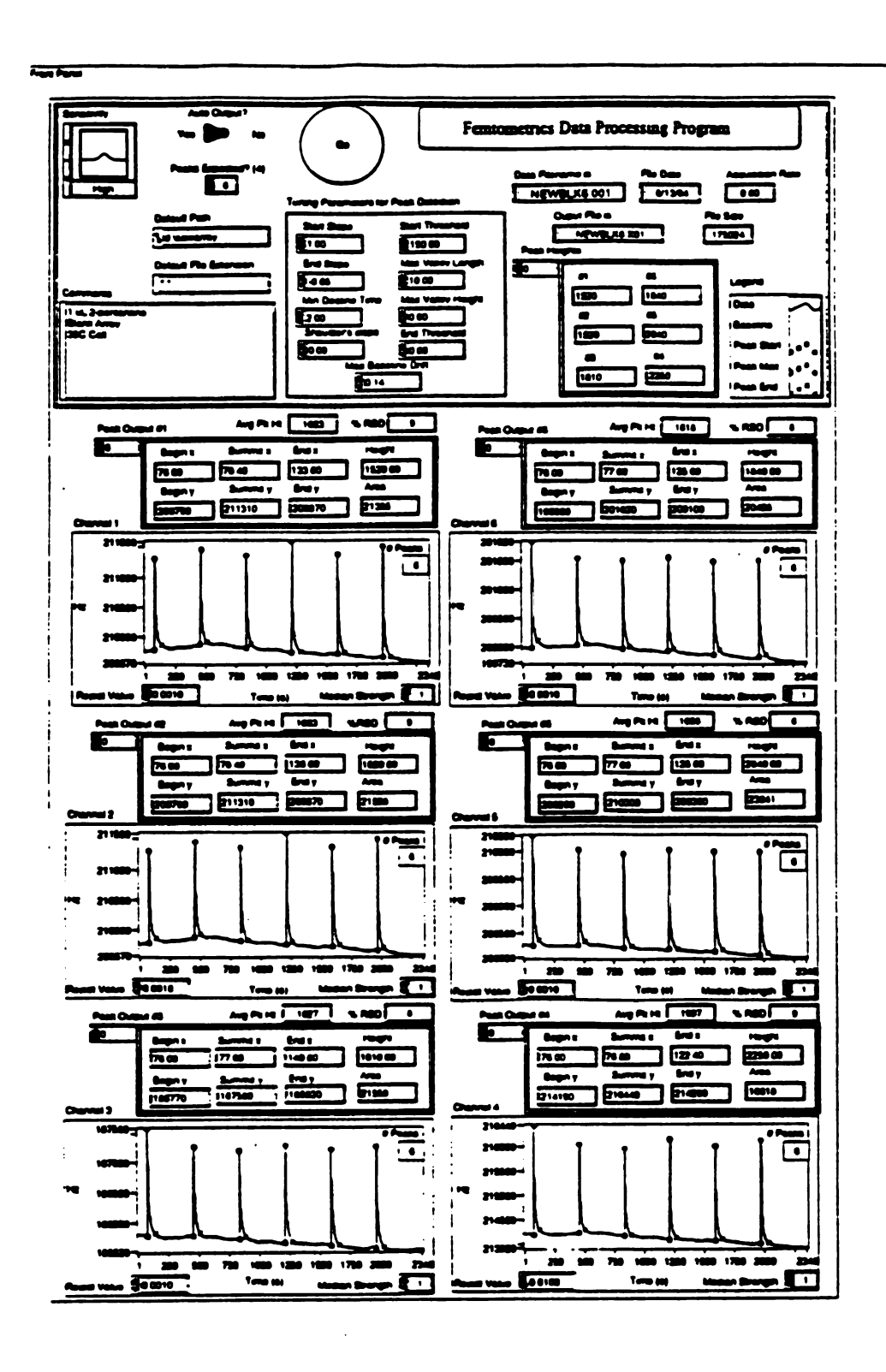


Figure 3.3. Output created by the LabView software written to process 6 channels of SAW data.

In our system, the major instrument variables that can be controlled are the temperatures of the sensor cell, transfer line, and splitting chamber as well as the carrier gas flow rate. We anticipate that the sensor cell temperature will influence the analyte residence time and adsorption/desorption equilibria in the cell. The temperature of the splitting chamber and transfer line will influence analyte arrival time by affecting the partitioning of the analytes during sample transfer from the injector to the sensor. Finally, the carrier gas flow rate will also affect the arrival and residence times of the analyte in the cell.

Effect of Sensor Cell Temperature. Figure 3.4 shows the effect of cell temperature on the response of an uncoated device to an injection of 3.0 μL of hexane followed by 3.0 μL of 1% (w/v) biphenyl in hexane. For a cell temperature of 60°C, the response to pure hexane is significantly lower than that observed for the biphenyl-hexane mixture. This difference can be explained in terms of the relative sensitivity of the blank to hexane and biphenyl. We have previously reported that enhanced adsorption of compounds with higher boiling points increases the sensitivity of the uncoated device to such analytes [36,38]. In addition, King [43] proposed that analytes with higher boiling points are able to achieve a higher level of partitioning into a film coated on a piezoelectric sensor. While partitioning cannot occur on the uncoated device, we believe it is reasonable to expect adsorption effects to produce similar results. Thus we anticipate that the response to biphenyl (bp = 256°C) would be much greater than to hexane (bp = 69°C). The large response to biphenyl leads to a larger response to the biphenyl-hexane mixture.

Most studies of coated SAW devices employ sensor temperatures less than 60°C in order to increase sensor response and prolong coating life. Figures 3.4b and 3.4c show that decreasing the cell temperature increases the magnitudes of the peaks observed following hexane and biphenyl-hexane injection. This can be attributed to greater analyte adsorption on the cooler device surface. The most significant change in sensor response

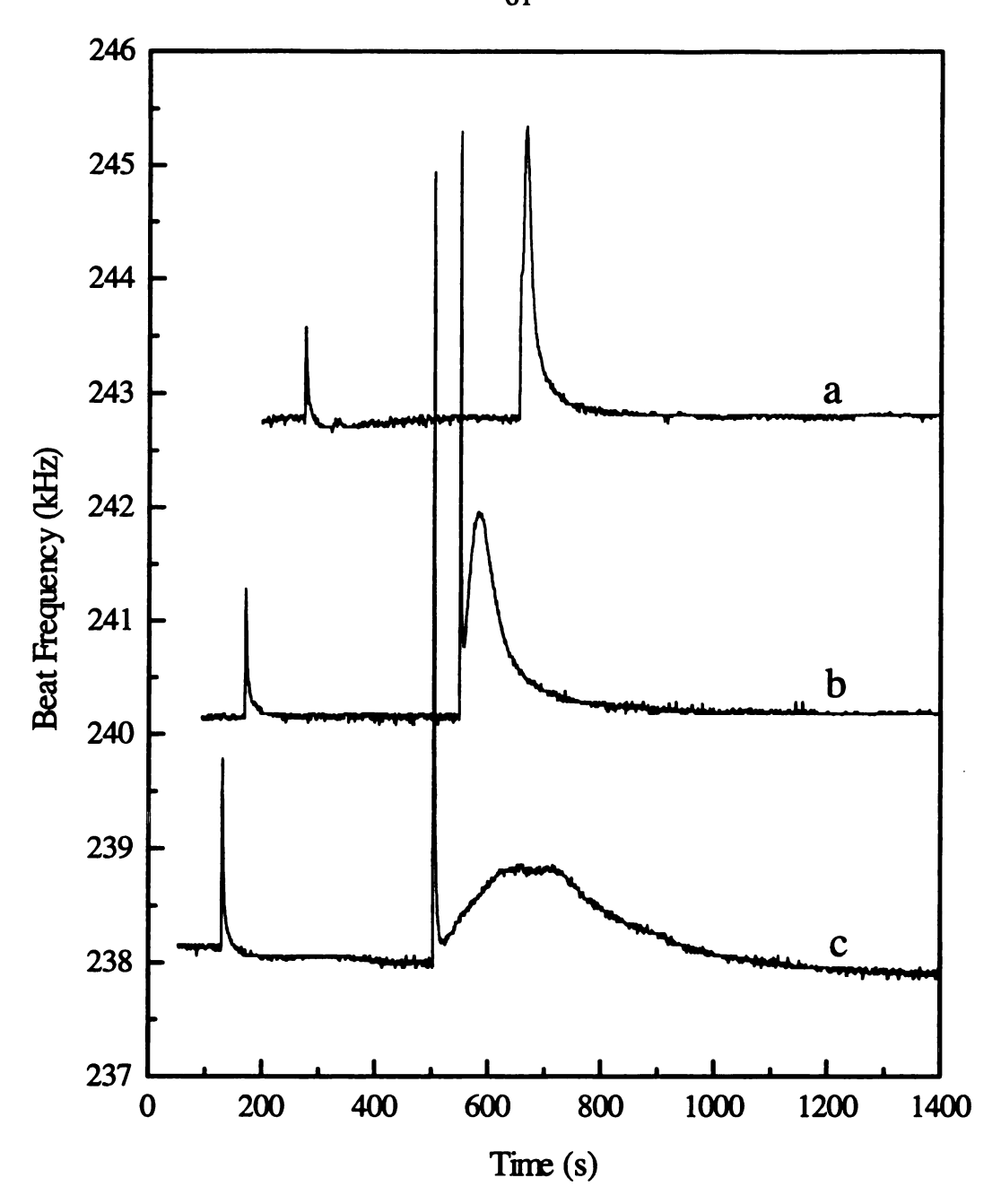


Figure 3.4. The effect of sensor cell temperature on the response of an uncoated device to injections of 3 µL of hexane followed by 3 µL of a 1% (w/v) mixture of biphenyl in hexane. Sensor cell temperatures = (a) 60°C, (b) 45 °C, and (c) 30°C. Splitting chamber temperature = 250°C. Transfer line temperature = 50°C. Carrier gas flow rate = 80 cc/min.

is the peak splitting observed for the biphenyl-hexane mixture. We believe that the narrow peak (designated henceforth as "hexane/biphenyl peak") is caused by rapid adsorption, desorption, and purging processes involving hexane and some of the biphenyl. After the hexane/biphenyl vapor responsible for the narrow peak leaves the cell, the biphenyl which initially adsorbed on the walls of the cell desorbs and can interact with the SAW device. The broadening observed on decreasing the cell temperature reflects the longer times required for such processes to occur in a cooler cell. Eventually, the remaining biphenyl is purged from the cell and the response returns to baseline. It is possible that the relatively large cell (volume ~15 mL) used for these studies is in part responsible for the degree of splitting shown in Figure 3.4. Larger surface area cells would be expected to show more pronounced adsorption effects in this experiment. However, the cell size is dictated by the dimensions of the array and the ease of array handling. Slightly smaller cell volumes are possible, but they require semipermanent device encapsulation and/or less effective flow splitting. Furthermore, experiments with these systems showed the same splitting phenomenon illustrated in Figure 3.4.

Effect of Splitting Chamber/Transfer Line Temperatures. Portable sensors are generally less elaborate than laboratory sensor test systems. One possible simplification for portable devices is to minimize the number of heat sources used in the system. Under such conditions, a thermal gradient will exist between the sample injector and the sensor device. We have simulated this situation by using only the splitting chamber heating cartridge to supply heat to the cell top. In this case, heat flow from the splitting chamber will increase the transfer line temperature. Figure 3.5 shows the effect of increasing splitting chamber/transfer line temperature on the response profiles obtained following injections of 3.0 μL of hexane and 3.0 μL of 1% (w/v) biphenyl in hexane. For all of the temperature combinations, the SAW response magnitude for pure hexane is essentially constant. This suggests that the combination of heat from the splitting chamber and the

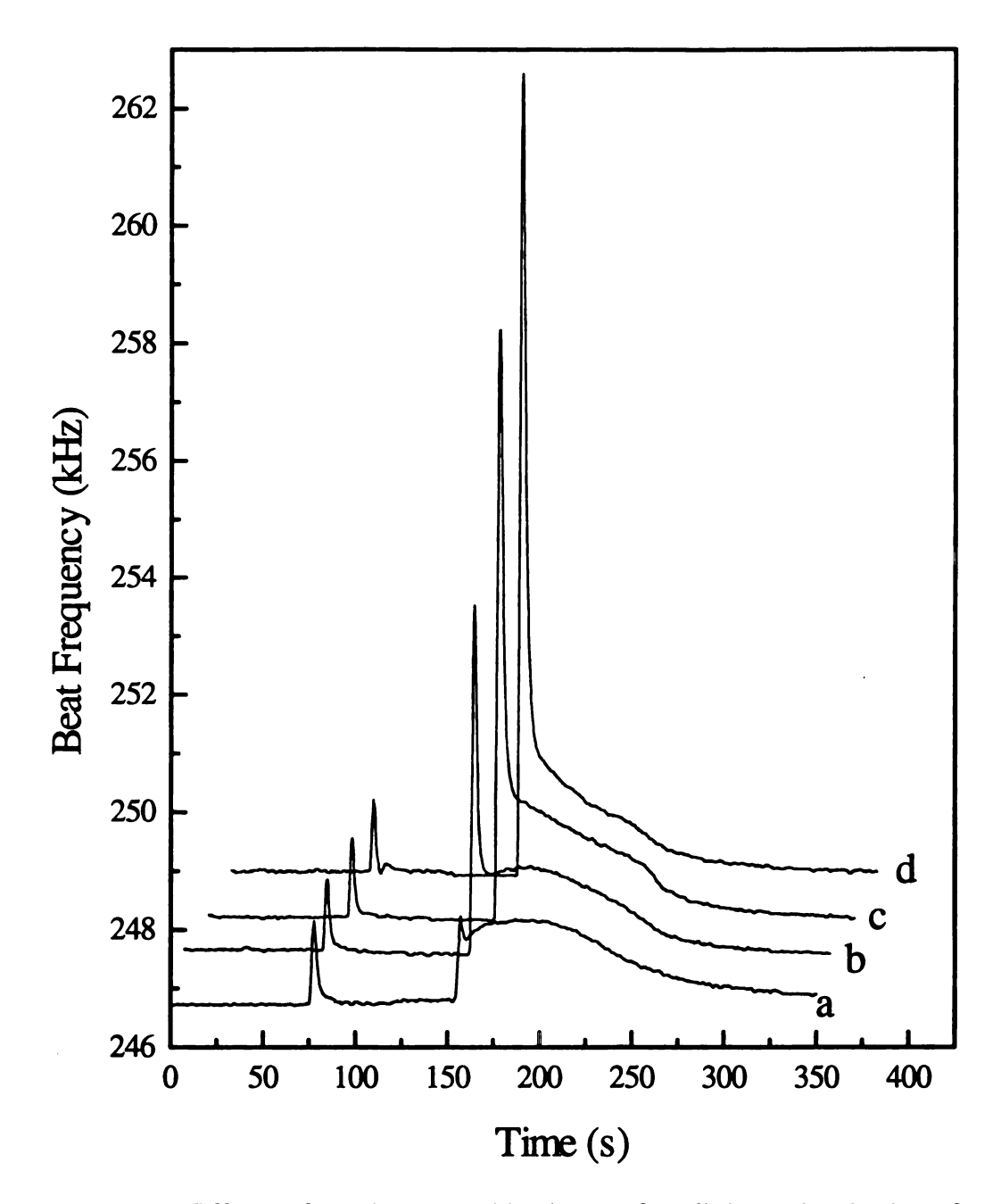


Figure 3.5. Effect of various combinations of splitting chamber/transfer line temperatures on the response of an uncoated device to injections of 3 μL of hexane followed by 3 μL of a 1% (w/v) mixture of biphenyl in hexane. Splitting chamber/transfer line temperatures = (a) 100/38°C, (b) 200/49°C, (c) 300/63°C, and (d) 400/77°C. Sensor cell temperature = 30°C. Carrier gas flow rate = 80 cc/min.

transfer line is sufficient to keep hexane in the vapor phase. However, this is not the casefor the biphenyl/hexane mixture. Note that for a splitting chamber/transfer line temperature of 100°/38°C (Figure 3.5a), the hexane and hexane/biphenyl peaks have approximately the same magnitude. This suggests that the biphenyl condenses in the chamber and transfer lines to such an extent that essentially none of the biphenyl reaches the sensor with the hexane. Increasing the splitting chamber/transfer line temperature increases the magnitude of the hexane/biphenyl peak. We attribute this to an increase in the amount of biphenyl arriving with the hexane. Finally, we note that the biphenyl peak shape is dramatically affected by the splitting chamber/transfer line temperature. This observation may be understood in terms of the arrival time of biphenyl and the desorption kinetics of the adsorbed analyte. For lower temperature combinations (Figures 3.5a and 3.5b), most of the biphenyl arrives after the hexane, adsorbs on the device surface and cell walls, and then slowly desorbs as described in the previous section. For higher temperatures, more biphenyl adsorbs and desorbs with hexane. The tailing observed for approximately 80 seconds after the hexane/biphenyl peak (Figure 3.5d) can be attributed to slow desorption of the remaining biphenyl from the surface of the SAW device.

The separation between the hexane/biphenyl peak and the peak attributed to pure biphenyl suggests a method for the determination of trace amounts of high boiling compounds in low boiling solvent matrices. Indeed, adsorption and thermal desorption methods have been used in combination with selective coatings to produce advanced sensor systems. Kindlund et al. [44] reported that water can be separated from organic species using thermal desorption in combination with a silicone oil preconcentrator. Grate et al. [19] have also demonstrated the advantages of this approach in a comprehensive study of a smart sensor system that employs thermally desorbed Tenax preconcentrator tubes and an array of four coated SAW devices.

Effect of Transfer Line Temperature. The effect of transfer line temperature on sensor response is most clearly illustrated with data obtained for a single component

sample. Figure 3.6 shows the effect of transfer line temperature on the response of an uncoated SAW device to 0.1 µL injections of trichlorobenzene (bp = 214°C). Both curves show a sharp increase in beat frequency approximately 2-3 seconds after injection. However, curve (a) is significantly broader than curve (b). Both curves show similar sloped falling edges. We believe that the shape of the response profile can be explained in terms of sample dispersion in the transfer lines and the sample concentration in the cell. For a transfer line temperature of 75°C, analyte dispersion in the lines results in a low, constant sample concentration in the test cell for a significant time interval. The result is a plateau in the response curve between 82 and 85 seconds. Increasing the transfer line temperature from 75° to 150°C produces a narrower response profile and a larger change in beat frequency compared to the corresponding features observed for the lower transfer line temperature. This can be attributed to less sample dispersion in the high temperature transfer lines and, consequently, a larger fraction of the TCB reaches the cell in a shorter period of time. We must note that preliminary experiments with low volume pulse injection systems that did not utilize heated transfer lines produced broad or irreversible response profiles that could be mistaken for selective analyte/film interactions.

Effect of Carrier Gas Flow Rate. Figure 3.7 shows the effect of carrier gas flow rate on the response of the uncoated device to injections of 3.0 μL of hexane followed by 3.0 μL of 1% (w/v) biphenyl in hexane. For a flow rate of 20 cc/min, both the hexane and biphenyl peaks are broadened by significant sample dispersion in the transfer lines and slow adsorption/desorption processes in the cell. Increasing the flow rate decreases the analyte dispersion and increases the rate of the adsorption/desorption processes. Consequently, the separation between the hexane/biphenyl and biphenyl peaks and the width of the biphenyl peak decreases.

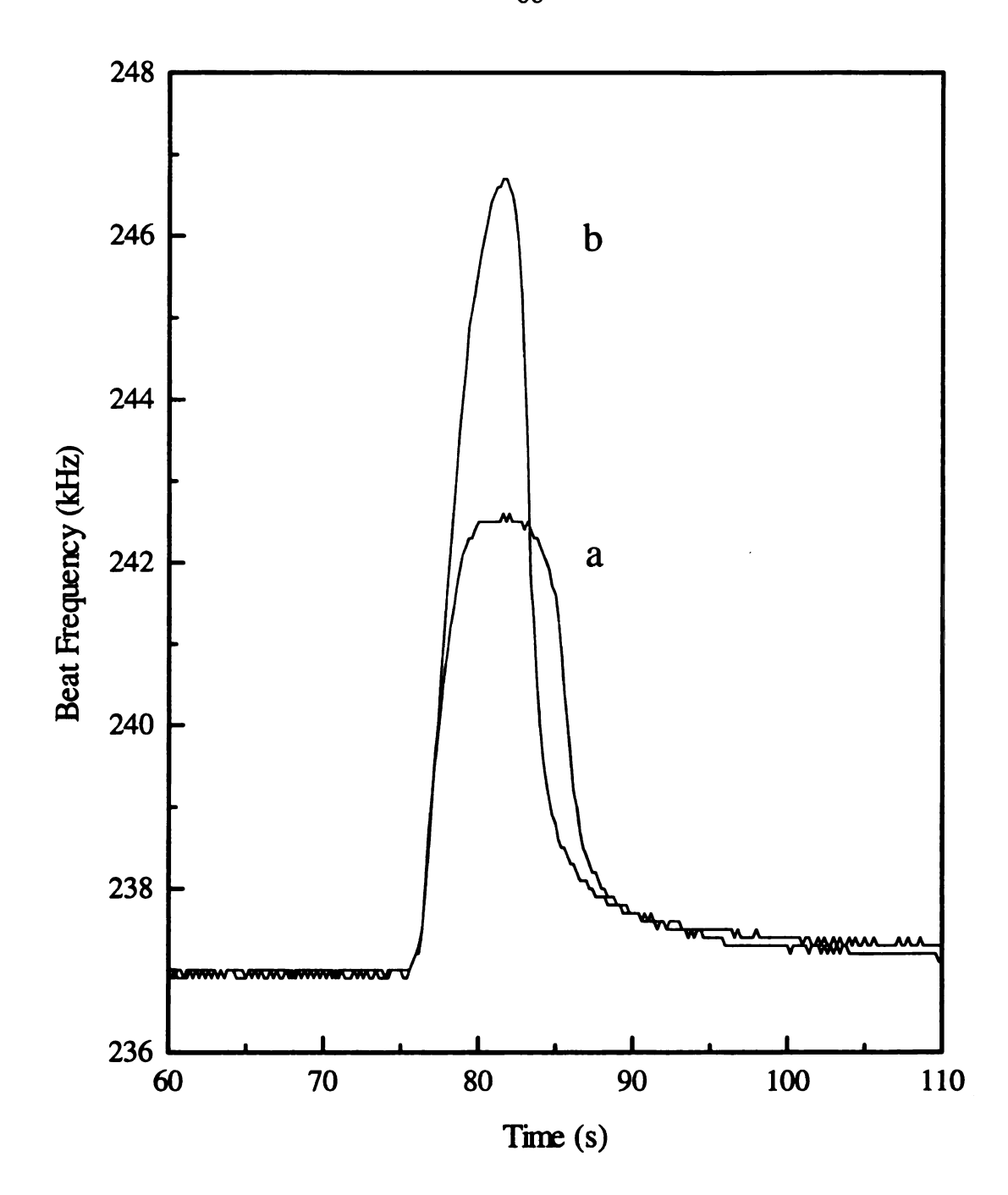


Figure 3.6. The effect of transfer line temperature on the uncoated device response to 0.1 μL injections of trichlorobenzene. Transfer line temperatures = (a) 75° C and (b)150°C. Splitting chamber temperature = 400°C. Sensor cell temperature = 30°C. Carrier gas flow rate = 80 cc/min.

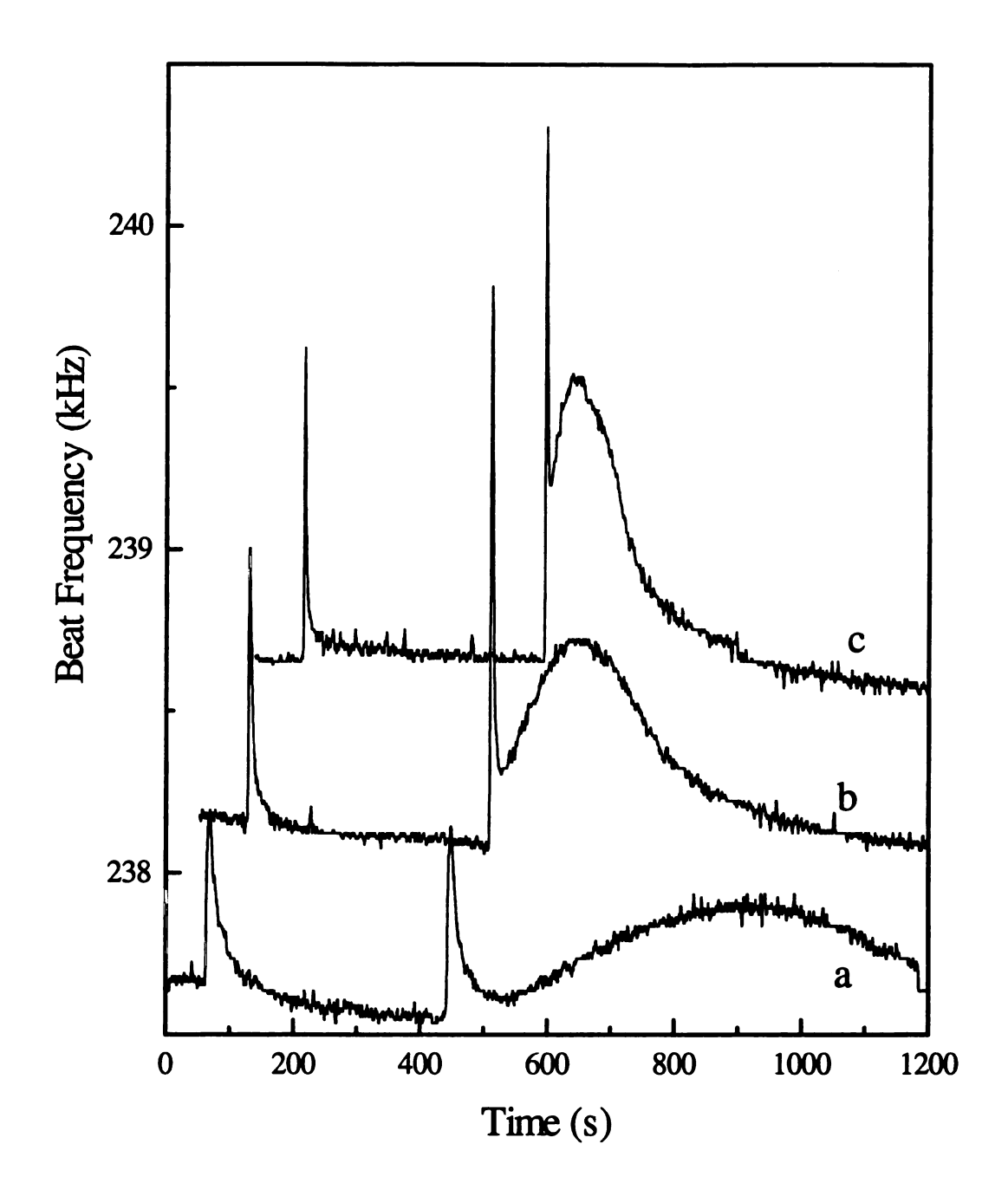


Figure 3.7. Effect of carrier gas flow rate on the uncoated device response to injections of 3 μ L of hexane followed by 3 μ L of a 1% (w/v) mixture of biphenyl in hexane. Carrier gas flow rate = (a) 20 cc/min, (b) 50 cc/min, and (c) 100 cc/min. Splitting chamber temperature = 250°C. Transfer line temperature = 50°C. Sensor cell temperature = 30°C.

Effect of Analyte Concentration. The response of a sensor to changes in analyte concentration is of interest for practical analytical devices and the fundamental study of sorption phenomena. Figure 3.8 shows the effect of hexane injection amount on the response of uncoated and 100 kHz poly(isobutylene) coated devices. Our results indicate that the uncoated device response increases linearly with hexane amount. However, the response curve obtained for the poly(isobutylene) coated device is nonlinear. Nonlinear calibration curves are not uncommon for coated devices. Wohltjen and Dessey [2] reported that the response of a DC 970 coated sensor used as a GC detector was nonlinear for 0-20 µg injections of o-chlorotoluene. Grate et al. [9] found that a fluoropolyol coated device gave a nonlinear response to dimethyl methylphosphonate in the concentration range of 1-10000 µg/L. Later, Grate et al. [19] reported a nonlinear response for the same vapor and film in a different SAW system over a vapor concentration range of 0-1500 mg/m³. Our experience with pulse injection systems has indicated that the concentration range over which sensor response is linear depends on a number of factors such as cell design, operating conditions, polymer coating, and analyte. However, we do not mean to imply that coated SAW device responses are inherently nonlinear. Snow and Wohltjen [12] demonstrated linearity for a poly(ethylene maleate) coated device exposed to 100-1000 ppm of cyclopentadiene. Frye et al. [45] showed that polystyrene coated SAW device responses were linear over a wide range of methanol partial pressures. Bowers et al. [39] reported that the response of a triethanolamine coated resonator to HCl was linear in the concentration range of 0.18-1 ppm. Figure 3.8 also shows that the poly(isobutylene) coated device is more sensitive than the uncoated sensor. Similar response enhancements have been observed by a number of investigators.

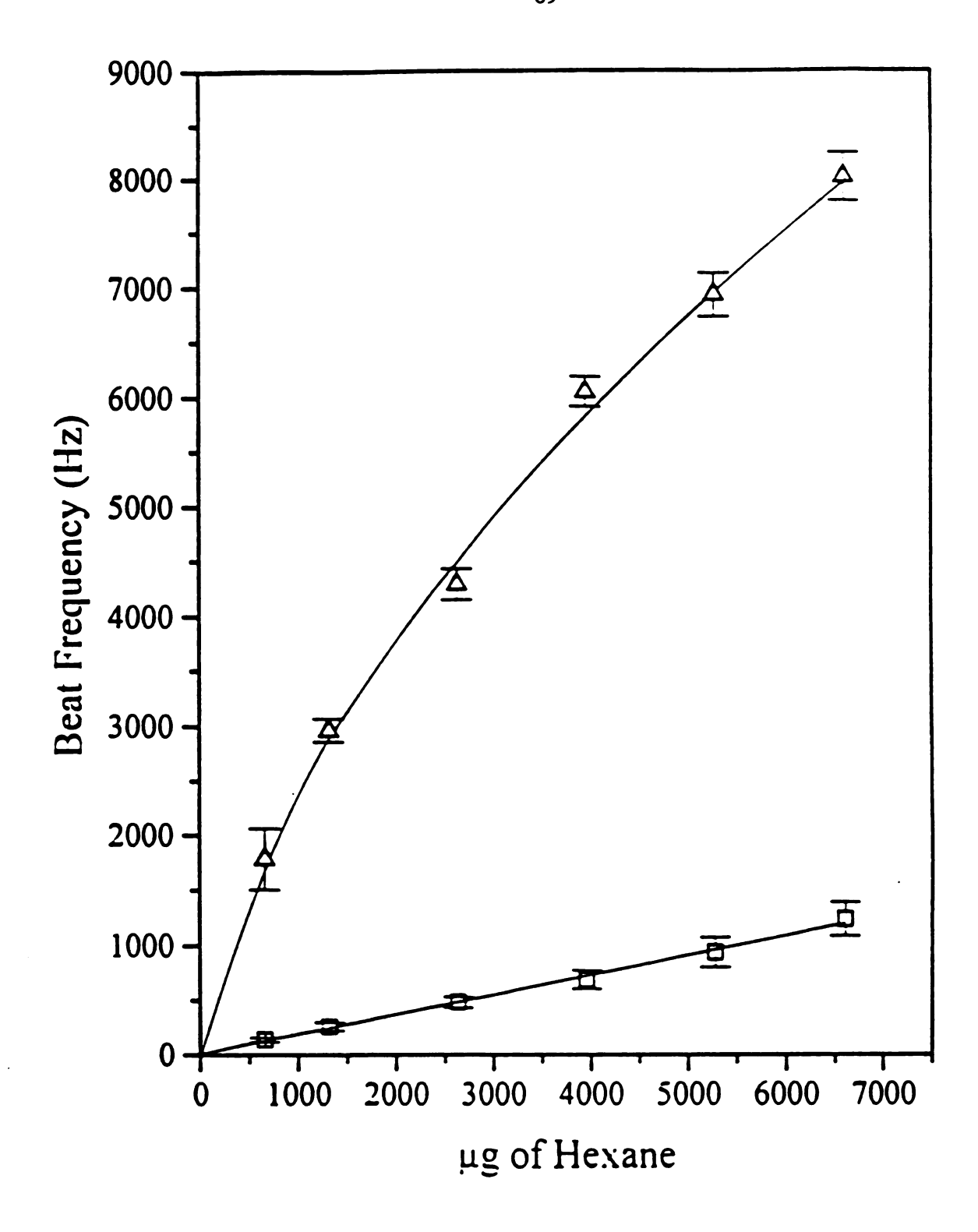


Figure 3.8. Calibration curves for hexane injected on a blank (\square) and poly(isobutylene) coated (Δ) device.

3.5 References

- 1. Wohltjen, H.; Dessy, R. Anal. Chem. 1979, 51, 1458.
- 2. Wohltjen, H.; Dessy, R. Anal. Chem. 1979, 51, 1465.
- 3. Wohltjen, H.; Dessy, R. Anal. Chem. 1979, 51, 1470.
- 4. Grate, J. W.; Martin, S. J.; White, R. M. Anal. Chem. 1993, 65, 940A.
- 5. Grate, J. W.; Martin, S. J.; White, R. M. Anal. Chem. 1993, 65, 987A.
- 6. Ballantine, D. S., Jr.; Wohltjen, H. Anal. Chem. 1989, 61, 704A.
- 7. Fox, C. G.; Alder, J. F. Analyst (London) 1989, 114, 997.
- 8. Nieuwenhuizen, M. S.; Venema, A. Sens. Mater. 1989, 5, 261.
- 9. Grate, J. W.; Snow; A.; Ballantine; D. S., Jr.; Wohltjen, H.; Abraham, M. H.; McGill, R. A.; Sasson, P. Anal. Chem. 1988, 60, 869.
- 10. Ballantine, D. S.; Rose, S. L.; Grate, J. W.; Wohltjen, H. Anal. Chem. 1986, 58, 3058.
- 11. Wohltjen, H. Sens. Actuators 1984, 5, 307.
- 12. Snow, A. W.; Wohltjen, H. Anal. Chem. 1984, 56, 1411.
- 13. Frye, G. C.; Martin, S. J. Appl. Spectrosc. Rev. 1991, 26, 73.
- 14. McCallum, J. J. Analyst(London) 1989, 114, 1173.
- 15. Katritzky, A. R.; Offerman, R. J. CRC Anal. Chem. 1989, 21(2), 83.
- 16. Carey, W. P.; Kowalski, B. R. Anal. Chem. 1986, 58, 3077.
- 17. Carey, W.P.; Beebe, K.R.; Kowalski, B.R.; Illman, D.L.; T. Hirschfeld, T. *Anal. Chem.* 1986, 58, 149.
- 18. Carey, W. P.; Beebe, K. R.; Kowalski, B. R. Anal. Chem. 1987, 59, 1529.
- 19. Grate, J. W.; Rose-Pehrsson, S. L.; Venezky, D. L.; Klusty, M.; Wohltjen, H. *Anal. Chem.* 1993, 65, 1868.
- 20. Katrinsky, A. R.; Savage, G. P.; Pilarska, M. Talanta 1991, 38, 201.
- 21. Nanto, H.; Kawai, T.; Sokooshi, H.; Usuda, T. Sens. Actuators B 1993, 13-14, 718.
- 22. Rose-Pehrsson, S. L.; Grate, J. W.; Ballantine, D. S., Jr.; Jurs, P. C. Anal. Chem. 1988, 60, 2801.
- 23. Zellers, E. T.; Pan, T-S.; Patrash, S. J.; Han, M.; Batterman, S. A. Sens. Actuators B 1993, 12, 123.
- 24. Grate, J. W.; Ballantine, D. S., Jr.; Wohltjen, H. Sens. and Act. 1987, 11, 173.
- 25. Nederlof, A. J.; Nieuwenhuizen, M. S. Rev. Sci. Instrum. 1993, 64, 501.

- 26. Munoz Leyva, J. A.; Hidalgo De Cisneros, J. L.; Garcia Gomez DE Barreda, D.; Beerra, Fraidias, A. J. *Talanta* 1994, 41, 159.
- 27. Ricco, A. J.; Martin, S. J. Sens. Actuators B. 1993, 10, 123.
- 28. Suleiman, A.; Guilbault, G. G. Anal. Chim. Acta 1984, 162, 97.
- 29. Thompson, M.; Stone, D. C. Anal. Chem. 1990, 62, 1895.
- 30. Hecki, W. M.; Marassi, F. M.; Kallury, K. M. R.; Stone, D. C.; Thompson, M. *Anal. Chem.* **1990**, *62*, 32.
- 31. Thompson, M.; Stone, D. C.; Nisman, R. Anal. Chim. Acta 1991, 248, 143.
- 32. Yan, Y.; Bein, T. J. Phys. Chem. 1992, 96, 9387.
- 33. Grate, J. W.; Abraham, M. H. Sens. & Act. B. 1991, 3, 85.
- 34. Janghorbani, M.; Freund, H. Anal. Chem. 1973, 45, 325.
- 35. Edmonds, T. E.; West, T. S. Anal. Chim. Acta 1980, 117, 147.
- 36. E.B. Townsend IV, J.S. Ledford, and D.P. Hoffmann, submitted to Sensors and Actuators.
- 37. E.B. Townsend IV, J.S. Ledford, and D.P. Hoffmann, submitted to Anal. Chim. Acta.
- 38. Patrash, S. J.; Zellers, E. T. Anal. Chem. 1993, 65, 2055.
- 39. Bowers, W. D.; Chuan, R. L.; Duong, T. M. Rev. Sci. Instrum. 1991, 62, 1624.
- 40. Martin, S. J.; Frye, G. C.; Senturia, S. D. Anal. Chem. 1994, 66, 2201.
- 41. Grate, J. W.; Klusty, M.; McGill, R. A.; Abraham, M. H.; Whiting, G.; Andonian-Haftvan, J. Anal. Chem. 1992, 64, 610.
- 42. Ballantine, D. S., Jr. Anal. Chem. 1992, 64(24), 3069.
- 43. King Jr., W. H. Anal. Chem. 1964, 36, 1735.
- 44. Kindlund, A.; H. Sundgren, H.; Lundstrom, I. Sens. & Act. B. 1984, 5, 1.
- 45. Frye, G. C.; Martin, S. J.; Ricco, A. J. Sens. Mater. 1989, 1, 335.

Chapter 4

Study of Poly(isobutylene) Coated Piezoelectric Mass Sensors in a Pulsed

Injection System

4.1 Abstract

The interactions of various classes of compounds with poly(isobutylene) coated surface acoustic wave (SAW) devices and quartz crystal microbalances (QCM) in a pulsed injection system have been examined. For the pulsed system, a new parameter (designated "pulse coefficient") has been developed that is analogous to the partition coefficient in a continuous flow system. Calculated pulse coefficients were similar in trend and slightly larger than calculated SAW coefficients and literature SAW and GLC partition coefficients reported for the same analytes. Using the pulse coefficients, Linear Solvation Energy Relationships (LSER) were calculated for the SAW and QCM. The results indicate that a poly(isobutylene) film interacts with analytes primarily through dispersion interactions. Thus, an enhanced response to alkanes is observed because of the dominant role of dispersion forces in the intermolecular interactions for both the polymer and the alkanes. LSER coefficients calculated for the pulsed injection system compare favorably with values reported for continuous flow SAW and GLC experiments.

4.2 Introduction

Surface acoustic wave (SAW) devices have been widely studied as mass sensors [1-16]. Typical devices employ polymer coatings that are able to interact selectively with the analyte of interest. If this coating is a soft, amorphous polymer above its glass transition temperature, then the frequency shift of the sensor resulting from the addition of a thin film coating is as described by Wohltjen [11]:

$$\Delta f = (k_1 + k_2) f_0^2 h \rho - k_2 f_0^2 h \left(\frac{4\mu}{v_R^2} \left(\frac{\lambda + \mu}{\lambda + 2\mu} \right) \right)$$
 (4.1)

where Δf is the frequency shift (hertz), $f_{\rm O}$ is the fundamental frequency of the device (hertz), k_1 and k_2 are material constants of the ST cut quartz substrate (-8.7 x 10⁻⁸ and -3.9 x 10⁻⁸ m²s/kg) [17], h is the film thickness (meters), ρ is the film density (kg/m³), μ is the shear modulus of the film material (N/m²), λ is the Lamé constant, and V_r is the Rayleigh wave velocity in the substrate (3300 m/s). The first term provides the frequency shift due to mass loading and the second term details the contribution from the mechanical properties of the film. If the shear modulus of the coating is small compared to the square of the wave velocity ($4\mu/V_{\rm R}^2$ < 100), then the second term is considered negligible and equation (4.1) simplifies to the more familiar expression:

$$\Delta f = (k_1 + k_2) f_0^2 h \rho (4.2)$$

This equation assumes that the film is an isotropic, nonconducting, nonpiezoelectric polymer film held above its glass transition temperature with a thickness less than one percent of the acoustic wavelength [11]. Similar expressions have been derived for the effect of vapor sorption on the frequency of the device.

Grate et al. [9] used partition coefficients to describe vapor sorption into materials used as SAW coatings. The frequency shift upon vapor sorption, Δf_V , and the partition coefficient, K_{SAW} , are related by the following expression:

$$\Delta f_{v} = \frac{\Delta f_{s} C_{v} K_{SAW}}{\rho_{s}} \tag{4.3}$$

where C_V is the vapor concentration, Δf_S is the frequency shift caused by the polymer coating, and ρ_S is the density of the polymer coating. This expression assumes that the response of the device is entirely due to mass loading [9].

The sorption of the vapor into the film depends largely on the solubility properties of both the film and the vapor [18]. Dominant interaction modes involve dispersion forces (induced-dipole/induced-dipole), dipole induction interactions (dipole/induced-dipole), dipole orientation interactions, and hydrogen-bonding. Originally, Hildebrand solubility parameters were thought to describe these interactions adequately, but more recently, solvation parameters have been proposed as better models [9,18]. If the response for several analytes that have different combinations of solvation parameters are known, the following equation can be used to describe the solubility properties of the film.

$$\log K = c + a \sum_{1} \alpha_{2}^{H} + b \sum_{1} \beta_{2}^{H} + \log_{1} L^{16} + rR_{2} + s\pi_{2}^{H}$$
 (4.4)

 $\Sigma \alpha_2^H$ is a measure of hydrogen-bond acid strength, $\Sigma \beta_2^H$ is a measure of hydrogen-bond base strength, $\log L^{16}$ describes dispersion interactions, R_2 is a quantitative measure of the ability of a solute to interact with a solvent through n and π electron pairs, and π_2^H measures the ability of a compound to stabilize a neighboring charge or dipole. A more detailed description of each variable and collections of solute parameters may be found in the extensive work of Abraham *et al.* [18-36]. From expression (4.3), K_{SAW} values can be calculated for each analyte and film. Once K_{SAW} values and the appropriate solvation parameters are known, linear solvation energy relationships (LSERs) can be developed to determine the values of the coefficients a, b, l, r, and s in equation (4.4). The relative magnitude of these coefficients describes the contribution of specific analyte/film interaction mechanisms to analyte partitioning [10,18].

In previous work, continuous flow sample introduction systems have been used to collect K_{SAW} data for comparison with K_{GLC} values [9,37]. For the same temperature, $\log K_{SAW}$ values were greater than $\log K_{GLC}$. This was attributed to differences in vapor concentration, temperature, and/or changes in the viscoelastic properties of the polymer film induced by vapor sorption [37]. K_{GLC} determinations were also combined with solute solvation parameters to explain phase interactions for a SAW coating [9,18]. More recently, Patrash and Zellers [38] have used a continuous flow system to examine the behavior of SAW devices coated with OV-275, OV-25, poly(phenyl ether), and

poly(isobutylene). These authors also reported detailed interpretations of SAW responses in terms of boiling point, solubility parameter, and LSER models.

Pulsed sample introduction has also been utilized widely in the study of mass sensors [18,39-45]. Janghorbani and Freund have successfully used a QCM as a GC detector [44]. Edmonds and West have used pulsed sample introduction in combination with QCMs coated with GLC phases to detect various organic species [45]. Grate and Abraham have pointed out that this type of sample introduction can be used in conjunction with laser or thermal desorption [18]. Grate et al. [46] have used thermal desorption of analyte from preconcentrator tubes to deliver pulses of gas to an array of SAW devices. While the specific details of pulsed introduction methods may vary, the analyte of interest usually reaches the SAW device as a plug, interacts with the coated surface, desorbs, and is rapidly swept out of the test cell.

In continuous flow sample introduction systems, the response is usually measured after the film has equilibrated with the analyte. The response magnitude is believed to depend only on the partition coefficient of the analyte into the film and any modulus changes that accompany analyte sorption. The pulse measurement is a dynamic one that may convolute analyte diffusion with partitioning phenomena and thus the applicability of equilibrium solubility models is questionable. Indeed, recent work has emphasized the importance of the response kinetics of quartz crystal microbalances when challenged with a vapor [47]. Freeman *et al.* [47] have shown that on a QCM, the rate constants for the response of AT100, OV-101, Carbowax 20M, and ethyl cellulose coatings to the same

vapor were different. It was also shown that the response of an ethyl cellulose coated sensor to three different vapors resulted in three different rate constants.

In this work, the response of poly(isobutylene) [abbreviated PIB] coated mass sensors to various analytes containing a variety of functional groups has been determined using a pulse injection system. To compare the results from the pulsed system to the more conventional continuous flow system, a new parameter, termed the "pulse coefficient" (P_{SAW} or P_{OCM}), is calculated using equation 4.5.

$$\Delta f_{v} = \frac{\Delta f_{s} C_{v} P_{SAW}}{\rho_{s}}$$
 (4.5)

This new parameter is analogous to the more traditional K_{SAW}. However, the pulse parameter does not represent a partition coefficient and may actually be a combination of contributions from both vapor/film diffusion kinetics and partitioning effects. We would like to determine if the film response kinetics reported by Freeman *et al.* [47] play an important role for our pulse measurements. Finally, the pulse coefficient is used in combination with analyte solvation parameters to develop LSER expressions for the PIB coated mass sensors.

4.3 Experimental

Materials. Poly(isobutylene) (MW = 380,000) was obtained from Aldrich chemical company. Analytes were obtained from either Aldrich or Baker chemical companies and used as received. Table 4.1 shows the boiling points and solvation parameters for the analytes examined in this study. Analytes were chosen to examine analyte/film interactions for molecules with a wide range of chemical functionalities,

List of analytes, boiling points, and the solvation energy parameters used in this work [18-36]. Table 4.1.

_																						
	Dipole	π_2^H	0.53	0.70	0.44	0.00	0.52	0.10	0.36	0.56	0.40	0.00	0.45	89.0	0.52	0.84	0.42	0.95	0.28	0.00	0.73	0.00
	Interactions Polarizability	R ₂	0.369	0.179	0.278	0.000	0.610	0.305	0.212	0.687	0.524	0.000	0.000	0.143	0.601	0.631	0.224	0.242	0.640	0.000	0.613	0.000
Dispersion		$logL^{16}$	1.830	1.696	0.970	2.668	2.786	2.964	1.764	2.819	3.000	3.173	0.260	2.755	3.325	3.020	2.301	2.894	3.580	3.677	2.865	4.182
H-bond	Base Stength	$\Sigma \beta_2^H$	0.13	0.49	0.47	0.00	0.14	0.00	0.56	0.15	0.03	0.00	0.35	0.51	0.14	0.52	0.48	0.31	0.00	0.00	0.29	0.00
H-bond	Acid Strength	$\Sigma lpha_2^H$	0.00	0.04	0.43	0.00	0.00	0.00	0.33	0.00	0.00	0.00	0.82	0.00	0.00	0.00	0.37	0.00	0.00	0.00	0.41	0.00
	Boiling	Point (°C)	31	26	65	69	80	81	82	%	87	86	90	101	111	116	117	120	121	126	131	151
		Analyte	furan	acetone	methanol	hexane	benzene	cyclohexane	isopropanol	thiophene	trichloroethylene	heptane	water	2-pentanone	toluene	pyridine	1-butanol	nitropropane	perchloroethylene	octane	pyrrole	nonane
		Number	1	7	က	4	2	9	7	∞	6	10	11	12	13	7	15	16	17	18	19	70

molecular weights, and boiling points. Furan, thiophene, pyridine, and pyrrole were studied to determine the selectivity for aromatic heterocycles. Benzene, 2-pentanone, pyridine, 1-butanol, and nitropropane were studied because they are used to determine McReynolds constants for chromatographic stationary phases [48]. In the context of LSER expressions, the alkanes mainly interact through dispersion interactions. Trichloroethylene and perchloroethylene interact through dispersion, polarizability, and dipole mechanisms. Furan, benzene, thiophene, 2-pentanone, toluene, pyridine, and nitropropane interact through dispersion, polarizability, dipole, and H-bond base type interactions. Acetone, methanol, isopropanol, water, and 1-butanol interact through all five mechanisms.

Surface Acoustic Wave (SAW) System. Data were obtained using a 200 MHz SAW resonator array microbalance (Femtometrics, Costa Mesa, CA) that has been described previously [49]. The array device consists of 6 individual resonators mounted on a single stage that is directly inserted into the circuit board. The frequency difference between each resonator and the separate reference device (beat frequency) is the measured signal. Power is supplied and frequency counted by an external unit provided by the manufacturer. The SAW device exhibits a 904 Hz frequency shift when perturbed by a 1 nanogram mass change.

A schematic diagram of the 13.5 mL cell and experimental apparatus is shown in Figure 4.1. Analytes were delivered to the cell as a pulse using a Varian autosampler Series 8000 and a Varian gas chromatograph injector operated at 300°C. The pneumatic

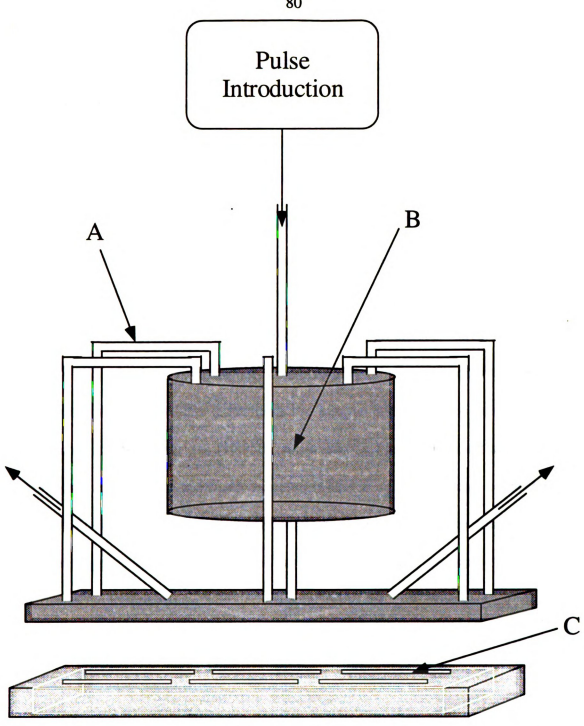


Figure 4.1. Schematic diagram of the SAW sensor test cell. The sample is introduced as a pulse and then split equally into 6 streams. Each of the streams is delivered directly onto the SAW surface. (a) is one of the six delivery arms, (b) is the mixing chamber, and (c) is one of the 6 resonators mounted on a gold stage.

pressure is provided from a standard laboratory gas cylinder, while purified gas with controlled flow rates are supplied to the injector by Porter Mass Flow Controllers. Both the actuators and the cell use nitrogen gas. The temperature of the test cell was controlled by resistance heating of the transfer line. Transfer line temperatures are approximately 120°C. Typical operating conditions are 40 cc/min flow of N₂ (99.95%, AGA Gas Co.) dried over molecular sieves and test cell temperatures of 30°C. Normally, six injections of each analyte were made on at least three devices to ensure reproducibility. Typical RSDs over all devices were 10%.

The vapor generation system and operating procedures have been detailed elsewhere [50]. Analyte concentration is controlled by adjusting the relative flow rates of carrier gas through a bubbler containing the analyte and a dilution gas line. Total flowrates of dry N₂ carrier gas (99.95%, AGA Gas Co.) are maintained at 100 cc/min. Vapor concentrations are measured using an in-line 5 cc sample loop connected to a Varian 3700 GC equipped with a flame ionization detector. Each run consists of a two minute nitrogen purge, vapor exposure for a period of time necessary for the SAW response to equilibrate, and a nitrogen purge equal to the time necessary for vapor/film equilibration. Data are collected at 2 Hz resolution. Poly(isobutylene) films are prepared by spray casting from dilute toluene or chloroform solutions (~500 ppm). Typical film thicknesses were 100 kHz, which corresponds to 0.012 μm. The devices were cleaned by rinsing with acetone and methanol, soaking in isopropanol, and drying in air.

SAW Data Acquisition and Manipulation. The beat frequency of each resonator was collected using a digital counting board (MetraByte, Taunton, MA) and

stored in a Gateway 2000 386-25 personal computer. The software used to collect the data was written by the manufacturer, and is capable of collecting data for all 6 channels at resolutions of 1-100 Hz (0.2-6 sec). The standard software has been modified by Femtometrics to allow for timed, multiple runs that fully utilize the capabilities of the Varian autoinjector. In this study, data analysis was performed using custom software written using LabView for Windows (v2.52, National Instruments, Austin, TX). This software separates the data output file into individual channels and displays the response of all 6 channels simultaneously on a single page. Additionally, the software counts peaks, determines peak heights, peak areas, and then calculates averages, standard deviations, and %RSDs. It also allows user selection of either none, Savitsky-Goolay smoothing, or median filtering of the data, and provides some control over the sensitivity of the peak determination. The capabilities of the software are described in further detail elsewhere [51].

Quartz Crystal Microbalance (QCM). Quartz crystal microbalance measurements were performed using 6 MHz quartz crystal microbalances from Maxtek Inc. (Torrance, Calif.). A model TM-100 Thickness Monitor (Maxtek Inc.) was used to determine the mass of polymer coating and the response of the coated device to analytes. The output voltage of the thickness monitor was recorded using a Hewlett-Packard 3394A integrator. The 6 MHz device exhibits a 53 Hz frequency shift when perturbed by a 1 microgram mass change.

The QCM sensor test apparatus shown in Figure 4.2 is similar to the SAW apparatus except that the volume of the cell is 8 mL. Analytes were delivered to the cell

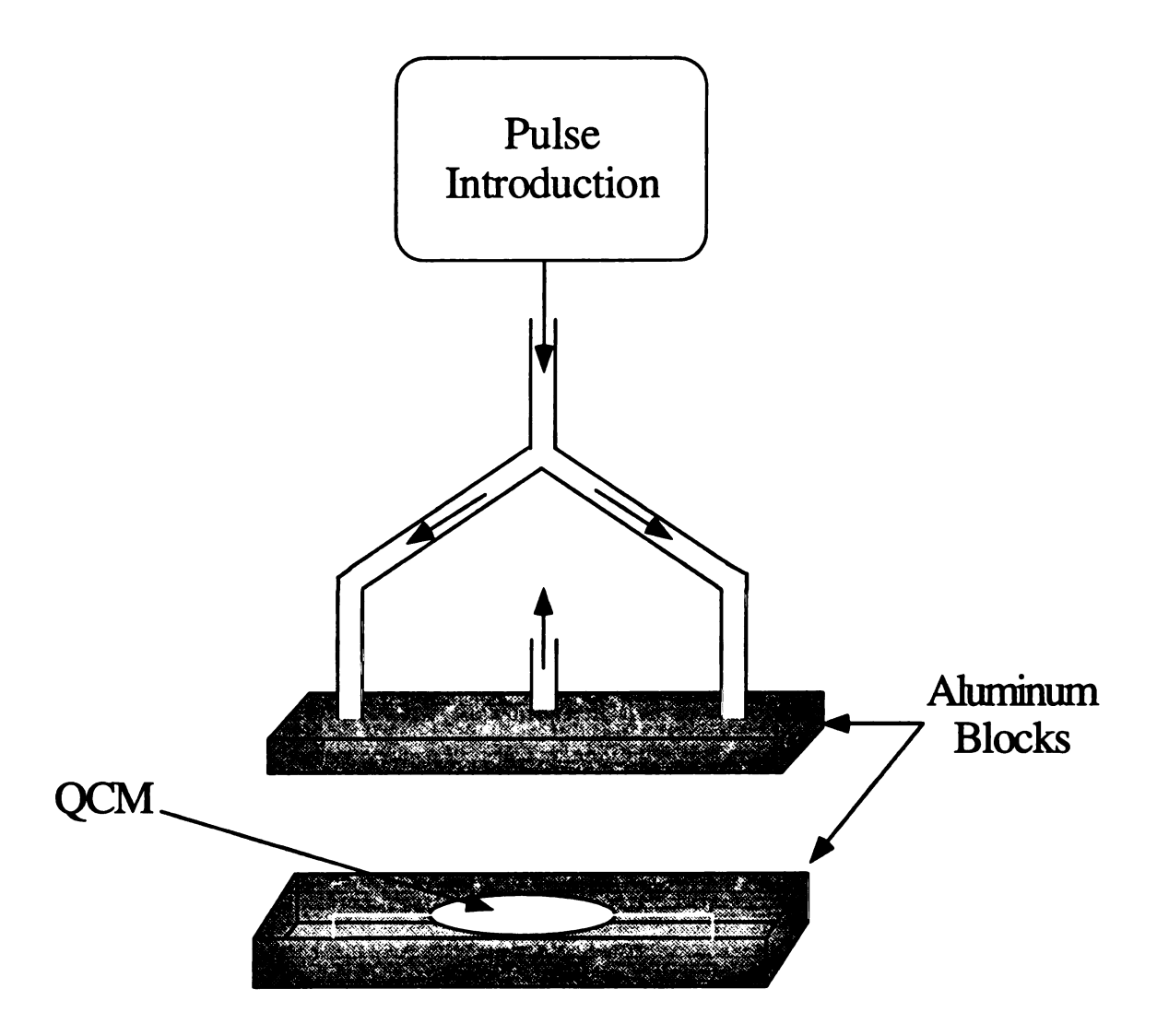


Figure 4.2. Schematic diagram of the QCM sensor test cell. The QCM is positioned in the center of the cell, and the sample is introduced as a pulse and then split equally into 2 streams. The streams are delivered to the left and the right of the device.

as a pulse using a gas chromatograph injector operated at 240°C. Typical operating conditions are 20 mL/min flow of N₂ (99.95%, AGA Gas Co.) dried over molecular sieve and a test cell temperature of 30°C. The temperature of the test cell was controlled by resistance heating of the transfer line. For the QCM measurements, at least three injections of each analyte were made to ensure reproducibility. For the blanks and each film, data were collected on at least three devices. The QCM data have typical RSDs of 6%.

QCM crystals were cleaned following procedures similar to those used for the SAW devices. Cleaned crystals were placed in the oscillator circuit and the thickness monitor set to zero. Crystals were spray coated with the polymer solution and allowed to dry in air. Films of approximately 0.038 µm thickness (~3.54 µg) were used in this study. In both types of acoustic measurements, analyte injection order was varied to minimize the effect of analyte order on sensor response. Mass sensor responses are reported as the maximum frequency shift in hertz per micromole (QCM) or nanomole (SAW) of analyte injected to normalize the response for each analyte. Responses are plotted against analyte boiling point to determine the effect of condensation on sensor response.

Linear Solvation Energy Relationship (LSER) Calculations. Linear solvation energy relationships were developed from equation (4.4) by multiple linear regression analysis using the analyte solvation parameters (Table 4.1) and the pulse coefficients calculated according to equation (4.3). Note that in most of this study P_{SAW} or P_{OCM} is

calculated instead of K_{SAW} . The vapor concentration (C_V) used in equation (4.3) is taken as the mass of analyte injected divided by the volume of the test cell. A Gateway 2000 4DX2-66V computer running Microsoft Excel (Microsoft Corporation, Redmond, WA) was used to calculate the multiple linear regressions. The solvation parameters not found in the literature were calculated in a manner consistent with those suggested by Abraham et al. [19-36].

4.4 Results and Discussion

Response of Uncoated Mass Sensors. QCM. Figure 4.3 shows the variation in sensor response as a function of analyte boiling point for the uncoated QCM device. With the exception of trichloroethylene (bp=87°C) and perchloroethylene (bp=121°C), the response of the uncoated QCM increases steadily with analyte boiling point. The large responses observed for trichloroethylene (TCE) and perchloroethylene (PCE) may be explained in terms of the surface structure of the QCM devices used in this work. Much of the QCM surface is covered with a gold film used to make electrical contact with the quartz piezoelectric crystal. It is well known that chlorine interacts strongly with gold. Thus we attribute the high responses measured for TCE and PCE to the strong interaction of the chloride substituent with the gold surface.

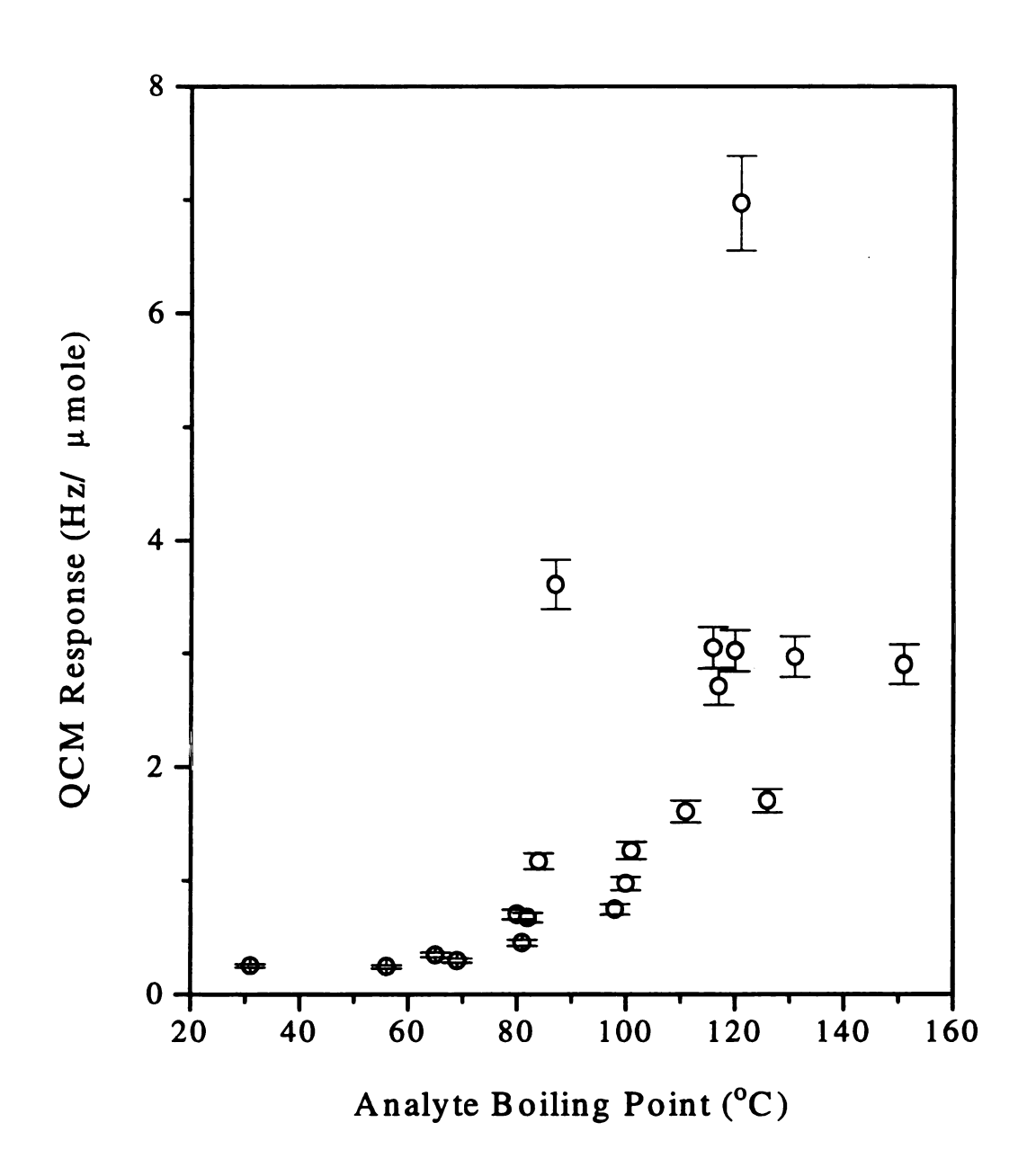


Figure 4.3. Variation of uncoated QCM device response (Hz/ μ mole) versus analyte boiling point.

SAW. The variation in sensor response as a function of analyte boiling point measured for the uncoated SAW device is shown in Figure 4.4. With the exception of isopropanol (bp=82°C), water (bp=100°C), and 1-butanol (bp=117°C), the response generally increases with analyte boiling point. Isopropanol, water, and 1-butanol exhibit larger frequency shifts than analytes of comparable boiling point. This enhanced response may be attributed to the attraction between these polar molecules and the polar SAW device surface (SiO₂), and the fact that alcohols tend to self associate. Martin *et al.* [52] have also shown that polar molecules bind more strongly to a polar quartz surface and that analyte-analyte interactions (self association) are significant for polar molecules.

The general trend of increase in frequency shift with increasing boiling point observed for the QCM and SAW devices indicates that the sensor response is strongly affected by analyte physisorption. King [53] proposed that analytes with higher boiling points are able to achieve a higher level of partitioning into a film. While it is not possible for partitioning to occur on an uncoated device, it is reasonable to expect condensation effects to produce similar results. Patrash and Zellers [38] have also shown that an increase in analyte boiling point increases the SAW response in continuous flow experiments.

Response of Poly(isobutylene) Coated Devices. QCM. Figure 4.5 shows the variation in sensor response as a function of analyte boiling point for the PIB coated QCM. The response trend is similar to that of the uncoated device; however, the response magnitudes are approximately three times larger. Table 4.2 shows the PIB coated/blank QCM response ratio calculated for each of the analytes. Responses for

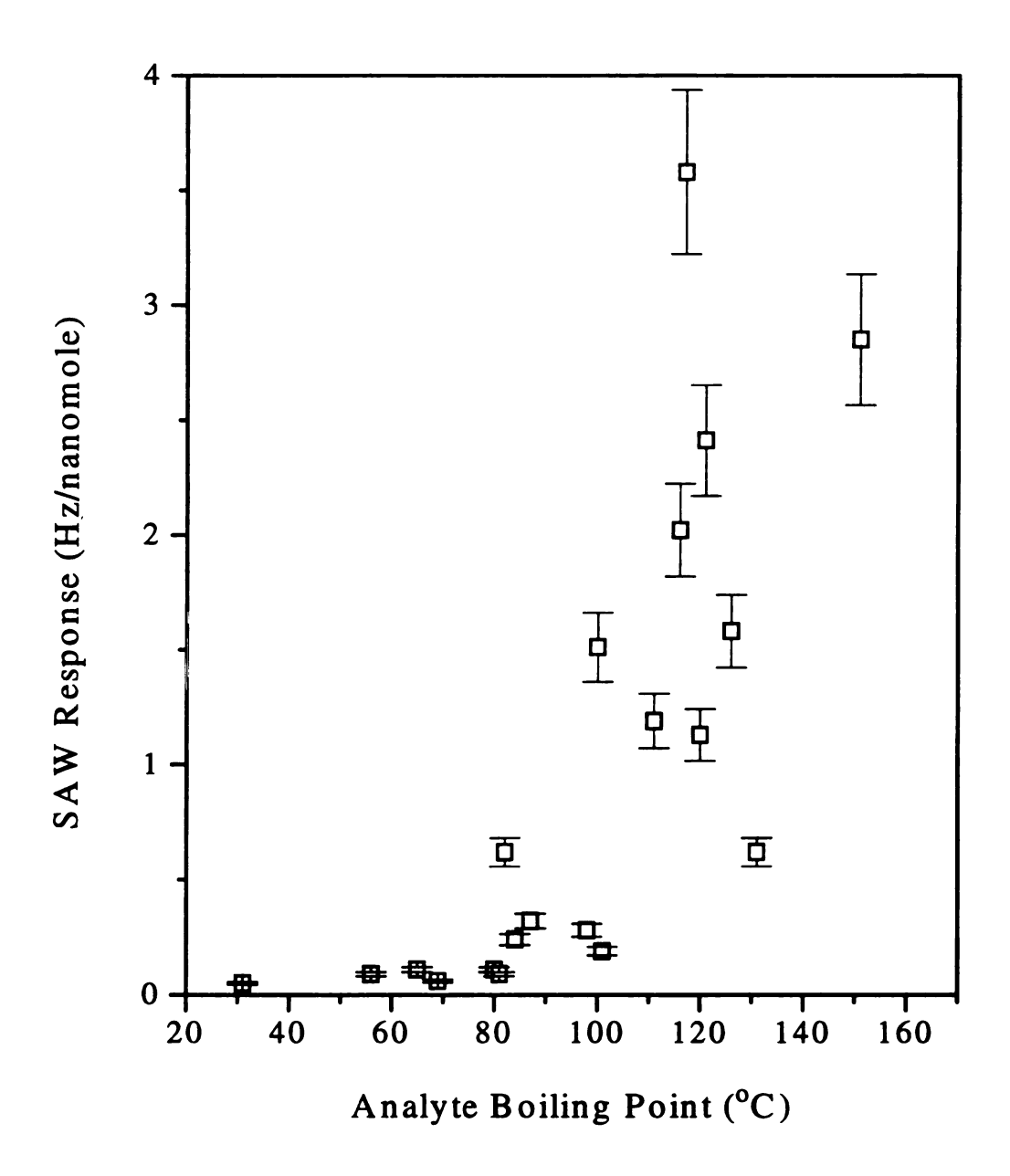


Figure 4.4. Variation of uncoated SAW device response (Hz/nanomole) versus analyte boiling point.

hydrocarbons such as hexane, cyclohexane, octane, and nonane are significantly enhanced for the PIB coated QCM. Isopropanol, water, and 1-butanol responses are similar to the values measured on the blank, while methanol is significantly lower.

As noted for the blank QCM (Figure 4.3), the responses measured for TCE and PCE are significantly greater than values observed for analytes of comparable boiling point. However, these results cannot be attributed to adsorption on exposed gold surfaces since the measured frequency shifts are more than three times those observed for the blank (Table 4.2). Equilibrium data (*vide infra*) collected for TCE and PCE using SAW devices do not indicate that these analytes have anomalously high diffusion rates in the PIB film. Unfortunately, the exact reason for the high response to TCE and PCE is not clear and these findings are under further investigation.

SAW. Figure 4.6 shows the variation in sensor response as a function of analyte boiling point for the PIB coated SAW device. The response for nonane (78 Hz/nanomole) has not been included in the plot in order to emphasize the response trend obtained for analytes of lower boiling point. As noted for the blank, the response of the PIB coated SAW generally increases with increasing analyte boiling point. However, the alcohol and water responses are no longer enhanced relative to the other analyte responses. In fact, only perchloroethylene and nonane could be considered enhanced relative to compounds with similar boiling points. Table 4.2 shows that the average response of the PIB coated SAW device is approximately nine times that of the blank device. The responses measured for acetone, methanol, isopropanol, 1-butanol, and

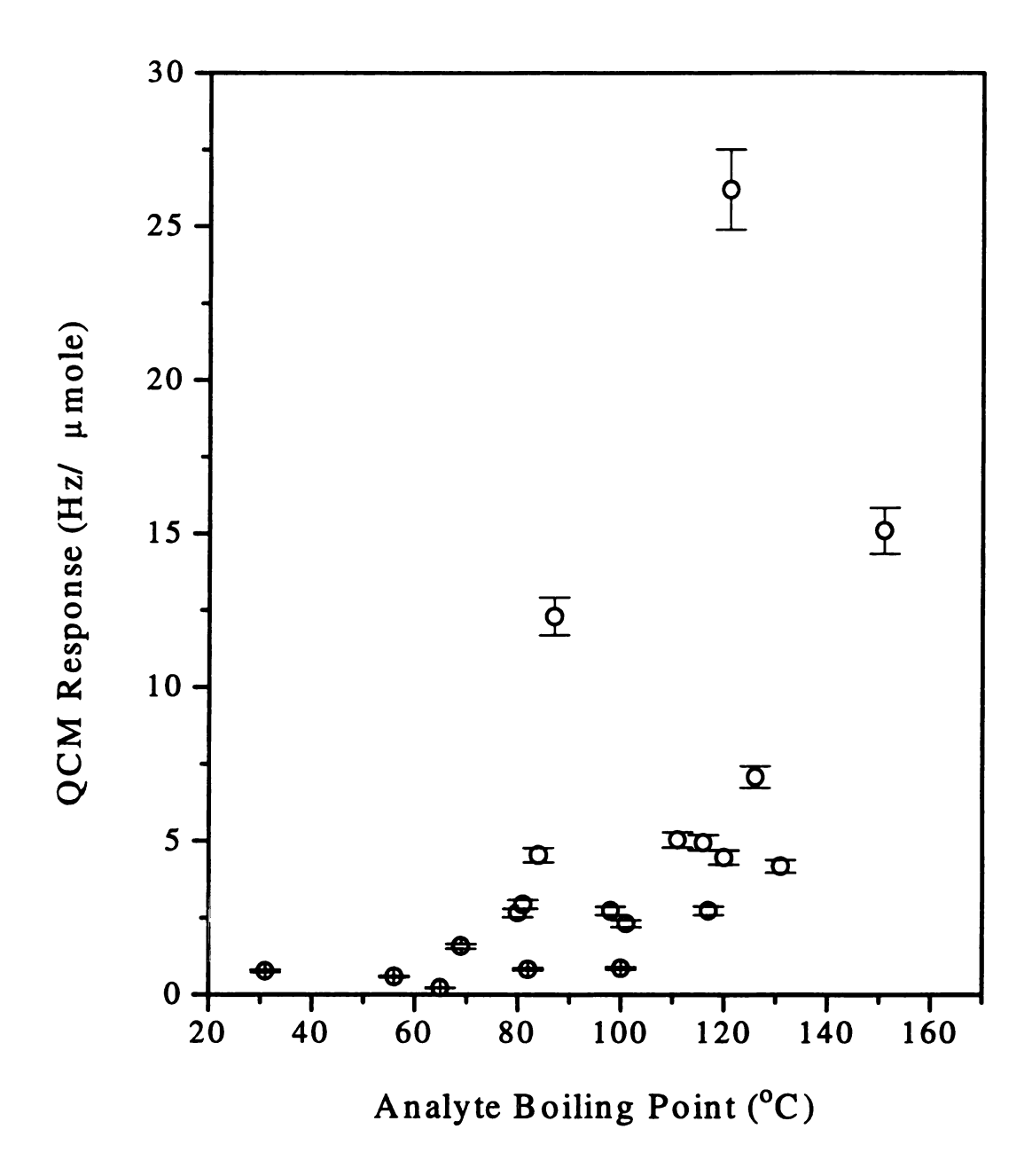


Figure 4.5. Variation in the response of poly(isobutylene) coated QCM device response (Hz/µmole) as a function of analyte boiling point.

Response ratios, pulse coefficients, and partition coefficients for the blank and PIB coated QCM and SAW devices. Table 4.2.

	PIB OCM ^a	PIB SAW b	PIB	PIB	PIB
Analyte	Blank QCM	Blank SAW	log(PQCM)	log(PSAW)	log(K _{SAW})
furan	3.0	8.6	2.20	2.89	
acetone	2.4	1.8	2.17	2.54	
methanol	9.0	8.0	2.16	2.52	1.89
hexane	5.3	14.0	2.36	3.05	2.72
benzene	3.8	12.4	2.67	3.35	
cyclohexane	6.4	20.7	2.66	3.42	
isopropanol	1.2	9.0	2.21	2.88	
thiophene	3.9	80.00	2.84	3.50	
trichloroethylene	3.4	11.6	3.08	3.55	3.27
heptane	3.7	19.8	2.60	3.84	
water	6:0	0.2	2.74	3.40	
2-pentanone	1.8	19.5	2.56	3.72	
toluene	3.1	5.0	2.91	3.90	3.42
pyridine	1.6	4.3	2.91	4.13	
1-butanol	1.0	1.2	2.69	3.85	3.54
nitropropane	1.5	6.0	2.83	3.14	2.62
perchloroethylene	3.8	6.9	3.37	4.09	3.90
octane	4.2	6.9	2.95	4.07	3.81
pyrrole	1.4	10.6	2.91	4.09	
nonane	5.2	26.6	3.20	4.86	

^aRSD is ±5% ^bRSD is ±7%

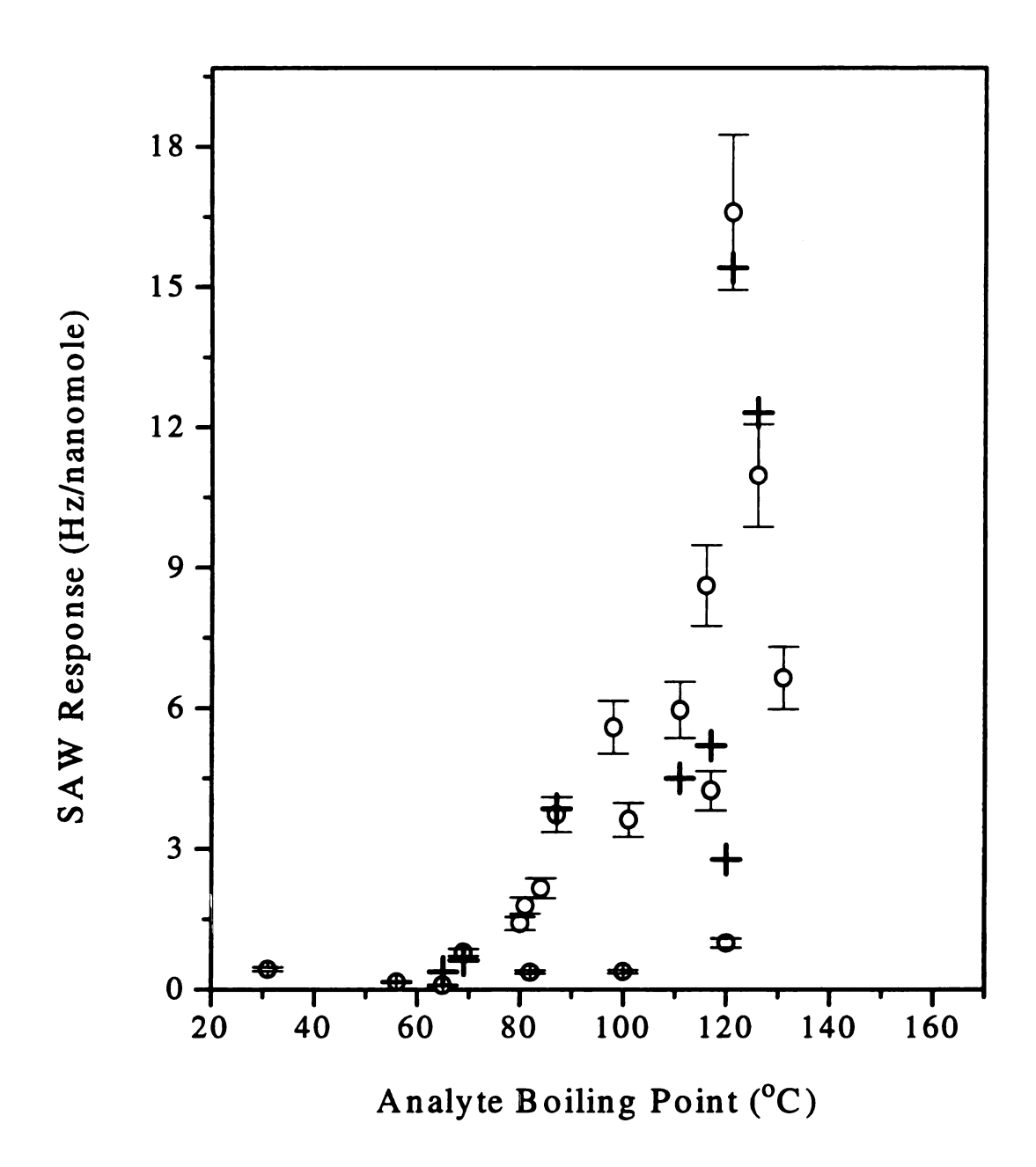


Figure 4.6. Variation in the response of poly(isobutylene) coated SAW device (Hz/nanomole) as a function of analyte boiling point for the pulse injection (O) and continuous flow (+) methods. The response for nonane (78 Hz/nanomole) has not been included in this plot (see text).

nitropropane are comparable to those obtained for the blank device while 2-pentanone and all of the alkanes (excluding octane) show large response enhancements.

The PIB coated SAW response observed for nonane is more than four times the value measured for any other analyte examined in this study. The high boiling point of nonane and the large solubility of alkanes in PIB should lead to considerable sorption of the molecule into the polymer film. However, extensive nonane sorption cannot completely explain the high nonane SAW response because we would also expect to observe a similar enhancement in the QCM data. We believe that the large SAW response to nonane may be attributed to viscoelastic effects that have been reported for PIB coated SAW devices [16,17,37]. Martin et al. [16] have shown that vapor sorption changes the modulii of the film. Ballantine [17] has shown that viscoelastic effects depend on the amount of analyte sorbed in the film and the thickness of the polymer coating. Apparently, condensation and sorption during our pulsed sample introduction results in sufficient nonane content to observe these effects in the SAW data. Similar phenomena may also occur for analytes with lower boiling points; however, the analyte concentration in the films must be too low to observe any significant effects.

Previously, Jurs et al. [54] reported that PIB was the most sensitive SAW coating among 10 coatings tested for isooctane. Our results indicate that there is a large enhancement in alkane response from the blank device to the PIB coated device. However, comparison of alkane responses with values measured for analytes of similar boiling point suggests that selective detection of alkanes in mixtures would be difficult.

Additionally, both Jurs et al. [54] and Grate et al. [37] have shown that for PIB, the frequency shift of toluene was similar to isooctane. In our work, the response to octane (bp=126°C) is larger than toluene. However, interpolation using our results (Figure 4.6) predicts that the responses of isooctane (bp=98°C) and toluene would be similar.

Jurs et al. [54] also reported that the frequency shift caused by water was similar to 1-butanol (both of which gave opposite difference responses). In our data, the magnitude of the water response is low (as noted by Jurs et al. [54]), but the 1-butanol response is greater than that due to water. The most likely explanation for the difference between the 1-butanol response reported in our work and by Jurs et al. [54] is that they used an uncoated delay line as the reference, while we use a sealed device. Jurs et al. [54] reported that their reference signal changed significantly in response to some vapors. Since PIB does not sorb most vapors strongly, they noted that their difference measurements for PIB may be less accurate.

In order to determine if the trend in SAW responses is affected by the method of sample introduction, eight analytes selected from different regions of the response curve were presented to the sensor under continuous flow conditions in order to obtain their equilibrium response. These results are also presented in Figure 4.6 (crosses). For the analytes selected, the responses measured using pulsed sample introduction are similar to those obtained from the equilibrium method. This suggests that the analyte diffusion rates in PIB are comparable and thus the method of sample introduction (pulse or continuous) has little impact on the response trend.

Evaluation of LSER Expressions. Pulse Coefficients. Table 4.2 shows the pulse coefficients calculated for the PIB coated QCM (P_{QCM}) and the pulse and selected partition coefficients calculated for the PIB coated SAW (P_{SAW}, K_{SAW}). The pulse coefficients for the SAW are larger than those calculated for the QCM. In general, the magnitude of the coefficients increases with increasing boiling point and magnitude changes are similar for P_{QCM} and P_{SAW}. We attribute the differences between P_{QCM} and P_{SAW} to the location of the sensor device relative to the inlet gas stream and the resulting effect on our calculation of vapor concentration (C_V) in equation (4.3). The SAW devices are located directly underneath the gas stream, while the QCM is positioned in the center of the cell. This makes our calculation assumption for C_V more accurate and more similar to a continuous vapor stream in the QCM system, while the actual vapor concentration above the SAW at the time of the measurement maybe much larger than our assumed concentration. This would result in higher P_{SAW} values for our measurements.

Comparison of the pulse and selected partition coefficients determined in this work with the partition coefficients for similar vapors reported by Grate *et al.* [9,37] and Patrash and Zellers [38] is shown in Table 4.3. In most instances, the relative magnitudes and trends of the coefficients are similar. However, the absolute magnitudes of the pulse coefficients are greater than the partition coefficient values. We believe that this can be attributed to the fact that the hot vapor (due to the heated injector) presented in the pulsed experiments is more soluble in the film than the room temperature vapor presented by continuous flow.

Comparison of LogPsaw, LogPocm, and LogKsaw with LogKsaw and LogKGLC values from the literature. Table 4.3

		This work		Patrash & Zellers [38] ^a	Grate et o	Grate <i>et al.</i> [9,37] ^b
	PIB @ 30°C	PIB @ 30°C	PIB @ 30°C	PIB @ 25°C	PIB	PIB @ 25°C
Analyte	log(PQCM)	log(PSAW) log(KSAW)	log(KSAW)	log(K _{SAW})	log(KSAW)	log(K _{SAW}) log(K _{GLC})
Methanol	2.16	2.52	1.89	1.92		
Hexane	2.36	3.05	2.72	2.78		
Benzene	2.67	3.35		2.90		
Cyclohexane	2.66	3.42		2.95		
Isopropanol	2.21	2.88		2.37		
Trichloroethylene	3.08	3.55	3.27	3.08		
Toluene	2.91	3.90	3.42	3.39	3.42°, 3.19 ^d	2.76
Pyridine	2.91	4.13		3.37		
1-butanol	2.69	3.85	3.54	3.11	3.15	2.20
Nonane	3.20	4.86		4.04		

^aData obtained with 200 kHz films on 158 MHz SAW devices. ^bData obtained with 280 kHz films on 200 MHz SAW resonators. CData obtained at 25°C. Data obtained at 35°C.

LSER Coefficients. Table 4.4 shows the results of the multiple linear regression analyses performed on data obtained from both the PIB coated QCM and SAW devices. Initially, regressions were performed using all the analytes. This resulted in LSER equations with very large a coefficients, suggesting that the film acts as a hydrogen bond donor. Since PIB is a nonpolar polymer, one would not expect hydrogen bond donation to be an important interaction mode for the film. Closer examination of the data reveals that the alcohols may be unfairly influencing the fit. The influence of these polar hydrogen bonding compounds can be seen in their high α and low dispersion solvation parameters. Grate et al. [37] have also reported that alcohols incorrectly influence regression analysis and removed alcohol data to produce improved regressions. Patrash and Zellers [38] reported that alcohols deviated significantly from predictions based on the boiling point model and performed a separate regression analysis for these analytes.

We have also examined the effect of removing alcohol data from our regression calculations. Following the removal of the alcohol data, the a coefficient is statistically insignificant (P_{stat}=0.06). Furthermore, the improved correlation coefficients (0.91) for both the SAW and QCM regressions, despite utilizing a relatively small number of analytes, demonstrates the influence of the alcohols on the fit. These fits indicate that PIB cannot act as a hydrogen bond acceptor, solute polarizability is not important, and dispersion interactions are the main mode for analyte/film interactions. Similar findings were reported by Grate and Abraham [18].

Table 4.4 also shows a comparison of the film coefficients determined in this study with similar work in the literature. Patrash and Zellers [38] found that both the

Results of LSER fits using the QCM and SAW data and different solvation parameters.^a **Table 4.4.**

Series	ပ	В	þ	l	L	S	correlation coefficient
SAW Results Initial Regression Only α and $\log L^{16}$	0.98 (0.028) 1.07 (0.002)	2.11 (4.1 x 10 ⁴) 2.09 (7.3 x 10 ⁻⁵)	0.03	0.87 (4.0 x 10 ⁻⁶) 0.84 (1.4 x 10 ⁻⁷)	-0.09 (0.81)	0.13	0.82
QCM Results Initial Regression Only α and logL ¹⁶	1.39 (7.3 x 10 ⁻⁵) 1.42 (1.6 x 10 ⁻⁵)	1.24 (7.6 x 10 ⁴) 1.03 (4.7 x 10 ⁻³)	-0.72 (0.057)	0.41 (7.8 x 10 ⁻⁵) 0.44 (2.7 x 10 ⁻⁵)	0.14 (0.54)	0.45 (0.12)	67.0
Patrash and Zellers [38] PIB (25°C) (full data set) PIB (25°C) (reduced data set)	-0.416 0.418	0.875 1.03	0.275 0.226	0.869		-	
Abraham et al. [27] Squalene (80°C) Squalene (100°C)	-0.21			0.735 0.674	0.11	0.08	
Abraham et al. [28] Squalene (121.4°C)	-0.202	-0.097		0.581	0.125	0.018	

^a P_{Stat} values are in parenthesis.

polarizablity and dipole coefficients did not make significant contributions to the fit and did not include their values. Comparing our data at 30°C to that of Patrash and Zellers [38], we find that there is a consistent difference between the dispersion terms in each case. Abraham *et al.* [27,28] performed LSER calculations for squalene, which may be considered a close GLC analog to PIB. In one instance, Abraham *et al.* [27,] found that squalene did not have significant α or β contributions, but later [28] reported significant α contributions for squalene. When comparing our values to those of Abraham *et al.* [27,28], it is important to emphasize that squalene is simply an approximation to PIB, and that the values for squalene were obtained at much higher temperatures. However, comparison of the data still indicates that both expressions predict dispersion to be the major mode of interaction. Other variations in the calculated LSER coefficients can be attributed to differences in the number and classes of compounds in the analyte sets.

Table 4.5 shows the calculated contributions from the common statistically significant parameters to the logK_{SAW} and logP_{SAW} term for analytes present in both our experiments and those of Patrash and Zellers [38]. The sum of the calculated contributions for the analytes do not equal 100% because not all of the contribution are presented. There should be some differences in the percent contribution from each type of interaction because the styles of the fits are different. Patrash and Zellers [38] fit only 4 parameters in the LSER expression. Nevertheless, the dispersion interactions for the hydrocarbons agree to within approximately 12%.

Table 4.5. Comparison of the contributions from each of the common statistically significant interaction parameters to $logK_{SAW}$ and $logP_{SAW}$ for poly(isobutylene).

	% contr	_	SAW and logK _{SA} logI	
Analyte	This work ^a	Ref [38] ^b	This work ^a	Ref [38] ^b
Methanol	36	20	33	44
Hexane	0	0	76	84
Isopropanol	24	12	53	65
Benzene	0	0	72	83
Cyclohexane	0	0	75	88
Trichloroethylene	0	0	74	85
Toluene	0	0	94	85
Pyridine	0	0	64	78
1-butanol	20	10	52.	73
Nonane	0	0	75	90

^aUsing the LSER fit obtained at 30°C with 100 kHz PIB films on 200 MHz resonator SAW devices. This work determined that b, r, and s terms are not significant. ^bUsing the LSER fit obtained at 25°C with 200 kHz PIB films on 158 MHz SAW devices. Patrash and Zellers determined that both the r and s terms are not significant.

4.5 Conclusion

Our work has shown that mass sensor responses obtained using a pulsed sample introduction technique can provide meaningful chemical insight into analyte/film interaction mechanisms for PIB films. In the absence of other complicating factors, we anticipate that similar success can be achieved in the study of any coating provided the relative analyte diffusion rates in the material of interest are comparable. Pulsed response data can be used to calculate pulse coefficients that are analogous to partition coefficients obtained from equilibrium data. We have shown that these pulse coefficients can be used to determine useful LSER expressions. This was demonstrated by examining the calculated contributions and types of interactions suggested by LSER coefficients. These contributions are similar to results obtained by others using equilibrium data. The calculated LSER expression for the film, used in conjunction with the analyte parameters, clearly shows the major mode of analyte/PIB interaction to be dispersion forces. This is also consistent with previously reported research. The magnitudes of the pulse coefficients are larger than partition coefficients determined in this study and in the literature. This variation may be attributed to our different method of calculation for the analyte vapor concentration and the increased solubility of hot gases in the film. Finally, it should be noted that this experimental approach is simple, convenient, and capable of providing fundamental insight into analyte/film interactions that occur in practical pulse sampling applications of mass sensors.

4.6 References

- 1. Wohltjen, H.; Dessy, R. Anal. Chem. 1979, 51, 1458.
- 2. Wohltjen, H.; Dessy, R. Anal. Chem. 1979, 51, 1465.
- 3. Wohltjen, H.; Dessy, R. Anal. Chem. 1979, 51, 1470.
- 4. Grate, J. W.; Martin, S. J.; White, R. M. Anal. Chem. 1993, 65, 940A.
- 5. Grate, J. W.; Martin, S. J.; White, R. M. Anal. Chem. 1993, 65, 987A.
- 6. Ballantine, D. S., Jr.; Wohltjen, H. Anal. Chem. 1989, 61, 704A.
- 7. Fox, C. G.; Alder, J. F. Analyst (London) 1989, 114, 997.
- 8. Nieuwenhuizen, M. S.; Venema, A. Sens. Mater. 1989, 5, 261.
- 9. Grate, J. W.; Snow; A.; Ballantine; D. S., Jr.; Wohltjen, H.; Abraham, M. H.; McGill, R. A.; Sasson, P. Anal. Chem. 1988, 60, 869.
- 10. Ballantine, D. S.; Rose, S. L.; Grate, J. W.; Wohltjen, H. Anal. Chem. 1986, 58, 3058.
- 11. Wohltjen, H. Sens. Actuators 1984, 5, 307.
- 12. Snow, A. W.; Wohltjen, H. Anal. Chem. 1984, 56, 1411.
- 13. Frye, G. C.; Martin, S. J. Appl. Spectrosc. Rev. 1991, 26, 73.
- 14. McCallum, J. J. Analyst(London) 1989, 114, 1173.
- 15. Katritzky, A. R.; Offerman, R. J. CRC Anal. Chem. 1989, 21(2), 83.
- 16 Martin, S. J.; Frye, G. C.; Senturia, S. D. Anal. Chem. 1994, 66, 2201.
- 17. Ballantine, D. S., Jr. Anal. Chem. 1992, 64(24), 3069.
- 18. Grate, J. W.; Abraham, M. H. Sens. & Act. B. 1991, 3, 85.
- 19. Abraham, M. H. Pure Appl. Chem. 1993, 65(12), 2503.
- 20. Abraham, M. H. Chem. Soc. Rev. 1993, 22, 73.
- 21. Abraham, M. H.; Whiting, G. S.; Doherty, R. M.; Shuely, W. J. J. Chem. Soc. Perkin. 2 1990, 1451.
- 22. Abboud, J.-L. M.; Kamlet, M. J.; Taft, R. W. J. Am. Chem. Soc. 1977, 99, 8325.
- 23. Abraham, M. H.; McGowan, J. C. Chromatographia 1987, 23, 243.
- 24. Abraham, M. H.; Whiting, G. S.; Doherty, R. M.; Shuely, W. J. *J. Chromatogr.* 1991, 587, 213.
- 25. Taft, R. W.; Abboud, J-L. M.; Kamlet, M. J. J. Am. Chem. Soc. 1981, 103, 1080.
- 26. Abraham, M. H.; Grellier, P. L.; McGill, R. A. J. Chem. Soc. Perkin Trans. 2 1987, 797.

- 27. Abraham, M. H.; Whiting, G. S.; Doherty, R. M.; Shuely, W. J. *J. Chromatogr.* **1990**, *518*, 329.
- 28. Abraham, M. H.; Whiting, G. S.; Doherty, R. M.; Shuely, W. J. J. Chromatogr. 1991, 587, 229.
- 29. Abraham, M. H.; Grellier, P. L.; Prior, D. V.; Morris, J. J.; Taylor, P. J. J. Chem. Soc. Perkin. Trans. 2 1990, 521.
- 30. Abraham, M. H.; Grellier, P. L.; Prior, D. V.; Duce, P. P.; Morris, J. J.; Taylor, P. J. J. Chem. Soc. Perkin. Trans. 2 1989, 699.
- 31. Abraham, M. H.; Duce, P. P.; Grellier, P. L.; Prior, D. V.; Morris, J. J.; Taylor, P. J. *Tetrahedron Lett.* **1989**, 29, 1587.
- 32. Abraham, M. H.; Duce, P. P.; Grellier, P. L.; Prior, D. V.; Morris, J. J.; Taylor, P. J. *Tetrahedron Lett.* **1989**, *30*, 2571.
- 33. Abraham, M. H.; Grellier, P. L.; McGill, R. A.; Doherty, R. M.; Kamlet, M. J.; Hall, T. N.; and Taft, R. W.; Carr, P. W.; Koros, W. J. *Polymer* **1987**, *28*, 1363.
- 34. Abraham, M. H.; Fuchs, R. J. Chem. Soc. Perkin. Trans. 2 1988, 523.
- 35. Kamlet, M. J.; Abboud, J-L, M., Abraham, M. H.; Taft, R. W. J. Org. Chem. *J. Org. Chem.* 1983, 48, 2877.
- 36. Patte, F.; Etcheto, M.; Laffort, P. Anal. Chem. 1982, 54, 2239.
- 37. Grate, J. W.; Klusty, M.; McGill, R. A.; Abraham, M. H.; Whiting, G.; Andonian-Haftvan, J. Anal. Chem. 1992, 64, 610.
- 38. Patrash, S. J.; Zellers, E. T. Anal. Chem. 1993, 65, 2055.
- 39. Suleiman, A; Guilbault, G. G. Anal. Chim. Acta 1984, 162, 97.
- 40. Thompson, M.; Stone, D. C. Anal. Chem. 1990, 62, 1895.
- 41. Hecki, W. M.; Marassi, F. M.; Kallury, K. M. R.; Stone, D. C.; Thompson, M. *Anal. Chem.* 1990, 62, 32.
- 42. Thompson, M.; Stone, D. C.; Nisman, R. Anal. Chim. Acta 1991, 248, 143.
- 43. Yan, Y.; Bein, T. J. Phys. Chem. 1992, 96, 9387.
- 44. Janghorbani, M.; Freund, H. Anal. Chem. 1973, 45, 325.
- 45. Edmonds, T. E.; West, T. S. Anal. Chim. Acta 1980, 117, 147.
- 46. Grate, J. W.; Rose-Pehrsson, S. L.; Venezky, D. L.; Klusty, M.; Wohltjen, H. *Anal. Chem.* 1993, 65, 1868.
- 47. Freeman, N. J.; May, I. P.; Weir, D. J. J. Chem. Soc., Faraday Trans. 1994, 90, 751.
- 48. McReynolds, W.O. J. Chromatogr. Sci. 1970, 8, 685.

- 49. Bowers, W. D.; Chuan, R. L.; Duong, T. M. Rev. Sci. Instrum. 1991, 62, 1624.
- 50. E.B. Townsend IV, Ph.D. Thesis, Michigan State University, 1995.
- 51. E.B. Townsend IV, J.S. Ledford, D.P. Hoffmann, accepted for publication in *Rev. Sci. Instrum*.
- 52. Martin, S. J.; Ricco, A. J.; Ginley, D. S.; Zipperian, T. E. *IEEE Trans. Ultrason.* **1987**, UFFC-34, 142.
- 53. King Jr., W. H. Anal. Chem. 1964, 36, 1735.
- 54. Rose-Pehrsson, S. L.; Grate, J. W.; Ballantine, D. S., Jr.; Jurs, P. C. *Anal. Chem.* **1988**, *60*, 2801.

Chapter 5

An FTIR/ATR Study of Sorbent Induced Polymer Swelling: Application to the Study of Surface Acoustic Wave Sensors

5.1 Abstract

Poly(isobutylene) films coated on surface acoustic wave (SAW) devices and FTIR/ATR internal reflection elements were exposed to nitromethane, isooctane, and perchloroethylene vapors. A correlation was found between the spectroscopic indication of vapor induced polymer swelling and the responses of polymer coated SAW devices to the same vapors. The sorption of perchloroethylene and isooctane caused PIB films to swell significantly while sorption of nitromethane swelled PIB films to a lesser degree. This correlates to literature swelling estimates determined for the same or similar vapors. It was noted that observed polymer swelling occurs nearly simultaneously with analyte sorption. Finally, both IR and SAW results indicate that the polymer swelling changes were reversible.

5.2 Introduction

Surface Acoustic Wave (SAW) devices have been widely studied as vapor sensors [1-15]. The response of such devices coated with thin elastic films has been described using an expression that includes contributions from mass loading and mechanical properties of the film [16]. Initially, the influence of thin film mechanical properties on

the sorption induced frequency shift of the device was thought to be negligible compared to mass loading effects. Thus, polymer-coated SAW devices were often considered to be simply mass sensors. However, it is now widely reported that changes in mechanical properties contribute significantly to the response of SAW-based vapor sensors [14,15,17-19].

Vapor sorption expands polymer volume [20] and, essentially, dilutes the film. This dilution reduces the polymer inter- and intra- chain interactions and decreases polymer modulus. Grate *et al.* [17] have suggested that for a polymer coated SAW device, temperature or vapor induced polymer swelling decreases the film modulus and SAW device frequency. Recently, Martin *et al.* [19] have provided extensive insight into film modulus changes caused by temperature and vapor sorption. They presented models that describe changes in velocity and attenuation for acoustically thin and thick polymer film coatings. These authors also described the dependence of the film thickness and film density on the amount and specific volume of the sorbed vapor.

We are interested in using FTIR/attenuated total reflection (ATR) spectroscopy [21,22] to examine analyte/film interactions that occur in acoustic sensor coatings. FTIR/ATR is often used for solution analysis. Polymer thin films have been examined using various types of contact samplers [23]. FTIR/ATR can also be used to study Polymer films coated onto the internal reflectance element (IRE). In addition, polymer coated IREs have been used to study liquid diffusion in thin polymer films [24-31] and sorption induced polymer swelling [32].

In this chapter, the use of FTIR/ATR to monitor changes in poly(isobutylene) band intensities caused by the sorption of analyte vapor is reported. These changes are interpreted in terms of swelling processes that occur in the polymer thin film. The impact of these swelling processes on SAW device response obtained using both pulsed and continuous flow sample introduction is discussed. Our choice of analytes has been guided by previous work [17] with sorption induced poly(isobutylene) swelling. Grate et al. [17] estimated that nitromethane should produce small swelling effects for poly(isobutylene), while isooctane and dichloroethane should cause large amounts of vapor induced polymer swelling. We selected nitromethane and isooctane from this set of analytes and added perchloroethylene for our study. We anticipate that perchloroethylene should behave similarly to dichloroethane.

5.3 Experimental

Chemicals. Poly(isobutylene) (abbreviated PIB) was obtained from Aldrich chemical company (MW = 380,000). Analytes were obtained from Aldrich chemical company and used as received.

Sensor Test Apparatus. SAW Device. Data were obtained using a 200 MHz SAW resonator array microbalance (Femtometrics, Costa Mesa, CA) that has been described previously [13]. The array device consists of 6 individual resonators mounted on a single stage. The frequency difference (beat frequency) between each resonator and the separate reference device is the measured signal. Power is supplied and frequency counted by an external unit provided by the manufacturer. The SAW device exhibits a

904 Hz frequency shift when perturbed by a 1 nanogram mass change. The SAW array was contained in a 15 mL brass test cell that has been described previously [33].

Sample Delivery. For pulsed injections, analytes were delivered using a Varian autosampler Series 8000 and a Varian gas chromatograph injector operated at 250°C. Typical operating parameters have been given previously [33]. In this study, a 40 cc/min flow of N_2 (99.95%, AGA Gas Co.) dried over molecular sieves and a test cell temperature of 30°C were used. Normally, six 0.2 μ L injections of each analyte (separated by 5 minutes) were made on at least three devices to ensure reproducibility.

Equilibrium measurements were performed using a vapor generation system following operating procedures that have been detailed elsewhere [34]. A series of 4 port and 6 port valves enable the flow to be directed to either the SAW device or the ATR accessory. Analyte concentration is controlled by adjusting the relative flow rates of N₂ carrier gas (99.95%, AGA Gas Co., dried over molecular sieves) through a bubbler containing the analyte and a dilution gas line. The total flow rate is maintained at 100 cc/min. Vapor concentrations are determined using an in-line 5 cc sample loop connected to a Varian 3700 GC equipped with a flame ionization detector. Each run consists of a two minute nitrogen purge, vapor exposure for a period of time necessary for the SAW response to equilibrate, and a nitrogen purge equal to the time necessary for vapor/film equilibration.

Equilibrium SAW response data were obtained using 0.02 - 0.04 g/L vapor streams. To simplify comparison, equilibrium response magnitudes presented in this paper have been normalized to constant vapor concentration (0.02 g/L). Pulse responses

were obtained using 0.2 µL injections of analyte. These injection volumes correspond to 0.009 - 0.02 g/L vapor concentrations if we assume 0.2 µL sample volumes in a 15 mL cell. Pulse response magnitudes have been normalized to 0.01 g/L vapor concentrations. We must emphasize that pulse and equilibrium responses cannot be compared directly since pulse vapor concentrations are never actually constant.

Data Acquisition and Analysis. The beat frequency of each resonator was collected using a digital counting board (MetraByte, Taunton, MA) and stored in a Gateway 2000 386-25 personal computer. The software used to collect the data was provided by the manufacturer. The standard software has been modified by Femtometrics to allow for timed, multiple runs that fully utilize the capabilities of the Varian autosampler. The pulse and equilibrium data were collected at resolutions of 100 Hz (1 pt/0.2 sec acquisition rate) and 2 Hz (1 pt/3 sec data acquisition rate), respectively. Typical RSDs were 10% for the pulse and less than 5% for the equilibrium measurements.

Data analysis was performed using custom software written in LabView for Windows (v2.52, National Instruments, Austin, TX). This software separates the data output file into individual channels and then simultaneously displays the response of all 6 channels on a single page. Additionally, the software counts peaks, determines peak heights, peak areas, and then calculates averages, standard deviations, and %RSDs. It also allows median filtering of the data and provides some control over the sensitivity of the peak determination.

FTIR/ATR. FTIR/ATR experiments were performed using a Mattson Instruments Galaxy 5020 FTIR spectrometer equipped with a wideband mercury cadmium telluride (MCT) detector. FTIR/ATR spectra were collected with 4 cm⁻¹ resolution. A commercial ATR accessory (Specac, Inc.) designed for HPLC detection has been modified to perform analyte/film studies. The attachment consists of a 500 μL cell in contact with a ZnSe internal reflection element (IRE). The cell temperature is maintained at 30°C using a temperature controlled recirculating water bath.

Sample Delivery. The fittings of the ATR cell have been altered to accommodate 1/4" o.d. (1/8" i.d.) stainless steel tubing. For equilibrium measurements, the inlet of the cell was connected directly to an outlet of the vapor generation system and analyte concentrations were identical to those used in the equilibrium SAW experiments (0.02 -0.04 g/L). For pulse injections, the inlet of the ATR cell was connected to a Varian gas chromatograph injector by a 4" long, 1/8" i.d. stainless steel transfer line. The transfer line was heated using nichrome wire. The injector and transfer line were heated to 250°C and 120°C, respectively. Analytes were injected into a 20 cc/min flow of N₂ (99.95%, AGA Gas Co., dried over molecular sieves). The injection volume for each analyte (1 µL) was the minimum amount necessary to produce useful spectra; however, due to the small volume of the ATR cell, the resulting maximum analyte concentrations were approximately 100 times higher than in the case of the continuous flow experiments (see Table 5.2). As in the case of the SAW measurements, we must note that pulse concentrations are only approximate.

Data Acquisition and Analysis. Two software packages supplied by Mattson (FIRST Macros) were used to collect FTIR/ATR data. The initial background spectrum of either the polymer film or the blank crystal was collected using a First software package. EnhancedFirst 1.6.2 was modified to collect time dependent FTIR/ATR data. The program used either the spectrum of the polymer coated IRE or a spectrum of the blank crystal as the background for further data collection. At least one spectrum was collected before the gas stream containing the analyte was introduced into the cell. Approximately eighty spectra (each spectrum is the sum of 10 scans taken at one second intervals) were obtained following the injection of each analyte. For continuous flow studies, up to 180 scans were collected.

Films. PIB films for the SAW devices were prepared by spray casting from dilute toluene solutions (~1000 ppm). Typical film thicknesses were 100 kHz, which corresponds to 0.012 μm. Prior to coating, the SAW devices were cleaned by rinsing with acetone and methanol, soaking in isopropanol, and drying in air. The ZnSe IRE was drop coated using the identical 1000 ppm PIB solution. The thinnest coating that could be detected by the FTIR was used. The calculated film thickness was 0.45 μm (*vide infra*). We have used drop coating on the IRE to facilitate the reproducible preparation of PIB films. However, it is possible that the different methods of film preparation lead to small differences in polymer film morphology in our SAW and FTIR/ATR experiments. Ballantine [35] has reported that the morphology of PIB films on SAW devices is influenced by coating technique.

5.4 Results

SAW Responses. Figure 5.1 shows typical responses obtained from PIB coated SAW devices exposed to each vapor using pulsed and continuous flow sample introduction. The responses measured for nitromethane are significantly lower than the responses observed for isooctane and perchloroethylene, regardless of the sample introduction method. For continuous flow sample introduction, the frequency shift measured for isooctane is greater than the perchloroethylene value; however, the pulse responses for these two analytes are similar.

Since pulse measurements involve a limited analyte/film contact time, the relative responses for analytes may be affected by the diffusion rates of the sorbates in the polymer film. In principle, analytes that diffuse more slowly through the polymer could give artificially low pulse responses compared to equilibrium values. Some insight into the diffusion rates of sorbates in the film can be obtained from the time dependencies of sorption and desorption processes measured with the equilibrium vapor streams. Figure 5.2 shows the normalized SAW responses to each vapor measured as a function of time (t^{1/2}), where t is the elapsed time after the SAW device beat frequency begins to increase in response to analyte vapor introduction (Figure 5.2a) or decrease due to analyte vapor

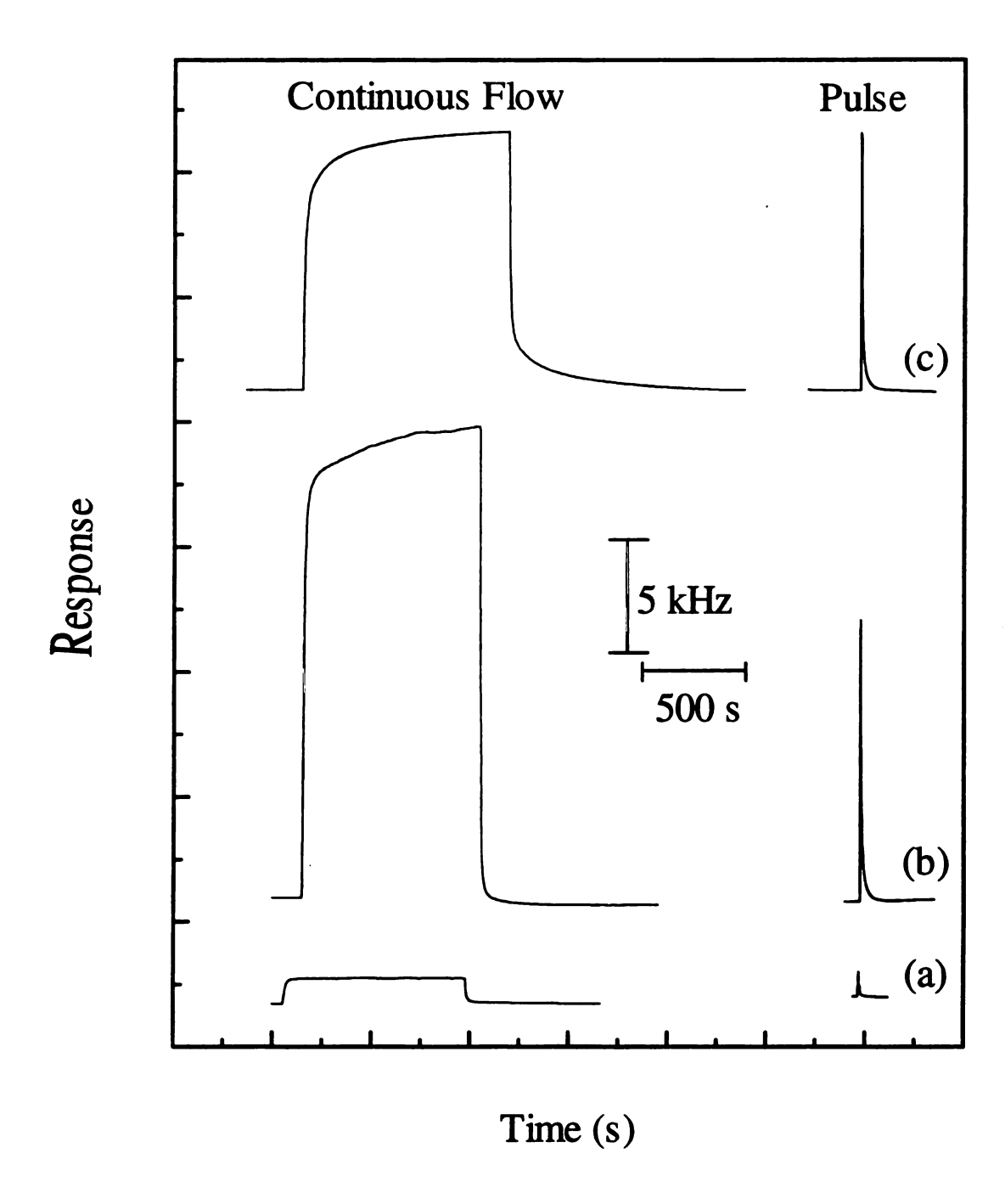
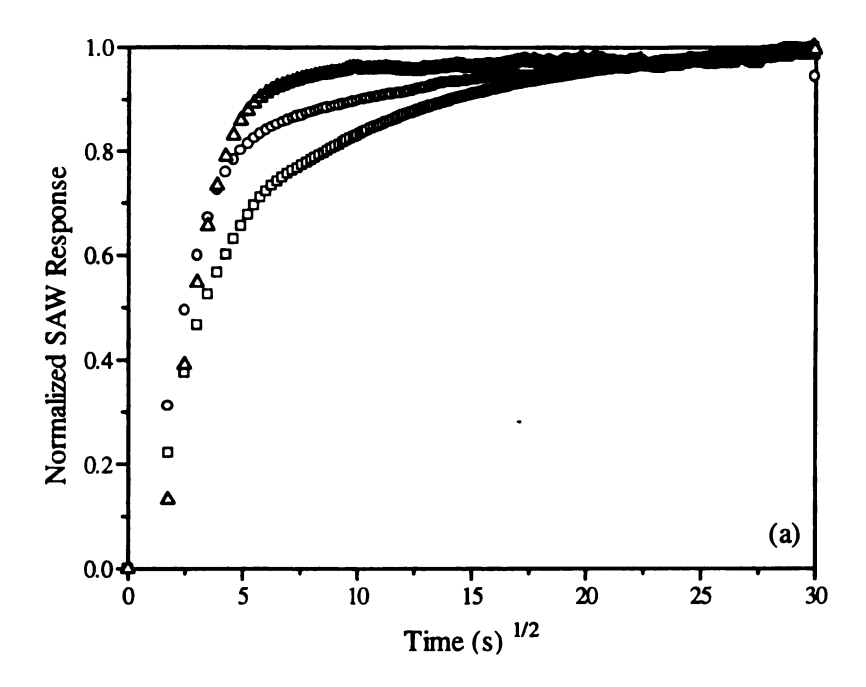


Figure 5.1. Normalized PIB coated SAW device responses to (a) nitromethane, (b) isooctane, and (c) perchloroethylene using continuous flow and pulsed injection sample introduction. Equilibrium and pulse responses have been normalized to analyte concentrations of 0.02 g/L and 0.01 g/L, respectively.



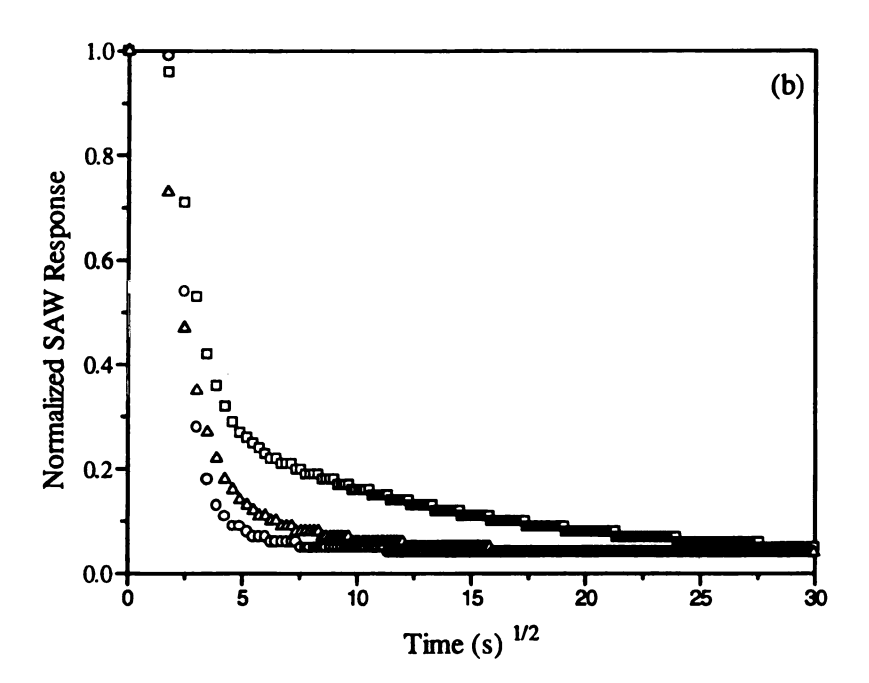


Figure 5.2. Variation in the normalized equilibrium frequency shifts versus time following $t^{1/2}$ for a PIB coated SAW device exposed to nitromethane (Δ), perchloroethylene (\square), and isooctane (O). (a) Rising and (b) Falling edges.

purging (Figure 5.2b). The rising edge profiles (Figure 5.2a) show considerable scatter in the normalized response to the analytes for $t^{1/2} < 5s$; however, the isooctane response is always larger than the value observed for perchloroethylene. Responses obtained at intermediate times ($5s < t^{1/2} < 15s$) suggest that nitromethane equilibrates most rapidly with the PIB film, followed by isooctane and perchloroethylene. The normalized responses obtained during analyte vapor purging are shown in Figure 5.2b. As noted in the rising edge profiles, some scatter in the normalized responses is observed; however, in most instances the values measured for isooctane are lower than the perchloroethylene response. The normalized nitromethane responses are comparable to the values obtained for isooctane. Finally, we should note that the device frequencies return to within 2% of the starting values after the analyte is purged from the cell.

FTIR/ATR Spectra. Analytes and PIB. Ideally, in order to use FTIR/ATR to examine the effect of analyte sorption on the intensity of polymer IR bands, a polymer band that does not significantly overlap with intense analyte bands should be available. Figure 5.3 shows the IR spectra measured for nitromethane, isooctane, and Perchloroethylene vapor streams using an uncoated IRE and a PIB spectrum obtained using a polymer coated IRE. Specific band assignments for the major vibrational modes of the analytes and PIB are given in Table 5.1. It is evident that there are no Perchloroethylene or nitromethane bands that interfere with the C-H stretching bands observed for PIB (3100-2750 cm⁻¹). However, as expected, isooctane has intense C-H stretch bands that would make it difficult to use this region to examine changes in the PIB spectrum arising from isooctane sorption. Further comparison of the PIB IR spectrum

with the spectra measured for the analytes suggests that the PIB CH₂ bending mode (1235 cm⁻¹) is the most intense PIB band that does not overlap with strong bands from any of the analytes.

Nitromethane Sorption. Figure 5.4 shows IR spectra obtained with a PIB coated IRE before (solid line) and after (dashed line) exposure to nitromethane using pulsed (Figure 5.4a) and continuous flow (Figure 5.4b) sample introduction. It should be noted that the CH₂ bending mode (1235 cm⁻¹) is the only band in this region that is due exclusively to PIB. Comparison of the intensity of this band before and during pulsed nitromethane exposure indicates that vapor sorption has little effect on the PIB band intensity. The spectrum measured for a PIB film equilibrated with nitromethane vapor shows a weaker NO₂ asymmetric stretch feature (1553 cm⁻¹) compared to the pulsed experiments due to the decreased vapor concentration (see Experimental Section and Table 5.2). The intensities of the PIB bands were unchanged during the entire vapor exposure time (approximately 30 minutes). The intensities of the C-H stretching bands for PIB (not shown) are also unaffected by nitromethane sorption.

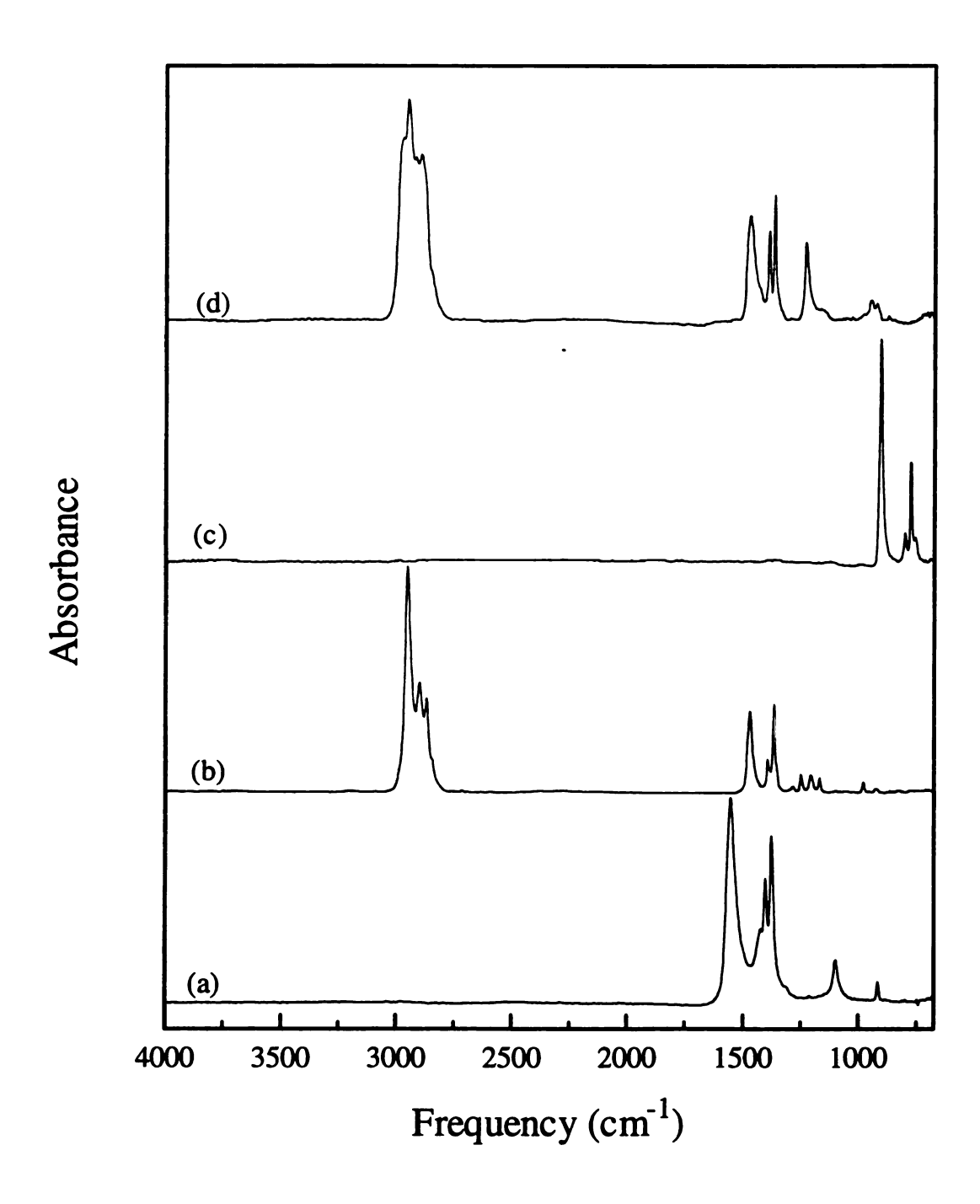
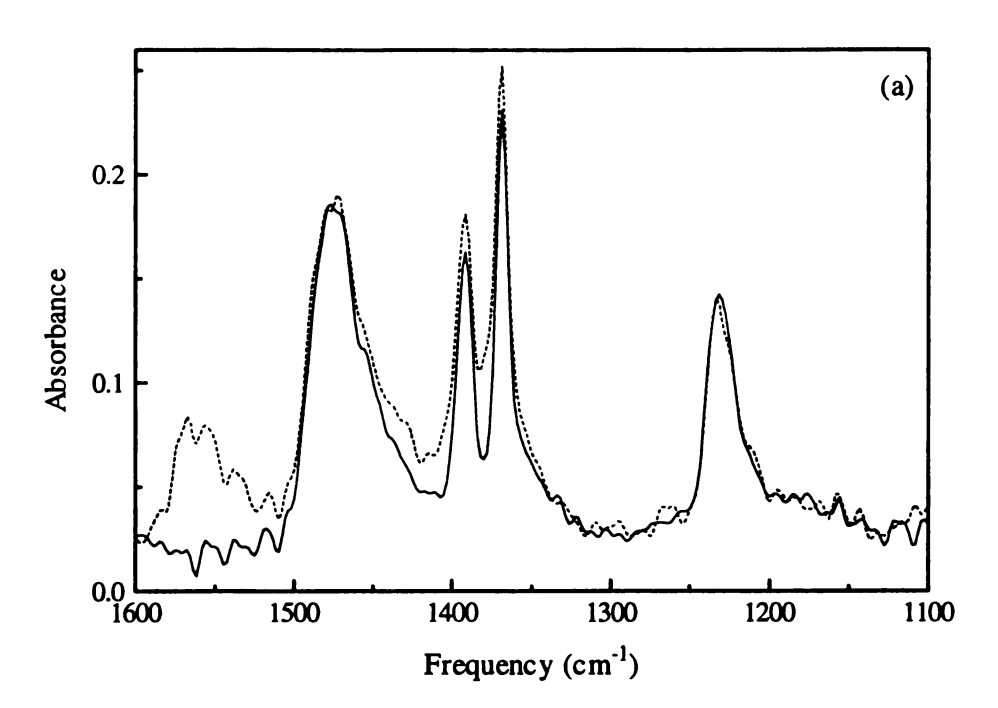


Figure 5.3. IR spectra of (a) nitromethane, (b) perchloroethylene, (c) isooctane, and (d) poly(isobutylene).

Assignments of the major IR bands for poly(isobutylene), isooctane, perchloroethylene, and nitromethane [36,37]. Table 5.1.

poly(is	poly(isobutylene)	isoo	isooctane	perchloroethylene	ethylene	nitromethane	thane
Band (cm ⁻¹)	Assignment	Band (cm ⁻¹)	Assignment	Band (cm ⁻¹)	Assignment	Band (cm ⁻¹)	Assignment
2955	vas CH3	2949	vas CH3	916	vas C-Cl	1553	vas NO2
2925	v_{as} CH ₂	2898	vas CH2, vs CH3	780	v _s C-Cl	1374	v _s NO ₂
2870	$v_S CH_3$	2871	v _s CH ₃			919	vas NO
2855	$v_{\rm S}$ CH ₂	1470	δ_{as} CH ₃				
1473	δ_{as} CH $_3$	1392	δas CH ₂				
1391	δ_{as} CH ₂	1369	$\delta_{ m s}$ CH $_{ m s}$				118
1368	$\delta_{\rm S}$ CH ₃						
1235	$\delta_{\rm S}$ CH ₂						
943	CH ₃ rock						



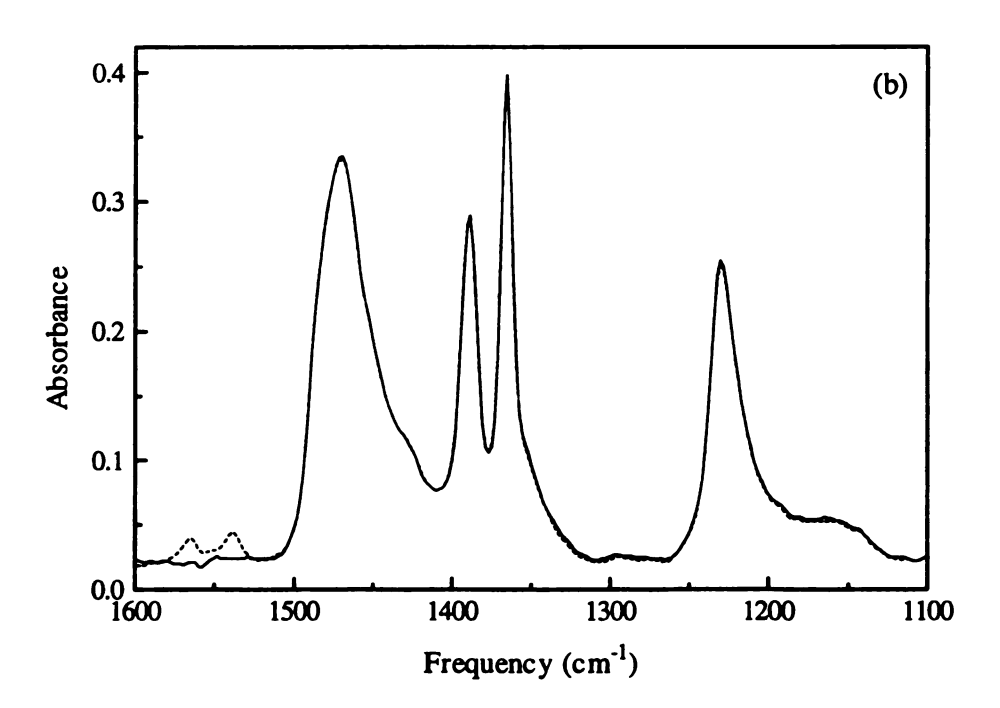


Figure 5.4. (a) IR spectra of a PIB film before exposure to nitromethane (solid line) and at maximum analyte intensity (dashed line) using pulsed sample introduction. (b) IR spectra before exposure to nitromethane (solid line) and during vapor/film equilibrium (dashed line) using continuous flow sample introduction.

Isooctane Sorption. The effect of isooctane sorption on the IR spectra measured for a PIB coated IRE is shown in Figure 5.5. For pulsed sample introduction (Figure 5.5a), intense bands characteristic of isooctane are observed at 1470 cm⁻¹ and 1369 cm⁻¹. In addition, the intensity of the δ_s CH₂ band of PIB (1235 cm⁻¹) decreases significantly in the presence of isooctane. An intense isooctane band should also be observed at 1392 cm⁻¹ (δ_{as} CH₂); however, we believe that the sum of the increase in this analyte band and the decrease in the intensity of the identical mode in PIB produces little change in this part of the IR spectrum. Equilibrium exposure to isooctane (Figure 5.5b) also leads to the observation of bands characteristic of the analyte and a decrease in the δ_s CH₂ band of PIB. For both pulsed and continuous sample introduction experiments, the spectra obtained after isooctane was purged from the film were identical to the initial film spectra.

Perchloroethylene Sorption. Figure 5.6 shows the effect of perchloroethylene sorption on the IR spectra measured for the PIB coated IRE. As noted for isooctane, sorption of perchloroethylene leads to a decrease in the PIB δ_s CH₂ band intensity. The intensities of the C-H stretching bands for PIB (not shown) also decrease on perchloroethylene sorption. As noted for isooctane, the spectra obtained after perchloroethylene was purged from the film were identical to the original film spectra.

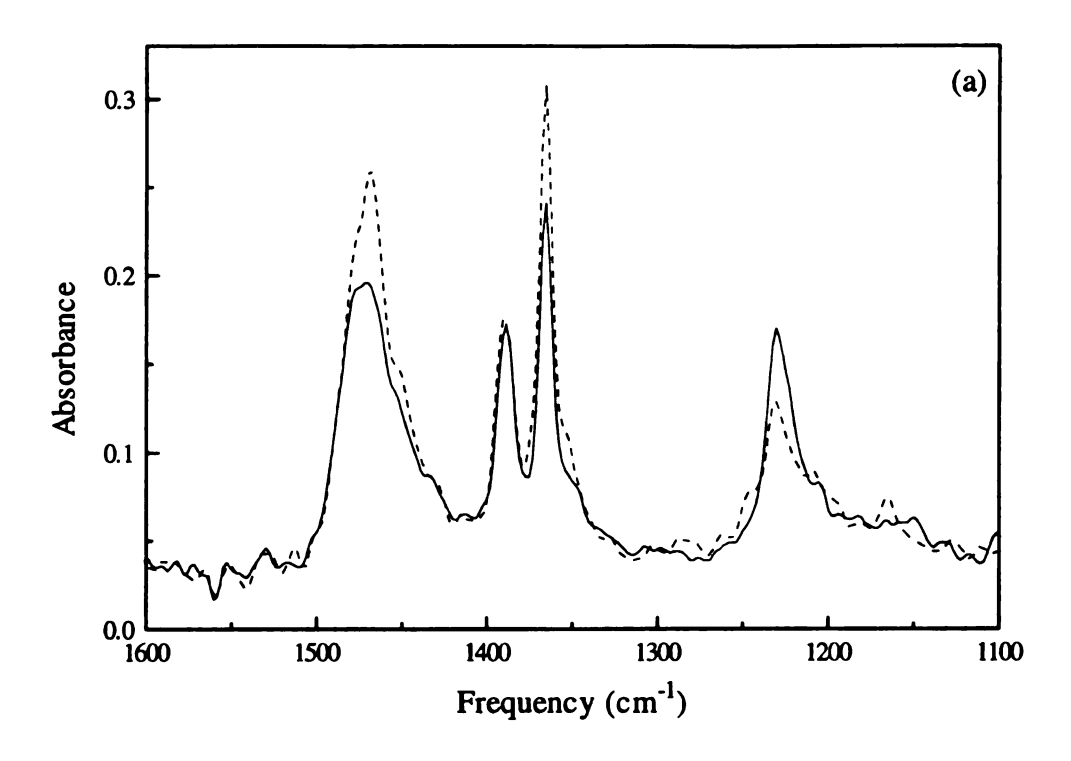
Figure 5.7 shows FTIR spectra measured during the sorption of perchloroethylene into a PIB film under continuous flow conditions. The intensities of the perchloroethylene bands increase with increasing exposure time, while the polymer bands

Comparison of vapor induced polymer swelling estimates¹⁷ to the change in integrated intensity of the C-H bending band of PIB (1235 cm⁻¹). **Table 5.2.**

	Estimated Polymer	Polymer		Continuous Flow	is Flow	Pulse	မ္
Vapor	Conc (g/L) (x 10 ⁻²)	Swelling, %	Vapor	Conc (g/L) (x 10 ⁻²)	Conc (g/L) % Change (x 10 ⁻²)	Conc (g/L) ^a % Change	% Change
nitromethane	1.6	0.05	nitromethane	2.0	0	2.0	-1
isooctane	4.5	1.2	isooctane	2.0	9	1.4	-13
dichloroethane	6.5	0.61	perchloroethylene	2.0	-2.5 ^b	3.2	-11

These values should be considered approximate since the concentration during pulsed injection is never constant.

^b Value is calculated based on a 4.0 g/L perchloroethylene concentration that resulted in a change of -5%.



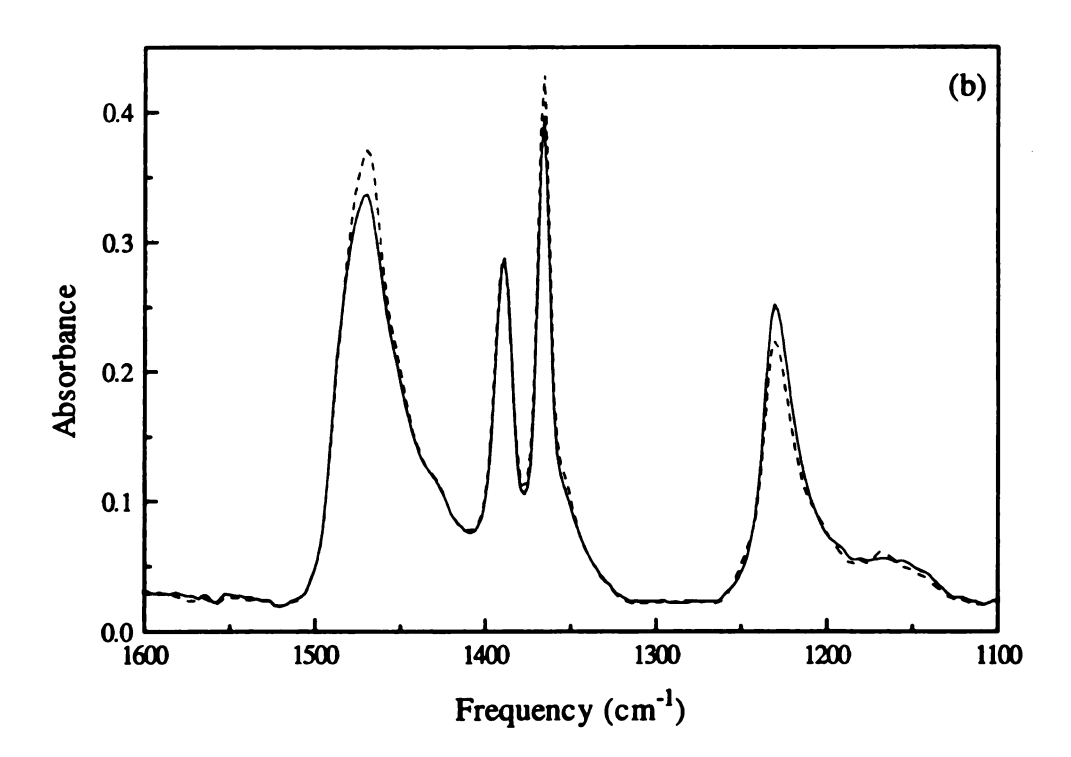
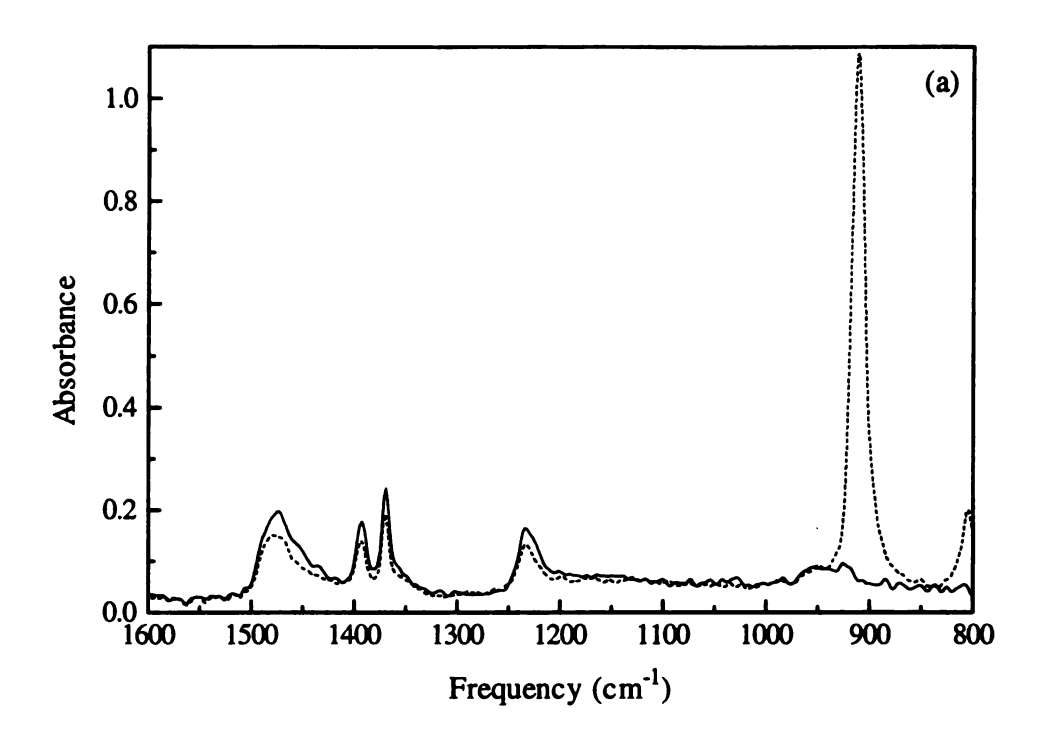


Figure 5.5. (a) IR spectra of a PIB film before exposure to isooctane (solid line) and at maximum analyte intensity (dashed line) using pulsed sample introduction. (b) IR spectra before exposure to isooctane (solid line) and during vapor/film equilibrium (dashed line) using continuous flow sample introduction.



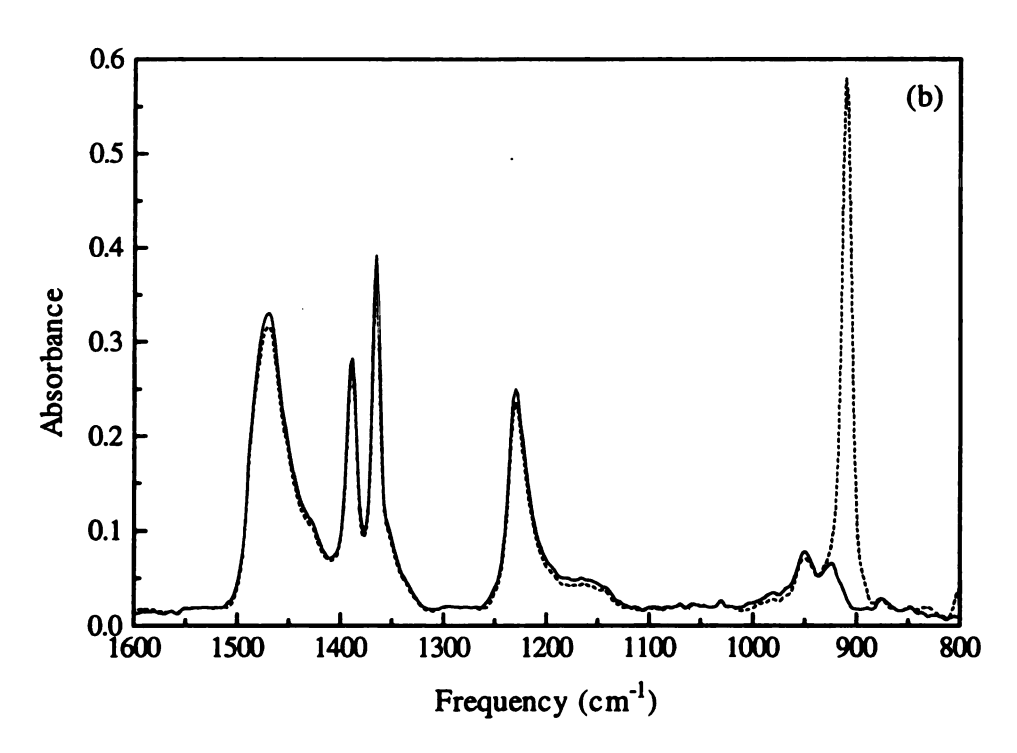
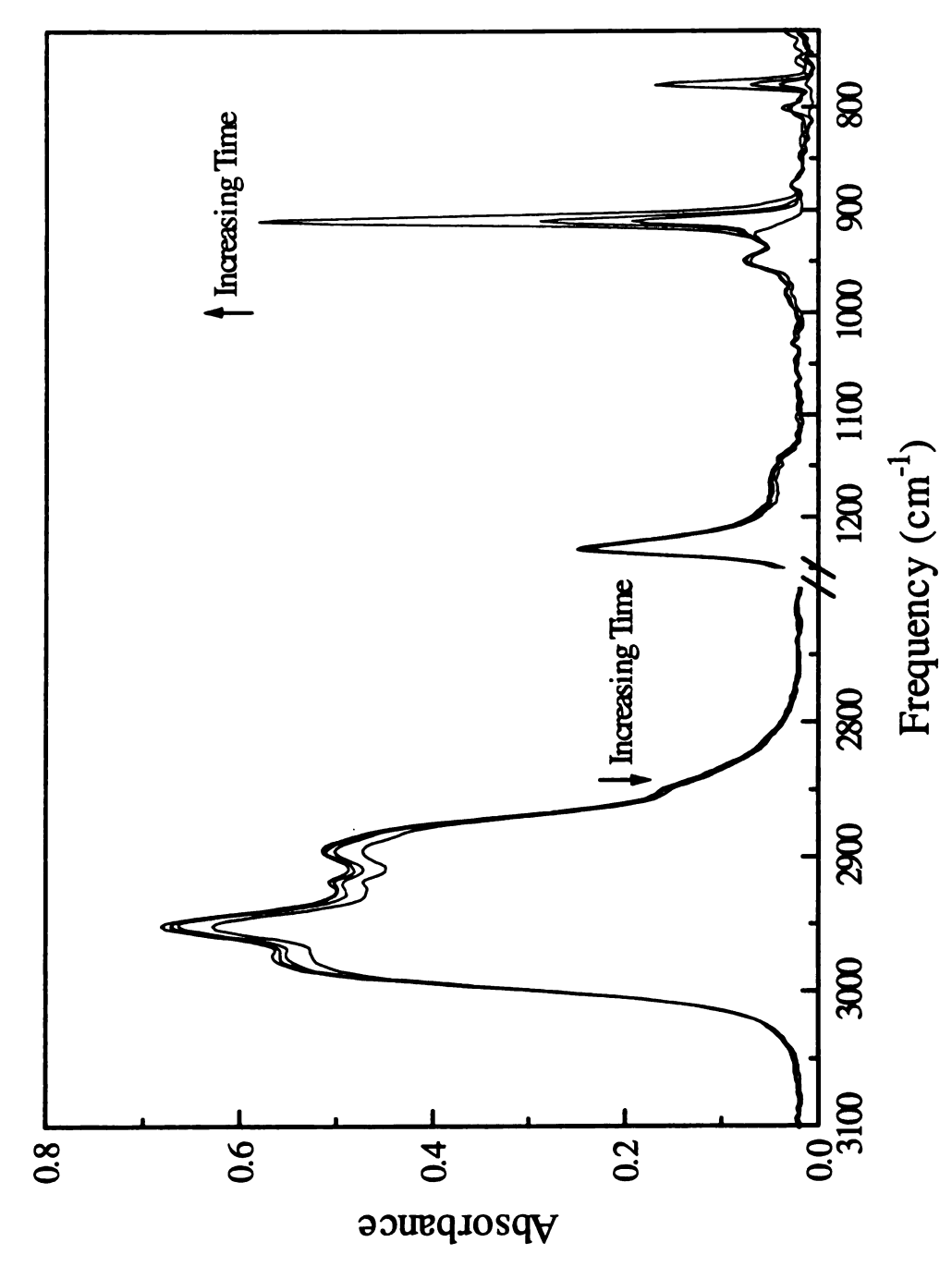


Figure 5.6. (a) IR spectra of a PIB film before exposure to perchloroethylene (solid line) and at maximum analyte intensity (dashed line) using pulsed sample introduction. (b) IR spectra before exposure to perchloroethylene (solid line) and during vapor/film equilibrium (dashed line) using continuous flow sample introduction.



IR spectra obtained as a function of time for a PIB film exposed to a continuous vapor stream of perchloroethylene. Figure 5.7.

show a corresponding decrease in intensity with time. Similar results were observed for isooctane and for both methods of sample introduction.

5.5 Discussion

FTIR/ATR Studies. In an FTIR/ATR experiment that employs a polymer coated IRE, decreases in polymer IR band intensities can occur due to a decrease in the ATR sampling depth and/or a decrease in the polymer concentration within the sampled volume. In principle, several vapor induced phenomena could lead to such decreases. Before examining these possibilities in detail, we must first consider the effect of ATR sampling depth and PIB film thickness on our measurements. Using refractive indices of 2.4 and 1.505 [38] for the ZnSe crystal and the PIB film, respectively, the penetration depth of 1200 cm⁻¹ radiation is calculated to be 1.68 μ m (θ = 45°). The quantity of polymer deposited onto the IRE is sufficient to produce a 0.45 μ m thick film if it is assumed that the polymer uniformly coats the ZnSe crystal. However, we must note that the morphology of the PIB films used in this study is not known and thus it is possible that the polymer is not evenly spread on the IRE. In such a case, it is likely that the film thickness is greater (and less) than the penetration depth of the evanescent wave in several areas of the coating.

Perhaps the most obvious explanation for our findings is a loss of contact between the PIB film and the IRE. Since polymer band intensities return to their initial values after the sorbate is purged from the film, we do not believe that an irreversible loss of polymer/IRE contact (i.e., polymer agglomeration or film lifting) can explain our results. It also seems unlikely that the PIB film redistributes over the IRE after sorbate is purged from the film. Indeed, changes in polymer IR band intensities are closely associated with the presence of sorbate (Figure 7). We believe that the most important vapor induced phenomena that could produce the IR band intensity changes observed in this study are refractive index effects and polymer swelling.

Refractive Index Effects. The penetration depth of the evanescent wave depends on the refractive index of the sampled medium [22]. For example, if vapor sorption decreases the refractive index of the sorbate/film system, then the ATR sampling depth and IR absorbance should decrease. The refractive index of the sorbate/film system (η_{mix}) can be calculated from an expression involving the fractional densities of the sorbate and film and the refractive indices of the pure components:

$$\eta_{\text{mix}} = \left(\frac{\rho_{\text{mix}}^{\text{vap}}}{\rho_{\text{vap}}}\right) \eta_{\text{vap}} + \left(\frac{\rho_{\text{mix}}^{\text{PIB}}}{\rho_{\text{PIB}}}\right) \eta_{\text{PIB}}$$
(5.1)

where ρ_{vap} , ρ_{PIB} , η_{vap} , and η_{PIB} are the densities and refractive indices of the pure vapor and film; ρ_{mix}^{vap} and ρ_{mix}^{PIB} are the densities of vapor and polymer in the film after the film volume has been increased by vapor induced swelling. Since the refractive index of perchloroethylene is comparable to that of the PIB film (Table 5.2), we do not anticipate that perchloroethylene sorption will significantly affect the refractive index of the system.

For equilibrium measurements with nitromethane and isooctane, we have used a calculation method similar to that described by Grate et al. [17] to determine the values of $\rho_{mix}^{\,vap}$ and $\rho_{mix}^{\,PIB}$ used in eq 5.1. The mass of vapor in the film was obtained from the K_{GLC} values taken from Grate et al. [17] and the experimental vapor concentration (Table 5.2). The swelled polymer volume was calculated by adding the volume of analyte in the film to the original film volume. The analyte volume was determined from the mass sorbed and the liquid density. We calculate the contribution of nitromethane and isooctane to the refractive index of the vapor/polymer mixture to be 8.7×10^4 and 7.7×10^4 10⁻³, respectively. The contribution from the PIB film to the refractive index (assuming a swollen film) for nitromethane is 1.505 and for isooctane is 1.497. Thus, the refractive indicies of the mixtures are estimated to be 1.506 (nitromethane/PIB) and 1.505 (isooctane/PIB). These calculations indicate that vapor induced changes in the refractive index of the system and, consequently, changes in the penetration depth of the evanescent wave, are insignificant. Thus, we do not believe that polymer band intensity decreases accompanying vapor sorption are a result of changes in the refractive index of the analyte/polymer system.

Polymer Swelling. If the polymer film swells upon vapor sorption, the density of the polymer decreases. For regions of the film that are thicker than the ATR sampling depth, such polymer swelling would decrease the intensity of the polymer IR bands. Since refractive index effects are minimal, we believe that the decreases in polymer band intensities observed in this work are primarily the result of vapor induced polymer

swelling. We are not aware of any other similar ATR studies of vapor induced polymer swelling. However, Balik and Xu [30] have used optical microscopy and FTIR/ATR to study water sorption into a latex polymer. They used an optical microscope to determine that water swells the polymer and noted a corresponding decrease in polymer IR band intensities during exposure of the film to water.

Table 5.2 shows the maximum change in PIB δ_s CH₂ band intensity during exposure of the polymer film to the analyte vapors under continuous flow and pulsed sample introduction conditions. For both vapor introduction methods, isooctane produces a larger intensity decrease than perchloroethylene and there is essentially no change in polymer band intensities during the sorption of nitromethane. Table 5.2 also shows the estimated percent polymer swelling caused by sorption of various concentrations of vapor reported by Grate *et al.* [17]. If we assume that perchloroethylene produces a change similar to that estimated for dichloroethane, the trend in vapor induced polymer IR band intensity changes is similar to the trend of vapor induced polymer swelling estimates.

been proposed to describe the response of polymer coated SAW devices to vapor sorption. The boiling point model relates the vapor/film partition coefficient to the analyte saturation vapor pressure and predicts that the log of the partition coefficient is directly proportional to the analyte boiling point [39]. Grate and Abraham [6,40] proposed the use of Linear Solvation Energy Relationships (LSERs) to elucidate chemical interactions occurring between a vapor and a film. Later, Patrash and Zellers [39] reported that LSERs could be used to understand and predict the responses of OV-275

(poly[bis(cyanoallyl)-siloxane]), OV-25 ([25% methyl] poly(methylphenylsiloxane)), poly(isobutylene), and poly(phenyl ether) coated SAW devices to a large number of analytes. We have also demonstrated that pulse responses obtained from a PIB coated SAW device can be interpreted using LSERs [41]. Each of the previous studies of PIB [39-41] have shown that this non-polar, hydrophobic polymer interacts with analytes primarily through dispersion forces.

Scheme 1 compares the analyte response order predicted using the boiling point and LSER models to the experimentally determined response order. The solvation parameters used for the LSER calculations are given in Table 5.3. Film coefficients were taken from Patrash and Zellers [39]. Both models fail to predict the response trend observed for these analytes accurately. Since the boiling point model does not consider any specific analyte/film interactions, it is not surprising to find that this model does not predict the correct response trend. In the case of the more sophisticated LSER model, it must be noted that predictions are appropriate for situations in which the SAW response is dominated by mass loading. If vapor sorption changes the mechanical properties of the film, the ability of the LSER model to predict sensor response is questionable. As noted above (Table 5.2), the IR band intensity decreases indicate that the amount of vapor induced polymer swelling decreases from isooctane > perchloroethylene > nitromethane. Thus, for this limited set of analytes, polymer swelling indicated by FTIR/ATR measurements correlates with the measured SAW device frequency shifts.

List of analytes, boiling points, refractive indicies, and solvation energy [40] parameters. Table 5.3.

			H-bond	H-bond	Dispersion		
	Boiling	Refractive	Acid Strength	Base Stength	1	larizability	Dipole
Analyte	Point (°C)	Index	$\Sigma lpha_2^H$	$\Sigma \mathfrak{b}_2^H$	$\log L^{16}$	R2	π_2^H
nitromethane	101	1.402	90:0	0.31	1.892	0.313	0.95
isooctane	86	1.391	0.00	0.00	3.106	0.000	0.00
perchloroethylene	121	1.506	0.00	0.00	3.580	0.640	0.28

Scheme 1. Experimental and predicted order of SAW device response magnitudes.

Model	Order		
Measured	isooctane > perchloroethylene > nitromethane		
Boiling Point	perchloroethylene > nitromethane > isooctane		
LSER	perchloroethylene > isooctane > nitromethane		

The FTIR/ATR results for isooctane and perchloroethylene are particularly useful for understanding the relative equilibrium SAW responses to these analytes. Our FTIR/ATR data indicate that isooctane swells the PIB film to a greater extent than perchloroethylene. However, the LSER model predicts that more perchloroethylene sorbs into the PIB film than isooctane. If the extent of swelling indicated by the FTIR/ATR data is proportional to the change in film mechanical properties caused by analyte sorption, our results suggest that mechanical effects contribute more to the SAW response for isooctane than for perchloroethylene. Thus, eventhough more perchloroethylene sorbs into the film, it appears that the isooctane induced mechanical effects lead to a larger SAW response for isooctane. Similar results have been reported by Martin et al. [19] in a thorough study of mechanical effects on the response of polymer coated SAW devices. These authors showed that mass loading accounts for 40% of the response observed for low concentrations of pentane using a 97 MHz SAW device coated with a 0.70 µm-thick PIB film. For trichloroethylene, mass loading accounted for 67% of the SAW response. Thus, effects other than mass loading (e.g., changes in mechanical properties) account for 60 and 33% of the responses to pentane and trichloroethylene, respectively. We believe

that our findings for isooctane and perchloroethylene are consistent with the work of Martin et al. [19].

Pulsed vs. Equilibrium Measurements. Many sensor applications require pulsed sample introduction. However, as noted previously, pulsed sampling may not allow the analyte to equilibrate with the sensor coating. Indeed, Freeman *et al.* [43] reported that an ethyl cellulose coated QCM showed different response rates to different vapors. They also reported different rate constants for the responses of AT100, OV-101, Carbowax 20M, and ethyl cellulose coatings to the same vapor [43].

We have found that the relative SAW responses of isooctane and perchloroethylene depend on the sample introduction method (Figure 5.1). It appears that the pulse isooctane response is lower than expected on the basis of equilibrium measurements. The sorption and desorption time dependencies shown in Figure 5.2 clearly indicate that isooctane does not diffuse through the PIB film more slowly than perchloroethylene. Thus we do not believe that the differences between pulse and equilibrium measurements are an artifact of analyte diffusion rates.

In principle, mass loading and mechanical effects may occur on different time scales. Frye et al. [44] have reported that the SAW response of a 1 µm-thick polysiloxane film to a low concentration of methanol consists of a rapid initial frequency decrease followed by a slower decrease. The initial shift was attributed to rapid diffusion of methanol through the film, while the slower decrease was ascribed to slow film processes such as polymer rearrangement/relaxation. In our experiments, the short analyte/film interaction time for the pulse measurement may limit the contribution of

slow processes to SAW response. However, our FTIR/ATR studies suggest that PIB swelling coincides closely with vapor sorption in both equilibrium and pulse experiments.

The apparent discrepancy between the pulse SAW response observed for isooctane and perchloroethylene and the SAW response expected on the basis of pulse FTIR/ATR indications of film swelling may be a consequence of the differences in film thickness and analyte concentration used in the two experiments. The PIB films used for the FTIR/ATR measurements are thicker than the films used for the SAW experiments (0.45 µm vs. 0.012 µm). In addition, the pulse analyte vapor concentrations required for the FTIR/ATR experiments are significantly higher than the equilibrium vapor concentrations (Table 5.2). For pulse experiments, the interaction of larger amounts of vapor with thicker polymer films (FTIR/ATR) may not produce the same phenomena as in the case of small vapor concentrations and thin films (SAW). In future pulse studies, we hope to make SAW and FTIR measurements under more similar conditions.

5.6 Conclusion

We have shown that FTIR/ATR spectroscopy can be used to monitor vapor induced changes in PIB film structure. Our initial experiments have focused on the relatively simple study of polymer swelling because the effect of this phenomenon on SAW device response is of significant current interest. Several logical extensions of this work are apparent. It has been suggested that more sensitive acoustic sensors can be constructed by emphasizing the effect of analyte sorption on the mechanical properties of polymer thin films versus simple mass detection. If suitable polymers for these new

sensors exhibit structure dependent IR spectra, FTIR/ATR studies may provide molecular level insight into the processes that contribute to the device response. Obviously, the mechanisms and operating parameters of reaction based sensors could be examined in greater detail using IR. In the study of more highly functionalized polymer coatings, strong analyte-film interactions could be probed using changes in analyte or polymer IR bands. Finally, irreversible sensor response caused by either permanent vapor sorption or altered film structure could be studied.

5.7 References

- 1. Wohltjen, H.; Dessey, R. Anal. Chem. 1979, 51(9), 1458.
- 2. Wohltjen, H.; Dessey, R. Anal. Chem. 1979, 51(9), 1465.
- 3. Ballantine, D. S., Jr.; Wohltjen, H. Anal. Chem. 1989, 61(11), 704A.
- 4. Fox, C. G.; Alder, J. F. Analyst 1989, 114, 997.
- 5. Nieuwenhuizen, M. S.; Venema, A. Sens. Mater. 1989, 5, 261.
- 6. Grate, J. W.; Snow; A.; Ballantine; D. S., Jr.; Wohltjen, H.; Abraham, M. H.; McGill, R. A.; Sasson, P. Anal. Chem. 1988, 60(9), 869.
- 7. Ballantine, D. S.; Jr.; Rose, S. L.; Grate, J. W.; Wohltjen, H. Anal. Chem. 1986, 58(14), 3058.
- 8. Wohltjen, H. Sens. Actuators 1984, 5, 307.
- 9. Snow, A.; Wohltjen, H. Anal. Chem. 1984, 56(8), 1411.
- 10. Frye, G. C.; Martin, S. J. Appl. Spec. Rev. 1991, 26(1&2), 73.
- 11. McCallum, J. J. Analyst 1989, 114, 1173.
- 12. Katritzky, A. R.; Offerman, R. J. CRC Anal. Chem. 1989, 21(2), 83.
- 13. Bowers, W. D.; Chuan R. L.; Duong, T. M. Rev. Sci. Instrum. 1991, 62, 1624.
- 14. Grate, J. W.; Martin, S. J.; White, R. M. Anal. Chem. 1993, 65, 940A-948A.
- 15. Grate, J. W.; Martin, S. J.; White R. M. Anal. Chem. 1993, 65, 987A-996A.
- 16. Tiersten, H. F.; Sinha, B. K. J. Appl. Phys. 1978, 49(1), 87.
- 17. Grate, J. W.; Klusty, M.; McGill, R. A.; Abraham, M. H.; Whiting, G.; Andonian-Haftvan, J. *Anal. Chem.* **1992**, *64*(*6*), 610.
- 18. Bartley, D. L.; Dominquez, D. D. Anal. Chem. 1990, 62, 1649.
- 19. Martin, S. J.; Frye, G. C.; Senturia, S. D. Anal. Chem. 1994, 66, 2201.
- 20. Rogers, C. E. in Polymer Permeability; Comyn, J., Ed.; Elsevier: New York, 1985; p 11-73.
- 21. Fahrenfort, J. Spectrochim. Acta 1961, 17, 698.
- 22. Harrick, N. J. Internal Reflection Spectroscopy, John Wiley and Sons: New York, 1967.
- 23. Internal Reflection Spectroscopy: Theory and Applications; Mirabella, F. M., Jr., Ed.; Marcel Dekker, Inc.: New York, 1993.
- 24. Fieldson, G. T.; Barbari, T. A. Polymer 1993, 34, 1146.

- 25. Farinas, K. C.; Doh, L.; Venkatraman, S.; Potts, R. O. *Macromolecules*, 1994, 27, 5220.
- 26. Heinrich, P.; Wyzgol, R.; Schrader, B.; Hatzilazaru, A.; Lubbers, D. W. Appl. Spectrosc. 1990, 44, 1641.
- 27. Meuse, C. W.; Tomellini, S. A. Anal. Lett. 1989, 22, 2065.
- 28. Xu, J. R.; Balik, C. M. Appl. Spectrosc. 1988, 42, 1543.
- 29. Fu, F. -N.; Fuller, M. P.; Singy, B. R. Appl. Spectrosc. 1993, 47, 98.
- 30. Balik, C. M.; Xu, J. R. J. Appl. Polym. Sci. 1994, 52, 975.
- 31. Marshbanks, T.L.; Ahn, D.J.; Franses, E.I. Langmuir 1994, 10, 276.
- 32. Stuart, B. H.; Williams, D. R. Polymer 1994, 35, 1326.
- 33. Townsend, E. B. IV; Ledford, J.S.; Hoffmann, D.P., accepted for publication in *Review of Scientific Instruments*.
- 34. Townsend, E. B. IV, Ph.D. Thesis, Michigan State University, 1995.
- 35. Ballantine, D. S. Jr. Anal. Chem. 1992, 64, 3069.
- 36. Calthup, N. B.; Daly, L. H., Wiberley, S. E. *Introduction to Infrared and Raman Spectroscopy*, 3rd ed., Academic Press: San Diego, 1990.
- 37. Silverstein, R. M.; Baffler, G. C.; Morrill, T. C. Spectometric Identification of Organic Compounds, 3rd ed., John Wiley & Sons: New York, 1974.
- 38. Aldrich Chemical Company.
- 39. Patrash S. J.; Zellers, E. T. Anal. Chem. 1993, 65(15), 2055.
- 40. Grate, J. W.; Abraham, M. H. Sens. & Act. B. 1991, 3, 85.
- 41. Townsend, E. B. IV, Ledford, J. S.; Hoffmann, D. P. submitted to Sensor and Actuators.
- 42. Abraham, M. H. Chem. Soc. Rev. 1993, 22, 73-83.
- 43. Freeman, N. J.; May, I. P.; Weir, D. J. J. Chem. Soc., Faraday Trans. 1994, 90, 751-754.
- 44. Frye, G. C.; Martin, S. J.; Ricco, A. J. Sens. Mat. 1989, 1-6, 335.

Chapter 6

Detection of Biphenyl and Pentachlorobiphenyl in Organic Solvents Using
Polymer Coated Surface Acoustic Wave Devices

6.1 Abstract

The responses of uncoated, poly(isobutylene), poly(vinyl alcohol), and OV-275 coated surface acoustic wave (SAW) devices to 4% (w/v) biphenyl or 500 ppm pentachlorobiphenyl (PCB) in acetone, methanol, or n-hexane have been determined using pulsed sample injection. Linear Solvation Energy Relationships (LSERs) are used to interpret uncoated and coated SAW device responses to the solvent and each analyte. The importance of dispersion forces in the interactions of PIB lead to large responses to hexane, while the hydrogen bond acid and polarity of PVA and OV-275 lead to large responses to methanol and acetone. For both biphenyl and PCB, the large response obtained with the PIB coated device suggests that dispersion forces are important for these analytes. PCB responses observed with PVA and OV-275 coated devices are not significantly larger than those obtained with an uncoated device. The nature of the solvent does not affect the sensor response to biphenyl. However, the response to PCB in hexane is larger than for PCB in methanol and acetone, regardless of polymer coating.

6.2 Introduction

Piezoelectric devices such as the surface acoustic wave (SAW) resonator have been widely employed for the construction of mass sensors because subnanogramchanges in the mass of the device surface produce readily measurable signals. By themselves, such devices are not chemically selective and thus a coating that interacts specifically with the target analyte is applied to the surface of the device [1-8]. Ballantine and Wohltjen [3] have noted that, when a good coating is available, it is possible to detect vapors at the 10-100 ppb concentration level, with selectivity of 1000:1 and a dynamic range of 3-4 orders of magnitude. However, it can be difficult to identify reversible analyte/coating systems that exhibit the requisite high selectivity. In addition, coatings that show 1000:1 selectivities may be inadequate for the detection of trace levels of one species in another if both molecules produce significant responses.

Limitations in sensor selectivity have lead to the development of array devices and chemometric techniques [9-17] as well as various sample clean-up methods [17,18] in an effort to improve the quality of mixture analysis. For example, Rose-Pehrsson *et al.* [10] used pattern recognition techniques to analyze data obtained from polymer coated SAW devices exposed to hazardous and nonhazardous vapors as either single or two component vapors. Their analysis produced unique fingerprints that could be used to detect toxic organophosphorus compounds in simple mixtures. They also reported that responses to mixtures were within 30% of the values estimated from the sum of individual vapors. Zellers *et al.* [15] also assumed SAW response additivity in order to simulate binary and

ternary mixtures using the data of Rose-Pehrsson et al. [10]. They subsequently applied extended disjoint principal-components regression analysis to improve the identification and quantification of components in the simulated mixtures.

Most previous reports of mixture analysis employed data obtained with sensors that had equilibrated with vapor streams. However, many practical applications of chemical sensors involve the analysis of pulsed vapor samples [9,17-25]. We have previously described the performance of a SAW array-based sensor test apparatus designed to analyze pulsed sample streams [26]. We have also shown that, under certain conditions, this method of sample introduction allows the separation of solvent matrix from analytes that have high boiling points. Similar phenomena have been observed by Kindlund et al. [18], who reported that water can be separated from organic species using thermal desorption in combination with a silicone oil preconcentrator. Grate et al. [17] also observed vapor separation during the application of a smart sensor system consisting of Tenax preconcentrator tubes and an array of four coated SAW devices. In addition, these authors noted that the presence of 2-propanol significantly reduced the sensitivity of four polymer coated SAW devices to the nerve gas soman [17]. This reduction was attributed to either a decrease in the collection efficiency of the preconcentrator tubes or a decreased sensor sensitivity to the test vapor in the presence of solvent, or a combination of both.

We are interested in the development of portable sensor systems for the detection of compounds of interest in waste management. Such analyses often require detection of the target analyte in the presence of excess organic solvent. In addition, typical

applications involve analyses of liquid and/or solid samples using various extraction or thermal desorption sampling methods. Thermal desorption generally produces pulses of sample vapor, while extraction and sample cleanup approaches require liquid sample injection. In this study, we have used a pulsed sensor system [26] for the analysis of 4% (w/v) biphenyl or 500 ppm pentachlorobiphenyl in hexane, acetone, and methanol using uncoated, poly(isobutylene), poly(vinyl alcohol), and OV-275 coated surface acoustic wave devices. Biphenyl and the three solvents were selected because of similarities to a number of environmentally important analytes and solvents, respectively. The films were chosen to provide a range of analyte(solvent)/film interactions and as such, would be logical candidates for SAW sensor array applications.

6.3 Experimental

Materials. Poly(isobutylene) (designated PIB, MW=380,000) and poly(vinyl alcohol) (designated PVA, MW=50,000) were obtained from Aldrich (Milwaukee, WI). Poly[bis(cyanoallyl)-siloxane] (designated OV-275) was obtained from Anspec (Ann Arbor, MI). 2,3,3',4,4'-pentachlorobiphenyl (designated PCB) was obtained from Ultra Scientific (Kingstown, RI). Biphenyl and all solvents were obtained from Aldrich and used as received. In this paper, n-hexane, acetone, and methanol are considered solvents, while the biphenyl and PCB will be referred to as analytes. All of the biphenyl mixtures were 4% (w/v) biphenyl/solvent, while the PCB mixtures were 500 ppm PCB/solvent.

SAW Test System. Data were obtained utilizing a SAW package available from Femtometrics (Costa Mesa, CA). This package consists of six individual 200 MHz SAW

resonator microbalances which exhibit a 904 Hz frequency shift when perturbed by a 1 nanogram mass change. The frequency difference (beat frequency) between each resonator and a separate reference device is the measured signal. Power is supplied and frequency counted using an external unit provided by the manufacturer.

The pulsed sensor test apparatus has been discussed in detail elsewhere [26]. A general overview of the apparatus is given in Figure 6.1. Analytes were delivered to the sensor cell using a Varian gas chromatograph injector operated at 250°C and either a standard syringe or a Varian autosampler Series 8000. The autosampler actuators and injector use nitrogen gas (99.95%, AGA Gas Co.). The nitrogen carrier stream used for the injector was dried over molecular sieves and the flow rate was controlled using Porter mass flow controllers. The splitting chamber was heated using a Variac and heater cartridge. Additional heat was applied to the transfer lines through resistive heating using Nichrome wire wrapped around the lines. The splitting chamber, transfer line, and cell temperatures were monitored using K-type thermocouples. The lid of the cell is cooled or heated (depending on the temperature of the transfer lines) with a recirculating water bath in order to provide the desired sensor cell temperature. The thermocouple used to monitor the cell temperature was placed near the SAW surface, underneath one of the transfer line outlets.

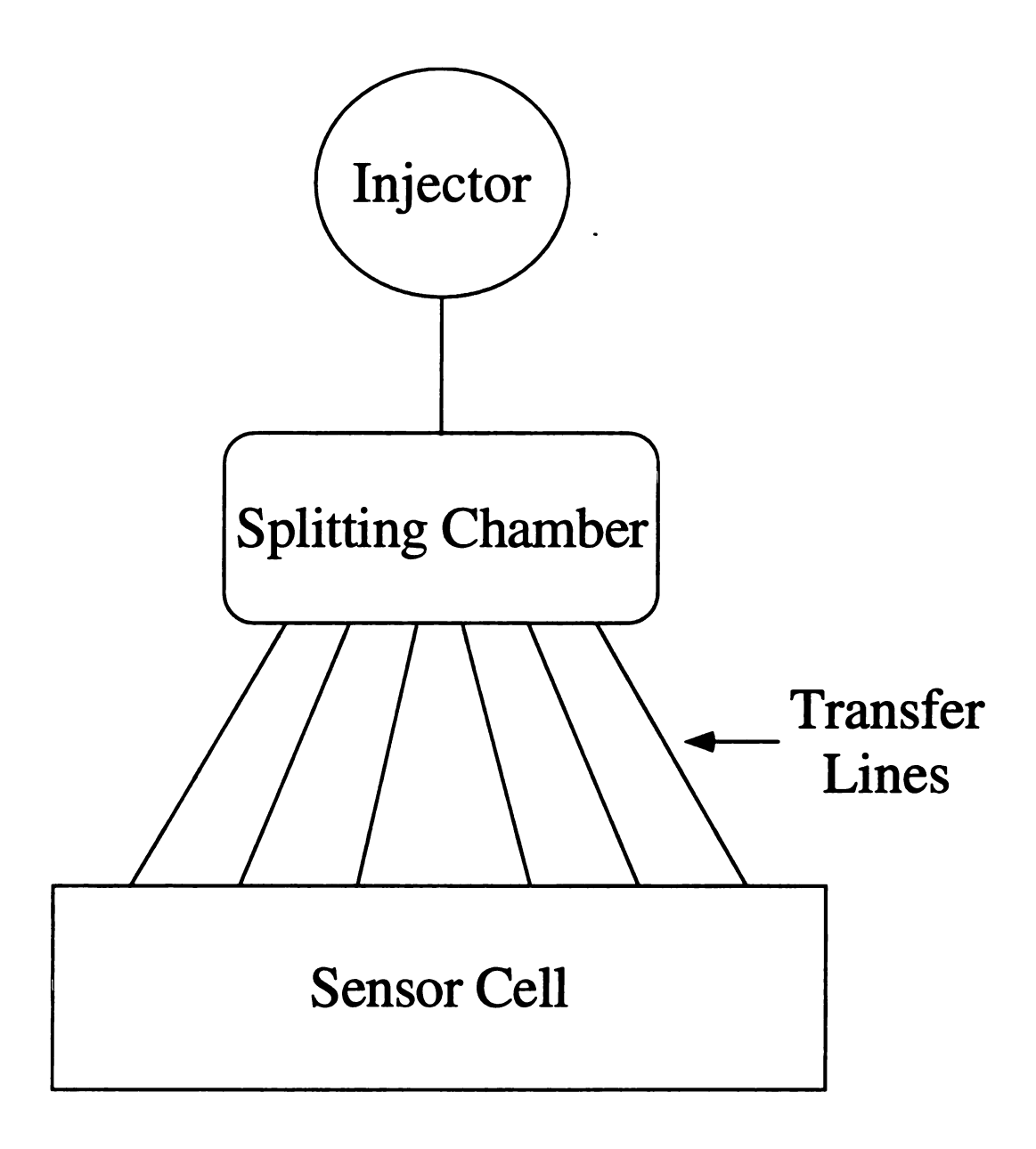


Figure 6.1 Overview of the sensor test apparatus.

In all cases, the splitting chamber temperature was maintained at 400°C. For the biphenyl/solvent mixtures, the carrier gas flow rate was 100 mL/min, the transfer line temperature was 120°C, and the cell temperature was either 30 or 60°C. As we have described previously [26] cell temperature affects the response profile obtained for mixtures of low and high boiling point compounds. At 30°C, the response for the biphenyl/solvent mixtures consists of two peaks: the first peak due to sorption/desorption of a mixture of solvent and biphenyl and the second peak due to sorption/desorption of biphenyl that was initially adsorbed on the walls of the cell. For a cell temperature of 60°C, a single peak is observed following mixture injection. Analyses of samples containing extremely high boiling point compounds such as PCBs are complicated by severe analyte condensation in test systems held at low temperature. Thus, all PCB analyses reported in this work are performed using high temperature cells that result in a single peak following injection of the PCB/solvent mixture. The conditions used for the PCB analyses were transfer line and cell temperatures of 160 and 75°C, respectively, and a carrier gas flow rate of 200 mL/min. We should note that these conditions are close to the upper limits of our test system.

Polymer Coatings. All SAW devices were pretreated for 10 minutes in an argon plasma (Harrick Plasma Cleaner, Harrick Scientific Corporation, Ossining, NY) before coating. 1000 ppm solutions of PIB in chloroform and OV-275 in acetone were airbrushed onto the surface of the crystal. PVA was dissolved in water to make a 10% solution, and then a portion of that solution was diluted 50/50 with methanol and airbrushed onto the surface of the SAW device. The frequency change for all devices

after coating was 50 ± 5 kHz. It should be noted that equivalent frequency shifts following coating does not necessarily imply that the surface coverage and/or morphology of the films are identical. Several researchers have noted problems with the spreading or wettability of films on SAW devices [27-30]. For example, poly(siloxanes) are reported to have poor wetting properties on SAW device surfaces [29].

Data Collection and Analysis. For each analyte/solvent mixture, a run consisted of a 1 μL injection of the solvent followed by a 1 μL injection of mixture. The solvent and mixture injections were separated by approximately 1-2 minutes. At least four injections of solvent and the mixture were made on two devices to ensure reproducibility. Injection order was varied to minimize the effect of solvent order on sensor response.

The beat frequency of each resonator was collected using a digital counting board (MetraByte, Taunton, MA) and stored in a Gateway 2000 386-25 personal computer. The software used to collect the data was modified by the manufacturer to take advantage of the capabilities of the autoinjector. All data were collected using an acquisition rate of 5 pt/sec (100 Hz resolution). Data analysis was performed using custom software written in LabView for Windows (v2.52, National Instruments, Austin, TX). The software separates the Femtometrics data file into individual channels, and then simultaneously displays the response of all 6 channels. The software also determines peaks and peak heights for each injection.

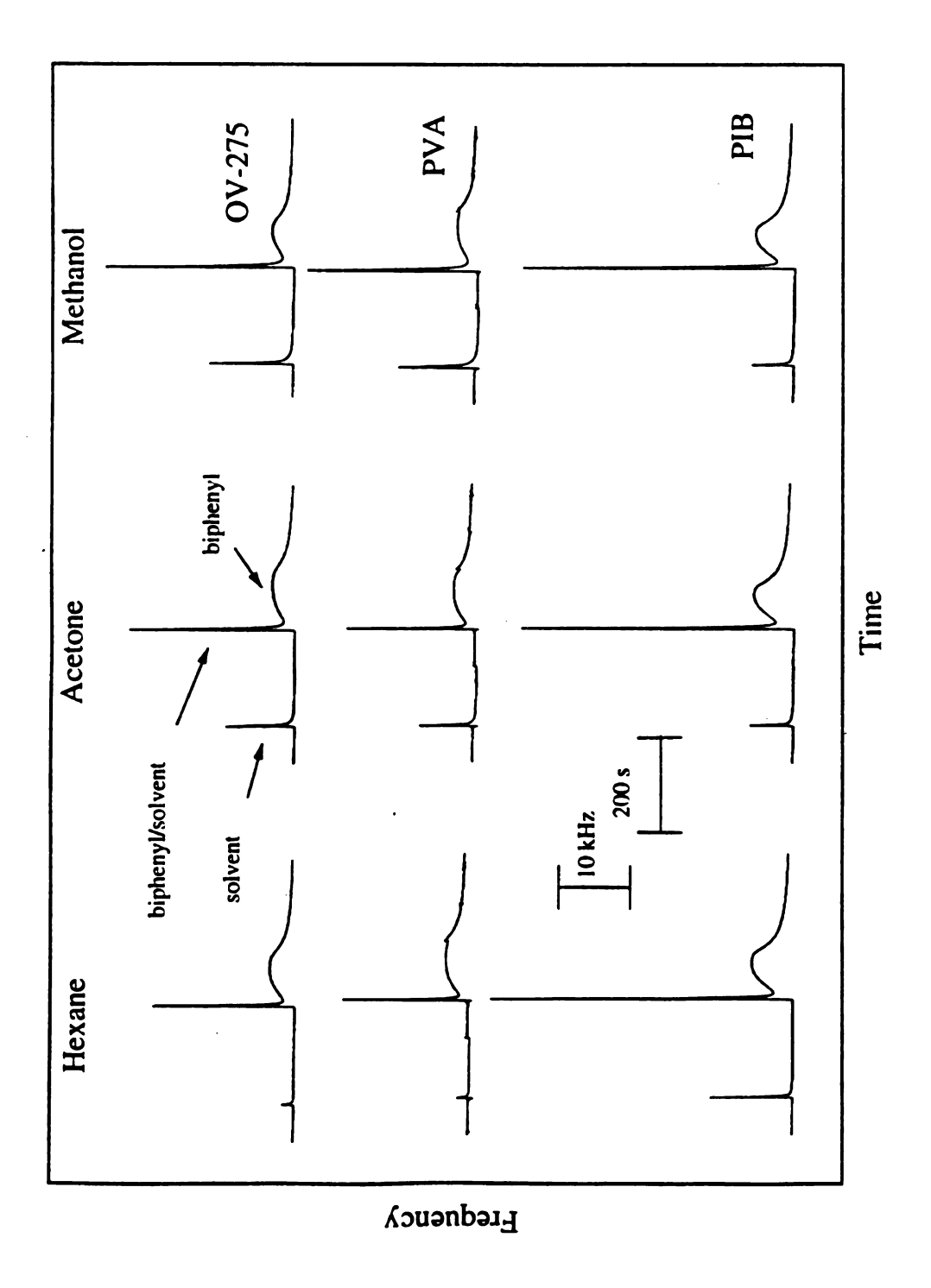
Sensor responses to pure solvents are reported as the maximum frequency shift in hertz observed following sample injection. Evaluation of solvent and analyte responses for mixtures is less straightforward. The frequency shift due to one component in a

mixture is often calculated from the difference in the frequency shift measured for the mixture and the other pure component. However, this approach may not be valid for data collected using a pulsed injection system since differences in solvent and analyte boiling points can lead to significantly different response profiles. For data obtained with high temperature cells (one peak following mixture injection), we have removed the contribution of the solvent to the mixture response by subtracting the entire solvent peak from the mixture peak profile. This was accomplished using the software package Origin (MicroCal Software, Northhapton, MA) by aligning the rising edges of the solvent and mixture peaks and taking the difference between the beat frequencies at the same instance in time relative to the start of each peak. Thus, responses reported for biphenyl and PCB (designated "biphenyl/mix" or "PCB/mix," respectively) are the maximum frequency shifts measured from response profiles obtained using this peak subtraction procedure. It should be noted that this calculation also assumes additive SAW responses. As noted above, two peaks are observed following injection of biphenyl/solvent mixtures into a system that employs a 30°C cell temperature. The biphenyl response from the first peak (designated as "biphenyl/mix) is determined using solvent subtraction. The response to biphenyl measured from the second peak is designated "biphenyl/pure."

6.4 Results

Figure 6.2 shows typical response profiles obtained after the injection of 1 µL of solvent followed by 1 µL of 4% (w/v) biphenyl/solvent using the coated SAW devices held at 30°C. The phenomena responsible for the response profiles have been described above (see Experimental). The average responses to the solvents and biphenyl/solvent mixtures measured using uncoated and coated devices are given in Table 6.1. For each pure solvent, the uncoated device gives the lowest response. The PIB coated device shows the largest response to hexane, while the PVA and OV-275 coated devices show the largest response for methanol. The PIB coated device gives the largest mixture response. The mixture responses measured with PVA and OV-275 coated devices are Table 6.1 also shows the biphenyl/mix responses calculated using solvent subtraction (see Experimental). The results indicate that the biphenyl/mix responses determined for a given film are essentially independent of solvent. The PIB coated device shows the largest biphenyl/mix response. The biphenyl/mix responses determined for PVA and OV-275 coated devices are similar. The biphenyl/pure peak magnitudes are also largest on the PIB coated device and essentially independent of solvent for all polymer coatings.

Figure 6.3 shows typical response profiles measured following the injection of 1 μ L of solvent and 1 μ L of 4% (w/v) biphenyl/solvent using polymer coated SAW devices held at 60°C. The peaks obtained following mixture injection are broader than the pure solvent peaks. The average response magnitudes are given in Table 6.1. The hexane,



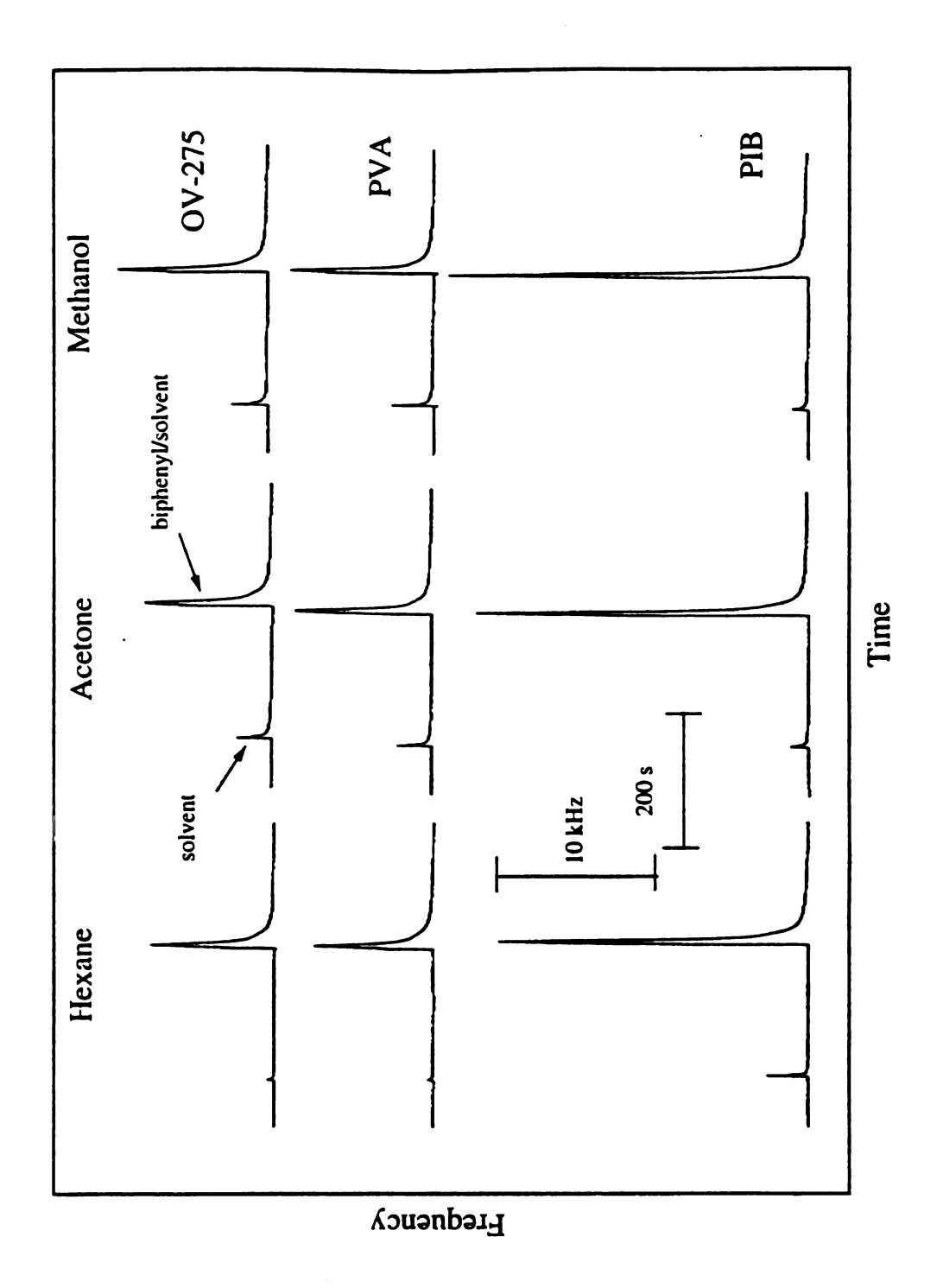
Typical response profiles obtained for the solvent and the biphenyl/solvent mixtures using poly(isobutylene), poly(vinyl alcohol), and OV-275 coated devices held at 30°C. **Figure 6.2.**

Table 6.1. The average measured and calculated responses (Hz) to the solvent, biphenyl/solvent mixtures, and biphenyl measured using uncoated and coated SAW devices held at 30°C and 60°C.^a

		30°C		l	60°C	
	Hexane	Acetone	Methanol	Hexane	Acetone	Methanol
Uncoated					-	
Solvent	900 (17)	1500 (18)	2300 (19)	500 (20)	600 (10)	700 (14)
Mixture	7200 (5)	8000 (12)	8500 (3)	3100 (14)	3500 (5)	3700 (5)
Biphenyl/Mix ^b	6400 (14)	6200 (13)	6000 (8)	3100 (16)	3500 (7)	3700 (3)
Biphenyl/Pure ^c	900 (14)	900 (10)	900 (12)			
PIB Coated						
Solvent	8300(9)	4400 (20)	5200 (14)	2600 (14)	1100 (3)	1100 (14)
Mixture	35400 (6)	31500 (7)	30900 (7)	18100 (15)	20300 (12)	23300 (9)
Biphenyl/Mix ^b	29700 (9)	28100 (8)	27200 (8)	18100 (18)	20300 (12)	23300 (10)
Biphenyl/Pure ^c	4400(12)	4200 (16)	4200 (17)			
OV-275 Coated						
Solvent	1200 (16)	6400 (8)	9100 (13)	400 (21)	2100 (9)	2400 (4)
Mixture	16000 (12)	21700 (7)	21600 (18)	7900 (6)	8500 (12)	10500 (5)
Biphenyl/Mix ^b	15500 (12)	12300 (9)	12700 (24)	7500 (6)	7800 (15)	8900 (7)
Biphenyl/Pure ^c	2900 (26)	2800 (33)	2700 (12)			
PVA Coated						
Solvent	1200 (9)	6300 (17)	9600 (7)	300 (22)	2700 (16)	3100 (20)
Mixture	14800 (5)	15800 (3)	20700 (2)	7300 (6)	9400 (9)	9700 (6)
Biphenyl/Mix ^b	14200 (5)	11100 (8)	12000 (6)	7300 (6)	8500 (8)	8700 (17)
Biphenyl/Pure ^c	2900 (11)	2800 (4)	2600 (11)		, ,	. ,

 ^a %RSDs are given in parenthesis.
 ^b Frequency shift calculated for the biphenyl by peak subtraction (see Experimental).

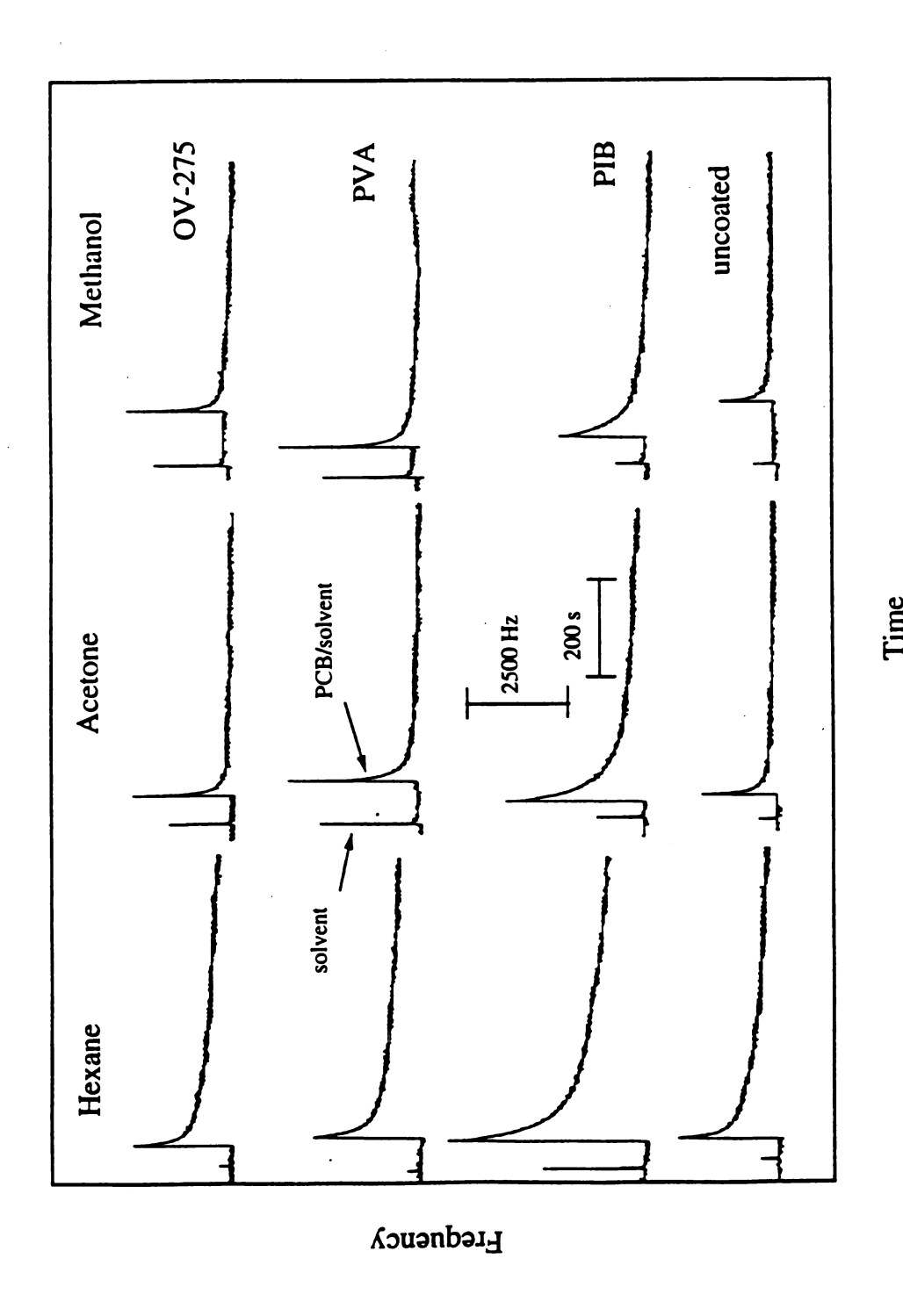
^c Frequency shift of the pure biphenyl peak following the biphenyl/mix spike at 30°C.



Typical response profiles obtained for the solvent and the biphenyl/solvent mixtures using poly(isobutylene), poly(vinyl alcohol), and OV-275 coated devices held at 60°C. Figure 6.3.

each film are identical to those observed with the lower cell temperature. Similar to the 30°C results, the PIB coated SAW device shows the largest mixture and biphenyl/mix responses for each solvent. In addition, variation in solvent has little effect on the biphenyl/mix responses obtained using each polymer coating.

Figure 6.4 shows typical response profiles obtained with uncoated and coated SAW devices held at 75°C following a 1 μL injection of solvent and a 1 μL injection of 500 ppm PCB/solvent mixture. In all cases, the PCB/hexane peak is broader than the PCB/acetone or PCB/methanol peak and does not completely return to baseline after 700 seconds. Table 6.2 shows the average frequency shifts measured for the solvent and PCB/solvent mixtures. The pure solvent responses measured with the uncoated and coated SAW devices are lower than the values obtained with a 60°C cell; however, the trends in solvent response are identical. Note that these response decreases can be attributed to both the increased cell temperature and the increased flow rate (100 vs. 200mL/min). The responses measured for each PCB/solvent mixture on the PIB coated device are larger than the responses measured for either the uncoated, PVA or OV-275 coated devices. Examination of the calculated PCB response in Table 6.2 (see Experimental) shows similar frequency shifts for the uncoated, PVA and OV-275 coated devices.



Typical response profiles obtained for the solvent and the PCB/solvent mixtures using poly(isobutylene), poly(vinyl alcohol), and OV-275 coated devices held at 75°C. Figure 6.4.

Table 6.2. The average measured and calculated responses (Hz) to the solvent, 2,3,3',4,4'-pentachlorobiphenyl(PCB)/solvent mixtures, and PCB measured using uncoated and coated SAW devices held at 75°C.

	Hexane	Acetone	Methanol
Uncoated			
Solvent	400 (18)	500 (16)	600 (19)
Mixture	2300 (10)	1700 (15)	1300 (28)
PCB/Mix ^b	2300 (14)	1700 (24)	1100 (52)
PIB Coated			
Solvent	2300 (21)	1000 (25)	800 (13)
Mixture	4800 (10)	3000 (16)	2000 (29)
PCB/Mix ^b	4400 (23)	2700 (20)	2000 (11)
OV-275 Coated			
Solvent	300 (21)	1700 (13)	1900 (12)
Mixture	2100 (9)	2300 (10)	2400 (7)
PCB/Mix ^b	2100 (11)	1400 (38)	1100 (34)
PVA Coated			
Solvent	300 (30)	2000 (25)	2100 (18)
Mixture	2400 (10)	3000 (15)	2600 (9)
PCB/Mix ^b	2400 (13)	1500 (26)	1400 (27)

[%]RSDs are given in parenthesis.

Frequency shift calculated for the PCB by peak subtraction (see Experimental).

6.5 Discussion

Influence of Solvation Phenomena on Sensor Response. The partitioning of vapor into a thin film acoustic sensor coating is often discussed in terms of expressions developed primarily to describe partitioning in gas chromatography [24,25,30-32]. Linear Solvation Energy Relationships (LSER) have been particularly useful for characterizing new materials [33] and GC stationary phases [34-36], understanding solvation processes [37,38], and interpreting SAW responses [32-40]. Patrash and Zellers [41] have reported that LSER coefficients can be used to describe the responses of SAW devices that have equilibrated with analyte vapor. Recently, we have demonstrated the validity of LSER expressions for the study of PIB coated devices using a pulsed injection system [42]. Our results suggest that if the relative analyte diffusion rates in a film are comparable, valid LSER coefficients can be determined for any coating using data collected with pulsed sample introduction.

LSERs describe analyte/film interactions in terms of five analyte solvation parameters and film coefficients:

$$\log K = c + a \sum \alpha_2^H + b \sum \beta_2^H + l \log L^{16} + rR_2 + s\pi_2^H$$
 (6.1)

 $\Sigma lpha_2^H$ is a measure of hydrogen-bond acid strength, Σeta_2^H is a measure of hydrogen-bond base strength, $\log L^{16}$ describes dispersion interactions, R_2 is a quantitative measure of the ability of a solute to interact with a solvent through n and π electron pairs, and π_2^H

measures the ability of a compound to stabilize a neighboring charge or dipole. Solvation parameters for the solvents, biphenyl, and selected chlorinated benzenes are given in Table 6.3. Parameters for PCBs are not available. The relative magnitude of the film coefficients (a, b, l, r, and s) determines the importance of specific vapor/film interaction mechanisms for a film. The coefficients reported for PIB and OV-275 are given in Table 6.3. For PIB, the LSER coefficients indicate that the polymer should interact with vapors primarily through dispersion interactions. The large a term is an artifact of the fit, and is often reported for PIB [41,42]. The coefficients for OV-275 indicate that it is highly polar (s coefficient) and interacts as a hydrogen bond base (a coefficient). The small l-coefficient suggests that dispersion forces will be less important for OV-275. Film coefficients for PVA are unavailable; however, we anticipate that this polymer should interact with analytes predominantly through hydrogen bond acidity and, to a lesser extent, dispersion forces.

Pure Solvent Responses. The solvent responses obtained with the uncoated and polymer coated SAW devices can be readily explained in terms of solvation interactions. The active area of the uncoated resonator surface consists of partially hydroxylated quartz and thus has polar and hydrogen bonding (acid and base) sites that can interact with adsorbed analytes. This suggests that the uncoated device should interact with hydrogen bonding and polar analytes more strongly than with nonpolar species. The responses measured for hexane, acetone, and methanol at 30, 60, and 75°C (Tables 6.1 and 6.2) are consistent with these expectations. In addition, the decrease in solvent response with

Table 6.3. List of boiling points and solvation parameters [29] for compounds used in this work and selected related species. The LSER coefficients available for the polymer films examined are also included.

Analyte	Boiling Point (°C)	$\sum \alpha_2^H$	$\sum \beta_2^H$	logL ¹⁶	R_2	π_2^H
acetone	56	0.04	0.49	1.696	0.179	0.70
methanol	65	0.43	0.47	0.970	0.278	0.44
hexane	69	0.00	0.00	2.668	0.000	0.00
biphenyl	256	0.00	0.22	6.014	1.360	0.99
benzene	80	0.00	0.14	2.803	0.61	0.59
chlorobenzene	132	0.00	0.07	3.657	0.718	0.65
1,2-dichlorobenzene	181	0.00	0.04	4.518	0.872	0.78
Polymer	_	a	b	1	r	s
poly(isobutylene) ⁴¹	_	0.875	0.275	0.869		_
OV-275 ⁴¹		3.03	0.616	0.615	_	1.88

increasing cell temperature is consistent with previous reports by a number of researchers [9,32,39,43-45].

The addition of a polymer coating generally increases the response of the device to the solvents. Notable exceptions to this statement are the hexane responses measured using PVA and OV-275 coated devices. The solvation parameters for hexane (Table 6.3) indicate that the only significant interaction mode for the molecule involves dispersion forces. Thus, it is not surprising to find that the blank and OV-275 coated devices show similar hexane responses since both surfaces are extremely polar and are not expected to exhibit significant dispersion interactions. The similarity of the hexane responses obtained with PVA and OV-275 coated devices suggests that the dispersion coefficient for PVA is closer to the value reported for OV-275 than for PIB.

The large hexane response measured with PIB coated devices is expected based on the importance of dispersion interactions for PIB (large l) and hexane (large $\log L^{16}$). Similar results for alkanes on PIB coated devices have been reported by others [32,41]. For example, Patrash and Zellers found that alkanes exhibit larger partition coefficients on PIB compared to similar boiling point compounds and smaller partition coefficients compared to the same compounds on OV-275 [41]. The solvation parameters for methanol show that the molecule has strong hydrogen bond accepting and donating properties ($\sum \alpha_2^H$, $\sum \beta_2^H$), and thus is able to interact through both donor and acceptor hydrogen bonds. Acetone is also capable of strong hydrogen bonding interactions (large $\sum \beta_2^H$ parameter). Given the film coefficients reported for OV-275 and anticipated for

PVA, resonators coated with these polymers should show large responses to methanol and acetone. The small dispersion solvation parameters (logL¹⁶) for methanol and acetone suggest that PIB coated devices should be less sensitive to these solvents. Patrash and Zellers [41] have also reported a larger partition coefficient for methanol in OV-275 compared to PIB. In summary, the responses of PIB, PVA, and OV-275 coated devices can be readily explained in terms of LSER principles. It should be emphasized that the ability to use equilibrium solvation parameters to explain pulse response trends suggests that any differences in analyte/film equilibration times are not significant for these systems.

Biphenyl Mixture Responses. The biphenyl SAW response obtained from a mixture can depend on factors such as biphenyl/solvent, solvent/film, and/or biphenyl/film interactions. Obviously, sensor responses observed using uncoated devices do not depend on any type of film interaction and thus most clearly define the effect of analyte/solvent interactions on our measurements. The similarity of biphenyl responses from different solvents measured using uncoated resonators (Table 6.1) suggests that the nature of the solvent has little effect on the amount of biphenyl sorption that occurs during an experiment. Further, these results indicate that the amount of biphenyl available to a coated device is essentially independent of solvent. Thus we believe that any differences in biphenyl response obtained with polymer coated SAW devices can be attributed to analyte(or solvent)/film interactions.

In principle, the nature of a solvent can influence acoustic sensor responses to mixtures in several ways. Solvent molecules could compete with trace analytes for

sorption sites in the coating. In addition, it is well known that vapor sorption expands polymer volume [46] and dilutes the film. The interaction of the analyte with the film may be affected by the presence of the solvent species or the change in polymer free volume. In this study, we have chosen solvents that interact with the polymer coatings to varying degrees. For example, hexane interacts more strongly with PIB than acetone or methanol. However, our results indicate that, as noted for the uncoated device, the nature of the solvent does not significantly affect the response of a given polymer to biphenyl (Table 6.1).

The solvation parameters for biphenyl (Table 6.3) suggest that the molecule can interact with solvents (and polymer coatings) using dispersion forces as well as polar and polarizability interactions. The magnitude of the dispersion solvation parameter (logL¹⁶) indicates that dispersion interactions should dominate the solvation properties of the molecule. Thus, it is not surprising to find that the PIB coated device gives the largest biphenyl response. However, closer examination of the biphenyl solvation parameters and polymer film coefficients suggests that the OV-275 coated device should also show a large response to biphenyl.

Patrash and Zellers have successfully used LSER expressions to predict the equilibrium response of polymer coated acoustic sensors to analytes [41]. Using the film coefficients for PIB and OV-275 and the solvation parameters for biphenyl (Table 6.3), we calculate that the logK_{SAW} for biphenyl on PIB is 5.64 versus 5.56 for biphenyl on OV-275. These results suggest that the biphenyl responses measured using PIB and OV-275 coated devices should be similar. However, as shown in Table 6.1, the biphenyl

response measured with the PIB coated resonator is approximately two times the value obtained using the OV-275 coated device. There are two possible explanations for this observation. First, the diffusion rate of biphenyl in OV-275 could be significantly lower than in PIB. This would lead to an anomalously low response to biphenyl using a pulsed sample delivery system that employs an OV-275 coated device. In essence, the use of an equilibrium model (LSER) to predict relative pulse responses is inappropriate if different sensors do not equilibrate with the analyte at the same rate. Second, it is possible that biphenyl sorption changes the mechanical properties of the PIB film [1,2,39] and, consequently, produces larger frequency shifts than those expected from analyte partitioning alone.

PCB Mixture Responses. In contrast to the results obtained for biphenyl, the PCB responses measured with the uncoated device indicate that solvent does affect the amount of PCB available for adsorption onto the SAW surface. Unfortunately, the exact reason for this observation is unclear. In principle, differences in PCB solubilities could lead to differences in the extent of PCB adsorption that occurs in our experiment. We might expect PCB condensation to be more pronounced from poorer solvents. However, the PCB concentration is very low (500 ppm) and hexane is a well known solvent for PCB test mixtures.

Comparison of the PCB responses measured with the polymer coated devices shows that solvent also affects the magnitude of the PCB response obtained with these sensors. However, solvent effects on the polymer coated device responses must be considered with respect to the uncoated results. Indeed, it should be noted that the

solvent dependencies observed for the coated devices are similar in relative magnitude to the trends observed for the uncoated device. Thus, we do not believe that solvent affects the PCB/film interaction and the differences in PCB response reflect only variations in the amount of analyte available to the device.

Unfortunately, solvation parameters for the specific PCB congener used in this study are unavailable. However, Table 6.3 lists parameters for benzene, chlorobenzene and 1,2-dichlorobenzene. The increase in dispersion solvation parameter (logL¹⁶) with increasing chlorine content suggests that a pentachlorobiphenyl compound will have a larger logL¹⁶ value than biphenyl. We also anticipate that the PCB congener will have significant R_2 and π_2^H values. As in the case of biphenyl, the importance of dispersion interactions should lead to a large PCB response using the PIB coated device. Based on the film coefficients reported for OV-275, one anticipates that a device coated with this polymer should also show a large PCB response. However, the PCB responses measured using the OV-275 coated device are not significantly greater than those obtained with the uncoated resonator. We believe that the similarity of PCB responses obtained with the uncoated and OV-275 (and PVA) coated devices indicates that the PCB does not absorb into the bulk of the film during our experiment. Since the solvation interactions between PCB and OV-275 (and presumably PVA) are favorable, we conclude that the diffusion rate of PCB in OV-275 and PVA is so small that PCB desorbs from the surface of the OV-275 and PVA coated devices before it has the opportunity to diffuse into the film. Apparently, the PCB diffusion rate in PIB is high enough to allow significant absorption;

however, we cannot eliminate the possibility that PCB induces changes in the mechanical properties of PIB that lead to an enhanced response.

6.6 References

- 1. Grate, J. W.; Martin, S. J.; White, R. M. Anal. Chem. 1993, 65, 940A-948A.
- 2. Grate, J. W.; Martin, S. J.; White R. M. Anal. Chem. 1993, 65, 987A-996A.
- 3. Ballantine, D. S., Jr.; Wohltjen, H. Anal. Chem. 1989, 61, 704A-715A.
- 4. Fox, C. G.; Alder, J. F. Analyst 1989, 114, 997-1004.
- 5. Nieuwenhuizen, M. S.; Venema, A. Sensors and Materials 1989, 5, 261-299.
- 6. Frye, G. C.; Martin, S. J. J. Appl. Spec. Rev. 1991, 26, 73-149.
- 7. McCallum, J. J. Analyst 1989, 114, 1173-1189.
- 8. Katritzky, A. R.; Offerman, R. J. CRC Anal. Chem. 1989, 21, 83-113.
- 9. Grate, J. W.; Abraham, M. H. Sens. & Actuators B 1991, 3, 85-111.
- 10. Rose-Pehrsson, S. L.; Grate, J. W.; Ballantine, D. S., Jr.; Jurs, P. C. Anal. Chem. 1988, 60, 2801-2811.
- 11. Amati, D.; Arn, D.; Blom, N.; Ehrat, M.; Saunois, J.; Widmer, H. M. Sens. Actuators B 1992, 7, 587-591.
- 12. Carey, W. P.; Beebe, K. R.; Kowalski, B. R. Anal. Chem. 1987, 59, 1529-1534.
- 13. Carey, W. P.; Beebe, K. R.; Kowalski, B. R.; Illman, D. L; Hirschfeld, T. *Anal. Chem.* 1986, 58, 149-153.
- 14. Carey, W. P.; Kowalski, B. R. Anal. Chem. 1986, 58, 3077-3084.
- 15. Zellers, E. T.; Pan, T-S.; Patrash, S. J.; Han, M.; Batterman, S. A. Sens. Actuators B 1993, 12, 123-133.
- 16. Yao, S.; Chen, K.; Nie, L. Anal. Chim. Acta 1994, 289, 47-55.
- 17. Grate, J. W.; Rose-Pehrsson, S. L.; Venezky, D. L.; Klusty, M.; Wohltjen, H. *Anal. Chem.* **1993**, *65*, 1868-1881.
- 18. Kindlund, A.; Sundgren, H.; Lundstrom, I. Sens. & Act. B. 1984, 5, 1-17.
- 19. Suleiman, A.; Guilbault, G. G. Anal. Chim. Acta 1984, 162, 97-102.
- 20. Thompson, M.; Stone, D. C. Anal. Chem. 1990, 62, 1895-1899.
- 21. Heckl, W. M.; Marassi, F. M.; Kallury, K. M. R.; Stone, D. C.; Thompson, M. *Anal. Chem.* **1990**, *62*, 32-37.
- 22. Thompson, M.; Stone, D. C.; Nisman, R. Anal. Chim. Acta 1991, 248, 143-153.
- 23. Yan, Y.; Bein, T. J. Phys. Chem. 1992, 96, 9387-9393.

- 24. Janghorbani, M.; Freund, H. Anal. Chem. 1973, 45, 325-332.
- 25. Edmonds, T. E.; West, T. S. Anal. Chim. Acta 1980, 117, 147-157.
- 26. Townsend IV, E. B.; Ledford, J. S.; Hoffmann, D. P., in press Rev. Sci. Instr.
- 27. McGill, R. A.; Grate, J. W.; Anderson, M. R. Interfacial Design and Chemical Sensing, ACS Symposium Series 561, 1994, 280-294.
- 28. Ballantine, D. S. Jr. Anal. Chem. 1992, 4, 3069-3076.
- 29. McGill, R. A.; Abraham, M. H.; Grate, J. W. ChemTech 1994, 24, 27-37.
- 30. McCallum, J. J.; Fielden, P. R.; Volkan, M.; Alder, J. F. Anal. Chim. Acta 1984, 162, 75-83.
- 31. Snow, A.; Wohltjen, H. Anal. Chem. 1984, 56, 1411-1416.
- 32. Grate, J. W.; Snow; A.; Ballantine; D. S., Jr.; Wohltjen, H.; Abraham, M. H.; McGill, R. A.; Sasson, P. Anal. Chem. 1988, 60, 869-875.
- 33. Abraham, M. H.; Du, C. M.; Grate, J. W.; McGill, R. A.; Shuely, W. J. J. Chem. Soc., Chem. Commun. 1993, 1863-1864.
- 34. Abraham, M. H.; Whiting, G. S.; Doherty, R. M.; Shuely, W. J. *J. Chromatogr.* 1991, 587, 229-236.
- 35. Abraham, M. H.; Whiting, G. S.; Doherty, R. M.; Shuely, W. J. J. Chem. Soc. Perkin. 2 1990, 1451-1460.
- 36. Abraham, M. H.; Whiting, G. S.; Doherty, R. M.; Shuely, W. J. *J. Chromatogr.* 1990, 518, 329-348.
- 37. Abraham, M. H. Pure Appl. Chem. 1993, 65, 2503-2512.
- 38. Abraham, M. H. Chem. Soc. Rev. 1993, 22, 73-83.
- 39. Grate, J. W.; Klusty, M.; McGill, R. A.; Abraham, M. H.; Whiting, G.; Andonian-Haftvan, J. *Anal. Chem.* 1992, 64, 610-624.
- 40. Grate, J. W.; McGill, R. A.; Abraham, M. H. *IEEE Ultrasonics Symp.* 1992, 275-279.
- 41. Patrash, S. J.; Zellers, E. T. Anal. Chem. 1993, 65, 2055-2066.
- 42. Townsend IV, E. B.; Ledford, J. S.; Hoffmann, D. P., submitted to Sens. Actuators.
- 43. King, Jr., W. H. Anal. Chem. 1964, 36, 1735-1739.
- 44. Guilbault, G. G.; Jordan, J. M. CRC Crit. Rev. Anal. Chem. 1988, 19, 1-28.
- 45. Townsend IV, E. B.; Ledford, J. S.; Hoffmann, D. P. submitted to Anal. Chim. Acta.

46. Rogers, C. E. in *Polymer Permeability*; Comyn, J., Ed.; Elsevier: New York, 1985; p 11-73.

